Doctoral Dissertations (All Dissertations, All Years)   Electronic Theses and Dissertations

2010-04-20

Ambulance Vibration Suppression via Force Field Domain Control

Paul D. Cotnoir
Worcester Polytechnic Institute

Follow this and additional works at: https://digitalcommons.wpi.edu/etd-dissertations

AMBULANCE VIBRATION SUPPRESSION VIA FORCE FIELD DOMAIN CONTROL

By

Paul David Cotnoir

A Dissertation

Submitted to the Faculty

of the

WORCESTER POLYTECHNIC INSTITUTE

in partial fulfillment of the requirements for the

Degree of Doctor of Philosophy

in

Manufacturing Engineering

April 20, 2010

APPROVED:

DISSERTATION COMMITTEE:

Professor Mustapha S. Fofana, PhD, WPI
Professor Richard D. Sisson, Jr., PhD, WPI
_____
Professor Sharon Johnson, PhD, WPI
Dr. Mustapha S. Fofana, Major Advisor
Professor Christopher Brown, PhD, WPI
Professor Kevin Rong, PhD, WPI
Professor Linda Esper, RN, MSN, MBA, EdD
– Becker College
_____
Dr. Richard D. Sisson, Jr. Director of   Stephen Haynes, Chief, UMass/Memorial
Manufacturing and Materials Engineering   EMS

Abstract

This PhD dissertation experimentally characterized the vibration amplitude, frequency, and energy associated with ambulance travel and defined the relationship of the vibration to safety, comfort and care of ambulance patients.

Average vertical vibration amplitudes of .46 to 2.55 m/sec^2 were recorded in the patient compartment of four ambulances over four road surfaces at three speed settings. Power spectrum analysis of the data revealed that the vibration energy and resulting vertical acceleration forces were concentrated in the .1 to 6 Hz range. Relationships between the measured ambulance vibration and the impact of whole body vibration on human physiology and performance were quantified. It was found that the accelerations measured in the ambulances were in excess of what is considered to be a normal human comfort level. Furthermore, the vibration measured was in a spectrum which could present physical impediments to optimum task performance for the on-board medical team. Phase portrait analysis combined with the power spectrum data revealed the presence of nonlinearities, stochastic fluctuations and time delays inherent in the data.

The ambulance vibration data was then used to create a unique analytical model and library of forcing functions corresponding to the vehicles, road surfaces and vehicle speeds that were tested. Using the example of a vibration absorbing force plate fit over an existing ambulance floor, it was demonstrated how the model and forcing functions could be used to develop a control law equation to select parameters for active control of vibration to produce sustainable regions of patient safety, comfort and care.

Acknowledgements

TABLE OF CONTENTS

LIST OF TABLES AND FIGURES

NOMENCLATURE

c_s	damping coefficient of shock absorber, $N\ sec\ /\ m$
c_t	damping coefficient of tire, $N\ sec\ /\ m$
E	elastic modulus, $psi\ (MPa)$
$F(t)$	road forcing function, N
g	acceleration due to gravity, $9.8\ m\ /sec^2$
$g(z)$	variable stiffness function, $kN\ /\ m$
$h(\dot{z})$	variable damping function, $N\ sec\ /\ m$
k_s	stiffness of vehicle suspension spring, kN/m
k_t	equivalent spring stiffness of tire, kN/m
k_p	stiffness of force plate, kN/m
m	mass, kg
m_s	sprung mass of vehicle, kg
m_u	unsprung mass of vehicle, kg
m_p	mass of force plate, kg
μ	deterministic bifurcation parameter
τ	Time delay, s
$-\sigma_0\gamma(t)$	stochastic noise term, m/sec^2
ω_n	natural frequency, Hz
ξ	damping ratio, $N\ sec\ /\ m$
z	relative displacement between sprung masss and tire, m
$z_g(t)$	vertical displacement function of tire at ground contact point, m
z_u	vertical displacement of unsprung mass, m
z_s	vertical displacement of sprung mass, m
z_1	vertical displacement of tire at ground contact point, m
z_2	vertical displacement of sprung mass, starting at equilibrium position, m
$\dot{z}$	relative velocity of sprung mass and tire, m/sec
$\dot{z}_u$	vertical velocity of unsprung mass, m/sec
$\dot{z}_s$	vertical velocity of sprung mass, m/sec
$\dot{z}_1$	vertical velocity of tire at ground contact point, m/sec
$\dot{z}_2$	vertical velocity of sprung mass, m/sec
$\ddot{z}$	relative acceleration of sprung masss and tire, m/sec^2
$\ddot{z}_u$	vertical acceleration of unsprung mass, m/sec^2
$\ddot{z}_s$	vertical acceleration of sprung mass, m/sec^2
$\ddot{z}_1$	vertical acceleration of tire at ground contact point, m/sec^2
$\ddot{z}_2$	vertical acceleration of sprung mass, m/sec^2

Ambulance Vibration Suppression via Force Field Domain Control

1.0 Executive Summary

The safety and comfort of passengers in acute care vehicles is an issue of major interest. Due to the already compromised health of most ambulance patients, and the relatively uncontrolled and limited health care environment of a moving vehicle, the risk of injury or death as a result of untoward events occurring during emergency transportation is high enough to warrant study. The current interest in health care reform and patient-centered care is creating significant pressure on the industry to continually improve services and expand the level and quality of care which can be provided.

Studies in the literature associated with ambulance modernization have revealed a need for greater patient comfort and safety during transport in order to reduce the likelihood of ride-induced patient trauma, increase the occupational safety of emergency medical service (EMS) crews, and to increase the scope and raise the standard of care of mobile, in-route treatment.

This study characterized the vibration amplitude, frequency, and energy associated with ambulance travel and the attendant impacts of road-induced vibration on patients and crew. Utilizing original vibration data collected from selected ambulances in concert with data from published studies, relationships between ambulance vibration and the impact of whole body vibration on human physiology and performance were quantified. Computational models of road-induced forcing functions of typical ambulance rides were developed based on a classic quarter car model of vehicle suspension. The unique contribution of this work to research in the field is threefold:

1) The experimental determination and analysis of vibration amplitude, frequency and energy unique to ambulance travel at a range of speeds, road surfaces and ambulance

type,

2) the association of those vibration characteristics which are specific to ambulance travel with known human physiological responses to whole body vibration with association to patient safety , care and comfort; and,

3) the creation of a library of forcing functions and ambulance vibration model which were created to simulate the travel of a typical ambulance over the undulating surface of a variety of common road surfaces at a broad range of frequencies.

The forcing functions and ambulance vibration model were utilized to develop a mathematical model of ambulance vibration control capable of accommodating the nonlinearities, stochastic fluctuations and time delays present in the ambulance vibration data. A generalized equation was derived for control of vibration attenuation solutions to accommodate typical allowable ambulance loads and road excitations.

The broader significance of this work lies in enhancing the patient-centered care associated with ambulance travel by improving patient comfort and safety through the assessment and administration of mobile medical interventions with improved precision, accuracy and safety.

2.0 Introduction

It is standard patient care policy to have EMS ambulance crews perform the minimum treatment necessary on-scene to stabilize and package the patient as quickly as possible. Therefore, a significant amount of basic, intermediate, and advanced life saving procedures must be carried out in the moving ambulance. This ensures a timely transport to an acute care facility. These same care guidelines typically call for no more than a 10 minute transport time for critically ill patients and no more than a 20 minute excursion for other medical or trauma patients. As our society becomes more and more litigious, and tort claims against emergency medical services increase, the safety of passengers in acute care vehicles is fast becoming an issue of major interest. Due to the already compromised health of most ambulance patients, and the relatively uncontrolled and limited health care environment of a moving vehicle, the risk of injury or death as a result of untoward events occurring during emergency transportation is high enough to warrant study.

The vast amount of the literature supports the evaluation of such risks of injury or fatalities involving ambulance patients and crews primarily in relation to accidents and crashes of emergency vehicles. This has led to the proposed establishment of new safety paradigms for emergency vehicles including: enhanced crash test requirements for ambulances, more stringent driver training and practice policies, changes to transportation systems engineering, better automotive engineering, and improved education of other road users, all targeted at reducing motor vehicle accidents involving emergency vehicles. The purpose of this study is to involve the characterization, modeling and the development of an engineered solution to enhance ride comfort and safety in an ambulance patient compartment.

In addition to the risks associated with motor vehicle accidents, ground transport of

injured patients to hospitals exposes the patient and ambulance emergency medical technicians (EMTs) to possibly hazardous shocks and vibrations, generated by travel at moderate to high speeds over uneven road surfaces. These shocks and vibrations are transmitted through the transport vehicle's chassis, rear suspension, body, and elastic contact surfaces to the occupants' tissue mass. Whole-body vibration can have a variety of detrimental physical effects on the human body which are either acute or chronic. All major systems of the body can be affected, including cardio-vascular and skeletal to endocrine, sensory and eye-motor functions.

International standards on whole-body vibration, typically, specify vibration exposure limits in terms of time, relating such limits to reduced comfort and fatigue-decreased proficiency. These exposure limits are typically expressed in charts which define a frequency weighted exposure time beyond which most individuals will experience discomfort or a variety of types of decreased physical, motor or sensory performance. While it is well understood that exposure to whole-body vibration is potentially injurious to human health, it is difficult to draw conclusions about the physical characteristics of shock and vibration or the mechanisms by which exposure to such excitations cause injury. Most studies which have evaluated the health effects of vehicle vibrations are epidemiological in nature.

The literature review explored three main categories of vibration effects on humans in ambulances: (1) Those in which road excitations directly impact patient health and safety due to physiological effects, (2) those in which road excitations may cause patients and EMS crew undue discomfort or occupational health problems, and (3) those in which road excitations limit the ability of EMS crews to provide advanced care and diagnosis due to activity interference effects. A study of the pertinent literature identified those vibrational frequencies and amplitudes which are most likely to cause injury and should be attenuated. The ambulance shock and

vibration effects studied were assumed to be whole body vibrations due primarily to road excitations.

In general, the dynamic ride characteristics of any road vehicle are influenced by road excitations, variations in vehicle velocity, and the stiffness and damping parameters of the vehicle. This study identified vibrations associated with normal emergency vehicle travel over standard road surfaces.

Ambulances in a typical urban setting, such as the area of study, Central Massachusetts around Worcester, Massachusetts (USA) and Northeastern Connecticut (USA), where this study was conducted, must negotiate a variety of road profiles at various velocities which lead to a broad spectrum of excitations in a variety of frequency regimes. These vibrations were correlated to a characterization of the road surface being traversed using data gathered directly from instrumented vehicles, from studies found in the literature, and from mathematical road models.

Over the last 40 years, a variety of analytical and empirical methods have been developed to predict discomfort caused by vehicle vibration due road excitations. Automotive designers design vehicle suspensions with a proper combination of stiffness and damping to support vehicle loads, isolate road shock from the passenger compartment, maintain vehicle contact with the road surface, and allow proper vehicle cornering. The common quarter-car mathematical model has proven to be an accurate tool for the design of vehicle suspensions where ride comfort is of prime importance. This study used this particular analytical model to determine the ability of an ambulance suspension to support the ambulance design load and isolate potentially harmful road excitations within the working space allowed.

Data from instrumented vehicles indicated that a standard ambulance chassis suspension

is incapable of adequately and reliably attenuating some of the harmful road excitations commonly encountered by these emergency vehicles. A secondary vibration attenuation system to augment the standard ambulance suspension could provide a workable solution.

Therefore, it was the goal of this study to:

1. **Experimentally determine** the vibrational amplitude, frequency and energy of a typical ambulance ride, and correlate those vibrational characteristics to human physical impacts on ambulance passengers and EMT crews.

2. Use the vibrational parameters to **characterize** road forcing functions to simulate typical ambulance travel over the undulating surface of a variety of common road surfaces at a broad range of frequencies to create a computational model of a vibration attenuation solutions.

3. **Model** a force field domain control system (FFDCS) embodied in a force plate design capable of working in tandem with a standard ambulance suspension system to attenuate the most harmful vibrations encountered by such a vehicle in normal service.

The broader significance of this study lies in enhancing the patient-centered care associated with ambulance travel by improving patient comfort and safety through the assessment and administration of mobile medical interventions with improved precision, accuracy and safety.

3.0 Literature review

3.1 The state of emergency ground transport

Over the last 40 years, the volume of non-hospital emergency care, its level of complexity and the required expertise of EMS personnel has all risen at a very high rate (Proudfoot, Romano, Bobick & Moore, 2003, p. 1629). In a recent article, Wired magazine, estimates that there are approximately 40,000 ambulances in service in the USA responding to an average of a half million 911 calls each day (Davis, 2003).

In a review of 326 insurance liability claims against emergency service (EMS) agencies, Wang, Fairbanks, Shah, Abo, & Yearly (2008) found that 122, or 37% of those claims were due to ambulance vehicle crashes or movement. The vast majority of peer-reviewed journal articles dealing with the safety and comfort of ambulance transport is associated with the evaluation of risk of injury or fatality primarily in relation to accidents and crashes of emergency vehicles. A selection of these studies is presented in Table 1.

Table 1. *Peer-reviewed studies dealing with risk of injury and death in ambulances*

Study Authors	Findings
Kahn, et. al., 2001	This study targeted ambulance crashes only from the NHTA Fatality Analysis Reporting System database and found that unrestrained patient compartment occupants were at the highest risk of injury in an accident. The authors also determined the typical high rate of speed of ambulance travel is often a contributing factor to accidents.
Maguire, et. al., 2002	The authors' analysis of various data sources suggests that the occupational fatality rates for EMS workers is greater than that of all workers and is on par with the fatality rates of other emergency public service workers.
	The results of this review of 49 independent studies of ambulance service occupational health issues corroborates other studies which indicate a higher

Sterud, et. al., 2006	standardized mortality rate than other professions, but further suggests additional risks of developing work-related health problems including: higher than normal rates of anxiety, general psychopathology, musculoskeletal problems and a higher standardized early retirement on medical grounds than the general working population.
Pirrallo & Swor, 1994	In this study, the authors failed to find any statistically significant differences in between the rate of fatal ambulance crashes during emergency or non-emergency use. The results of this study led the authors to conclude that the data was unable to provide much in the way of objective measures which would be useful in developing policies to decrease the number of fatal ambulance crashes.

In an effort to reduce the occupational hazards associated with EMS opearations and improve ambulance safety, Dr. Nadine Levick, MD, MPH, CEO of Objective Safety Inc., along with others working in the field of transportation safety, has proposed the establishment of new safety paradigms for emergency vehicles. These include: enhanced crash test requirements for ambulances, more stringent driver training and practice policies, changes to transportation systems engineering, better automotive engineering, and improved education of other road users, all targeted at reducing motor vehicle accidents involving emergency vehicles. A selection of studies analyzing and describing a variety of enhancements to ambulance safety is presented in Table 2.

Table 2. *Peer-reviewed studies dealing with suggested remediation to enhance ambulance safety*

Study Authors	Findings
Levick & Grzbieta, 2008a	In this study, the authors propose that ambulance design and safety testing should be on par or exceed accepted automotive guidelines for dynamic crashworthiness test procedures.
Johnson, et. al., 2006	The authors' surveyed 302 EMS personnel regarding child and provider restraints for ambulance patient compartment occupants. Results of the survey suggest restraints are underutilized. Conclusions included that improved equipment may help alleviate some risk and allow for safer ambulance transport of pediatric patients.

Siedel & Greenlaw, 1986	This study corroborates the Johnson study and calls for a means of safely restraining infants and children in ambulances.
Elling, 1989	In this study, the author suggests the creation of better ambulance driver education programs, making ambulance drivers more aware of the hazards inherent in emergency vehicle travel, and adjusting agency standards to require ambulances to come to full stops at all stop signs and red lights, etc.
Levick & Swanson, 2005	This study investigated the feasibility of using an on-board computer monitoring system in ambulances to improve driver risk behaviors. Results included an increase of 15 miles between penalty counts, a drop in seatbelt violations and 20% saving in vehicle maintenance costs within a 6 month period. 36 vehicles with 250 drivers covered 1.9 million miles over an 18 month test period.
Levick & Grzebieta, 2008b	The authors identify safety testing requirements for ambulances, outline the basic principles of crashworthiness design and evaluate the design and construction of characteristic ambulances from a safety perspective. Detailed information on design and construction is included.

The intent of the researchers listed in Table 2 was to improve the occupational safety of ambulances through the avoidance of traffic accidents or the addition of safety devices. While some of those measures may also accrue to the comfort and safety of ambulance patients, the policies or design recommendations do not speak directly to the detrimental effects of routine ground vehicle travel resulting from road-induced shocks and vibrations. Due to the already compromised health of most ambulance patients, and the relatively uncontrolled and limited health care environment of a moving vehicle, the risk of injury or death as a result of untoward events occurring during emergency transportation must also be considered. The same is true of the occupational hazards of chronic EMS personnel exposure to shock and vibration.

In addition to the risks associated with motor vehicle accidents, ground transport of injured patients exposes both the patient and ambulance EMTs to possibly hazardous shocks and vibrations, generated by travel at moderate to high speeds over uneven road surfaces. These shocks and vibrations are transmitted through the transport vehicle's chassis, rear suspension, body and elastic contact surfaces to the occupants' tissue mass (Goldman & Gierke, 1960, p. 9) .

In general, the dynamic ride characteristics of any road vehicle are influenced by road excitations, variations in vehicle velocity, and the stiffness and damping parameters of the vehicle (Tamboli & Joshi, 1999, p. 194).

3.2 Road surface as a source of vehicle vibration excitation

Methodologies for the characterization of the forcing functions which are produced by vehicles travelling over road surfaces, which in turn lead to the shocks and vibrations transmitted to vehicle passengers, is found in the literature associated with vehicle suspension design for enhanced ride comfort (Parsons & Griffin, 1983; Stephens, 1977; Gillespie, 1992; Genta, 1997; Wong, 2001) as well as in studies dealing with the occupational hazards of chronic exposure to vehicular vibration (Paddan & Griffin, 2002; Griffin, 1990).

In some studies, approximate mathematical models of road surface excitations are developed analytically or through computer simulation studies (Amman, Pielemeier, Snyder & Toting, 2001; Wambold, 1986, Rui, Saleem & Zhou, 1997; Gobbi, Levi & Mastinu, 2006, Pesterev, Bergman & Tan, 2004; Tamboli & Joshi, 1999; Green, Golding, Aulukh, Faldon, Murphy, Bronstein, & Gresty, 2008). Green et. al. studied the effects of off-road vehicle travel on human respiration and cardiovascular performance. They simulated off-road travel dynamics in a mechanical apparatus. In previous studies, they determined the various shock and vibration characteristics of typical road features. For potholes they "distributed (mean 4s intervals) transient tilt-and-return triangular displacements of 1.5s duration and +/- 0.5g peak accelerations" over a background excitation at combined frequencies of 0.075, 0.2, and 0.5 Hz (Green, et. al., 2008, p. 2). In their study, Optimum design of a passive suspension system of a vehicle subjected to actual random road excitations, Tamboli & Joshi compared the power spectra of a sinusoidal excitation to the spectra of actual road excitations (1999, p. 200). This is

shown in Figure 1.
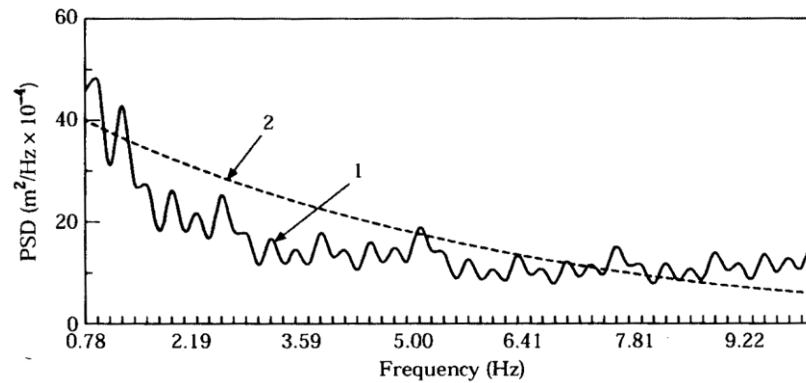
Figure 1. *Comparison of power spectral density of (1) actual and (2) formulated road excitations. (Tamboli & Joshi, 1999, . p200)*

The authors concluded this to be an adequate approximation of the actual displacement-time history shown in Figure 2 (Tamboli & Joshi, 1999, p. 200).
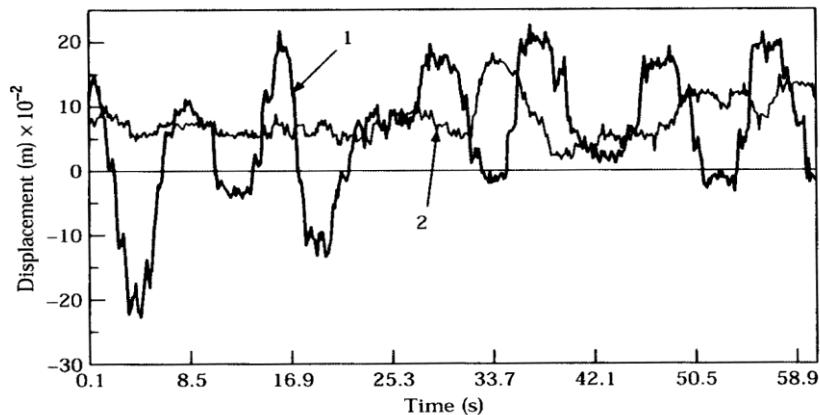
Figure 2. *Example displacement-time history of (1) actual highway travel and (2) actual city travel. (Tamboli & Joshi, 1999, p. 200)*

Many empirical vehicle vibration studies only use actual random road excitations which are gathered directly from instrumented vehicles or passengers (Papagiannakis, 1997; brown, Mear, Moore, Kannapan, Marshek, Cuderman, & Efatpenah, 1992; Kao & Perumaiswami, 1997). In general, vehicle suspension response to road excitations has been explored

experimentally through the use of shake table tests, ride simulator experiments, ride

measurement in vehicles, and subjective ride assessment (Barak, 1991, p.54).

In their study, *Evaluation of whole-body vibration in vehicles,* Paddan & Griffin (2002),

measured the vibration in 100 different vehicles and assessed the results relative to both ISO and

british international vibration standards. Typical frequency-weighted vibration amplitudes for

the 25 cars tested in their study is excerpted and shown in Table 3..

Table 3. *Frequency-weighted vibration amplitudes measured on cars, from Paddan and Griffin (2002, p.200)*

	BS 6841 (1987)								ISO 2631 (1997)			
	Equivalent r.m.s. acceleration (m s-2 r.m.s.)				Seat vertical. acceleration (m s-2 r.m.s.)				Most severe axis. acceleration (m s-2 r.m.s.)			
Vehicle type (#)	Med.	Min.	Max.	Std. Dev	Med.	Min.	Max.	Std. Dev	Med.	Min.	Max.	Std. Dev
Car (25)	0.45	0.32	0.75	0.14	0.37	0.25	0.61	0.10	0.39	0.26	0.75	0.14

Of great interest here is the range of frequency-weighted amplitudes from .26 to .75

m/sec^2, which is typical for road vehicle studies of this type. The vibration amplitudes of all the

vehicles tested by Paddan and Griffin ranged from a minimum of .14 m/sec^2 to 1.52 m/sec^2

(2002, p. 200).

Two international vibration standards were compared in the Paddan and Griffin study

(2002). Data for the study was gathered in accordance with the accepted vibration measurement

methods outlined in ISO 2631-1, 1997 (International Organization for Standardization 1997 ISO

2631-1, 1997) and BS 6841 (British Standards Institution 1987 BS 6841, 1987). Both standards

require the vibration amplitude data to be calculated using a vibration dose value (VbV) which

accounts for the frequency, the amplitude and the length of exposure to the vibration under investigation. For the British standard, the acceleration information is obtained for 4 axes, while for the ISO standard, only the most severe axis is reported when assessing health or perception risks. For comfort studies each axis data point is reported and the total vibration (triaxial sum) value is used. Regardless of the standard chosen, for all 100 vehicles tested over 461 experimental runs, Paddan and Griffin found that for the majority of measurements, the vertical axis on the seat pan provided the worst case frequency-weighted acceleration readings and that the vertical acceleration component dominated the r.m.s. vibration values (Paddan, et. al., 2002, p. 198 - 206).

The actual frequencies and amplitudes of the input excitations experienced by road vehicles can be highly variable and location dependent. Consider the variability and range displayed in the power spectrum curves for the 25 cars studied by Paddan and Griffin, reproduced here in Figure 3. While vibration time histories will vary by location and measurement method, the power spectral density, which identifies the major frequency components of vehicle vibration is fairly consistent across many studies.

For this study, the measurement and acquisition of actual displacement time histories for ambulance travel over the area of study, exhibiting a variety of surface conditions, was used in concert with data gleaned from the literature and analytical models. Particular attention was paid to those excitations which resulted in ambulance cabin frequencies and amplitudes shown by previous studies to have the greatest effect on human beings.
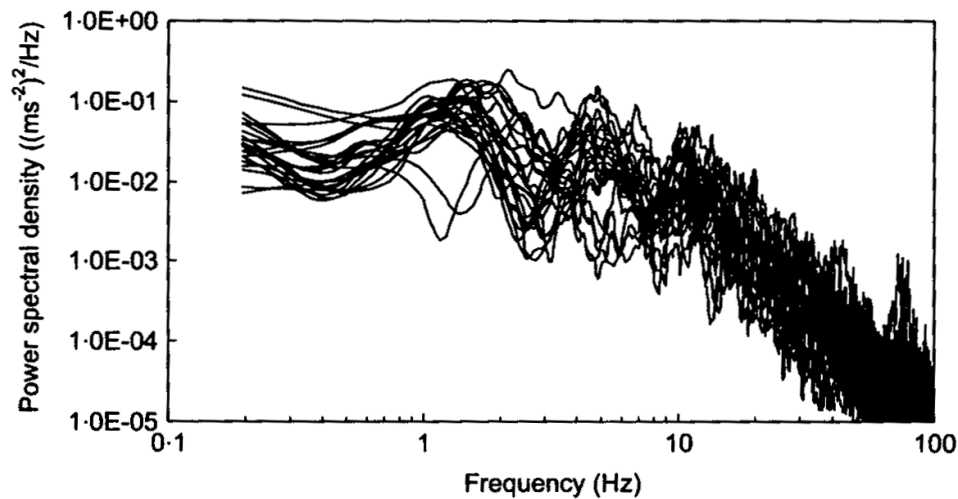
Figure 3. *Example* p*ower spectal density of vertical vibration measurement on seats of the 25 cars tested by Paddan & Griffin (2002, p203)*

3.3 Human whole-body vibration response and measurement

Any study of human shock and vibration must begin with a few definitions. For this study, the term *shock* will be used in its engineering sense, as defined by Goldman and Gierke as, "a force of significant amplitude which reaches its peak value in less than a few tenths of second and is of no more than a few seconds of total duration" (1960, p. 7). The term *vibration* will be used to refer to alternating forces with periodic tendencies which are of sufficient amplitude to be humanly perceived, but are of generally lower amplitude and longer duration than shocks. The terms *mechanical noise* and *random shocks* will describe excitations which fall somewhere between a shock and a vibration and may be treated as either a vibration spectrum or as repeated, individual shock loading (Goldman & Gierke, 1960, p. 7-8).

Studies of the detrimental effects of whole-body shock and vibration often concentrate on the analysis of occupational exposures and the development of standards for limits of exposure for industrial health and safety (Paschold, 2008; Lundstrum, Holmlund & Lindberg, 1998; Vibration Injury Network, 2001;). Lately, however, an enlightened attitude as well as the

litigious nature of our modern society has pushed the growth of human factors engineering and ergonomics into the spotlight. The extreme sports industry, the military/space/aeronautic industry and the simple desire of humans to continually stretch their abilities to new levels at work and at play, has required a fundamental re-thinking of design processes for moving vehicles and devices. For this reason many studies have been completed attempting to draw connections between vibration exposure and more general health effects that go beyond the purely occupational (Goldman & Gierke, 1960; Mansfield, 2006).

International standards on whole-body vibration typically specify vibration exposure limits in terms of time, relating such limits to reduced comfort and fatigue-decreased proficiency. Griffin's comparison of various whole-body vibration standards has shown that while it is well understood that exposure to whole-body vibration is potentially injurious to human health, it is difficult to draw conclusions about the physical characteristics of shock and vibration or the mechanisms by which exposure to such excitations cause injury (1998).

Over the last 40 years, a variety of analytical and empirical methods have been developed to predict discomfort caused by vehicle vibration. Parsons and Griffin (1983) have reviewed a number of these, identifying the variables which have been studied. These include: vibration axis, vibration frequency, vibration level, multiple frequency vibration, random vibration, duration of vibration, impulsive vibration, multiple axis vibration, input point to the body and subject posture.

The basicentric coordinate system as described in ISO 2631-(1997), and shown in Figure 4. is commonly used in vibration measurement experiments

This study utilized a slightly different coordinate system in order to make
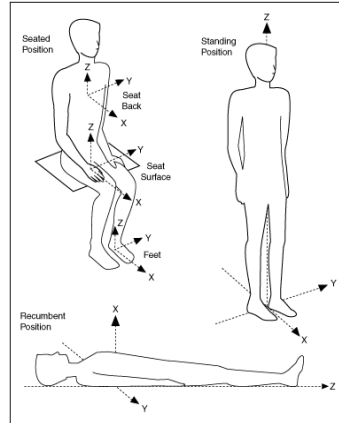
Figure 4. *Coordinate system for vibration measurement of ambulance occupants. ISO 2631-1, 1997*

correspondence with vibration measuring equipment and vehicle models less confusing and more convenient. This orientation of the coordinate axes is shown in Figure 5.
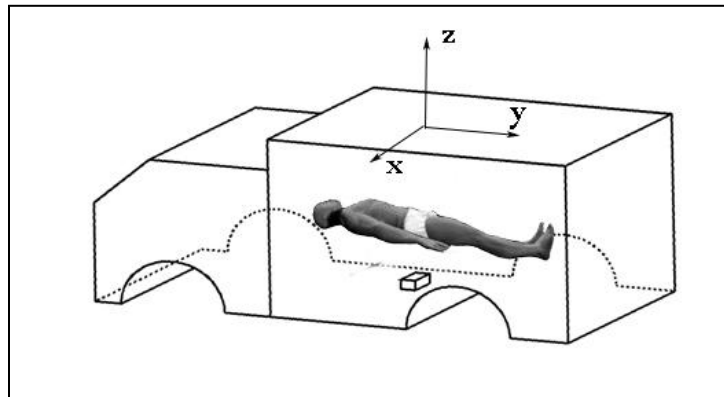
Figure 5. *Orientation of measurement axes for experimental tests*

This study included the modelling of an ambulance suspension system as analyzed by utilizing a standard quarter car model with a single degree of freedom in the vertical axis. For this reason, focus was placed on the vertical vibrations transmitted to the body of a supine ambulance patient through the supporting surfaces acting along the z-axis and to the body of a standing EMT through the ambulance floor also acting along the z-axis in order to better

correlate measured vibration with vehicle model, health effects and road excitations.

While it is recognized that longitudinal and transverse accelerations exist in the ambulance compartment, they are often due to quick starts, rapid decelerations, or sharp turns which can be significantly reduced by driver instruction and training.

The international vibration standards, especially ISO 2631, specify test methods which define specific points of vibration body entry and vibration source body contact points, most notably the seat and the ischial tuberosities with frequency weightings based on vibrations transmitted through the body along the spinal column. This is shown anatomically and schematically in Figure 6 (Goldman, et. al., 1960, p. 32).
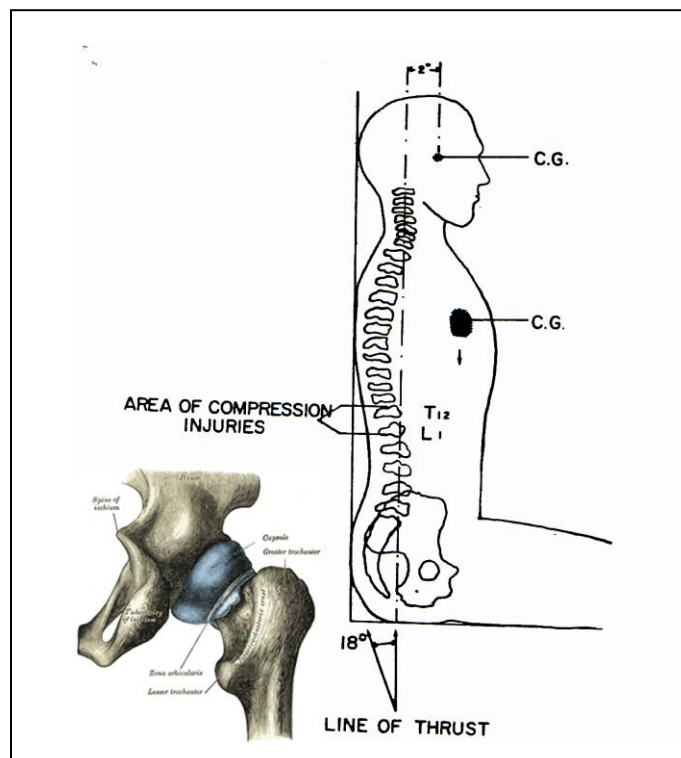
Figure 6. *Schematic and Anatomical representation of ischial tuberosity*

Tuberosity of the ischium. (2009, May 7). In *Wikipedia, The Free Encyclopedia*. Retrieved 13:48, May 7, 2009, from http://en.wikipedia.org/w/index.php?title=Tuberosity_of_the_ischium&oldid=288471336

Risks of occupational-related lower back disorders have long been associated with whole-body vibrations originating from the operation of motor vehicles (Waters, Rauche,

Genaidy & Rashed, 2007). Postures such as sitting, which enhance the transmission of vibration through the spine to the head should therefore be avoided (Yue, et. al., 2007, p. 124). This is why vibration standards apply primarily to seated individuals and puts more emphasis on musculoskeletal discomfort than on other, possibly more significant (for ambulance patients or standing EMTs), vibration-induced pathologies which arise from exposure to vibrations in other postures. Figure 7 graphically shows the various contact points of entry for vibration when subjects are in a recumbent position.
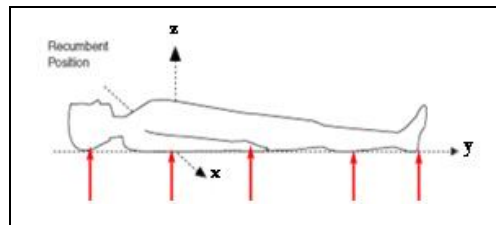
Figure 7. *Points of vibration entry in recumbent or supine subject*

The contact points normally associated with vibration entry to a standing individual can be seen in Figure 8.
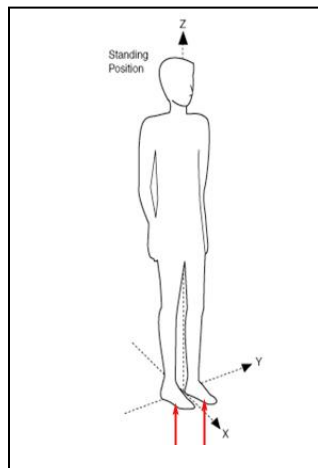
Figure 8. *Points of vibration entry in standing subject*

The effect of vibrations on standing or recumbent subjects is not well defined, despite a growing number of citations in the literature which address the effects of posture and body

resonance on whole-body vibration perception, health, comfort, and biomechanical response

(Matsumoto & Griffin, 1998; Miwa, 1982; Miwa, 1975; Miwa, 1969; Huang & Griffin, 2009;

Huang & Griffin, 2008; Huang & Griffin, 2008a). A general conclusion of these studies points to

the non-linear nature of biodynamic responses to vibrations (vibrational transmissibility,

apparent body mass and mechanical impedances) in supine, semi-supine and standing postures.

This nonlinearity is due at least in part to the thixotropic nature of the body's soft tissue through

which the vibrations are transmitted (Huang & Griffin, 2009, p. 451). What has been

documented clearly, however, is the variation of spinal loadings due to various postures. These

have been measured by Wilke, et. al. (Wilke, Neef, Caimi, Hoogland, & Claes, 1999) and are

summarized in Table 4, as adapted from Mansfield. (2006, p. 42).

Table 4. *Spinal loads for various postures as referenced by Mansfield*

Posture	% of load on spine
Recumbent	20 %
Sitting slouched	54%
Sitting relaxed w/o backrest	92%
Standing (relaxed)	100%
Sitting actively straightening back	110%
Sitting with maximum flexion	166%

Other considerations, such as muscle tension, which may be of significant concern in

coupling the vehicle vibrations to the human body, are also largely ignored in the standards.

Therefore, while there are international standards, and a significant amount of literature

on those elements of whole-body vibration which can lead to sound conclusions about vehicle

comfort, there are far fewer studies which directly link vehicle vibration studies to health or

injury risks (Vibration Injury Network, 2001). In attempting to draw a link between whole-body

vibration and its effects on human biological systems due to resonances, Paschold has reported

the natural frequencies of the human body and various parts from various studies (2008, p. 54).

This is shown in Table 5.

Table 5. *The natural frequencies of the human body and its various parts as summarized*
by Paschold

Study authors	Natural frequency (Hz)	body, part or organ
Randall, Matthews & Stiles, 1997	12	Whole body, standing
Brauer, 1994	4 -6	Whole body, seated
Brauer, 1994	3- 4	Whole body, supine
Wasserman, 1996	4- 8	Whole trunk, vertical
Kroemer and Grandjean, 1997	4*	Lumbar vertebrae
Brauer, 1994	20-30	Head, relative to body
Kroemer and Grandjean, 1997	5-30*	
SafetyLine Institute	20- 30	
Mansfield, 2006	20	
Kroemer and Grandjean, 1997	20- 70*	Eyes
SafetyLine Institute, 2007	20- 90	
Kroemer and Grandjean, 1997	5*	Shoulder girdle
Kroemer and Grandjean, 1997	3- 6*	Stomach
SafetyLine Institute	4- 5	
Kroemer and Grandjean, 1997	4- 6*	Heart
Kroemer and Grandjean, 1997	10-18*	bladder

*seated posture

In his *Handbook of Human Vibration*, Griffin (1990) separates human response to

vibration into three broad categories: activity interference, physiological effects including short

and long term occupational hazards and pathological effects. This study addressed the

physiological, occupational, and activity interference effects. The physiological effects bear

greatly on the short-term, acute effects of ambulance vibration on health-compromised patients

and the long-term occupational effects associated with EMT service. The activity interference

effects of vibration play a role in establishing the level of impairment EMTs experience due to

vehicle-induced shock and vibration.

3.4 Human physiological responses to vibration

Griffin organizes human physiological responses to vibration into seven systemic

categories: (1) cardiovascular, (2) respiratory, (3) endocrine and metabolic, (4) motor processes,

(5) sensory processes, (6) central nervous system, and (7) skeletal (1990, p. 174 – 186). All the

responses identified within the categories listed are assumed to result from the tissue strains

induced by the mechanical loads associated with the vibrational accelerations (Mansfield, 2006,

p. 73). Mansfield summarizes some salient physiological studies on human vibration response in

his *Literature review on low frequency vibration comfort*, from which selected citations are

reproduced below in Table 6.

Table 6. *Peer-reviewed studies dealing with general physiological responses to whole-body vibrations as reported by Mansfield*

Systemic Category	Study Authors	Findings
Cardiovascular (cv)	**Griffin, 1990, p174**	In the range of 2 – 20 Hz, moderate to high magnitudes of vertical vibration produce a cv response similar to moderate exercise including elevated heart and respiration rates as well as an increase in cardiac output, mean arterial blood pressure, pulmonary ventilation and oxygen uptake. All these effects increase with increasing vibration magnitude around major body resonant frequencies.
	Uchikune, 2002, p 203-206	A 4% increase in heart rate was measured when seated subjects in a high speed vehicle were exposed to vertical vibrations in the range of 1.6-2.3 Hz and magnitudes of .26 - .43 m s-2 r.m.s., a 4% increase in heart rate. Subjects were seated and vibration measurements were made at their heads.
	Yue & Mester, 2007a, p. 107	The authors of this study, associated with vibration assisted conditioning, found that human exposure to vibrations in the 40-50 Hz range resulted in an increase in the maximum shear stress at the walls of major coronary arteries and veins at even at local amplitudes as small as 50 μm. This vessel dilation phenomenon has potential benefits for athletes due to the

		increased blood flow capacity, but may present health risks for individuals with existing cardiovascular conditions.
Cardiovascular (cv) (cont'd)	**Yue & Mester, 2007b, p. 123**	• The results of this study suggest that whole body vibrations which produce local vibrations in excess of 40 μm lead to the dilations of small blood vessels, particularly arterioles of up to 30%. This dilation led to a significant observed reduction of total peripheral resistance – an important ability of the human body to prevent the blood pressure from getting too high during high levels of exertion. • The distribution of local vibrations is dependent on the vibration amplitude and body transmissibility. • Transmissibility depends on vibration frequency and location as well body posture and muscle state. • Vibrations are transmitted through both muscle and skeleton separately and in concert. Transmissibility through muscle tissue varies with muscle activation.
	Green, et. al., 2006	In simulated rides over rough road surfaces, subjects displayed prolonged mild hypocapnia (lower than normal levels of CO_2 in the blood stream brought on by tachypnea (elevated respiratory frequency) along with initial increases in heart rate and blood pressure. The authors feel this could be significant for individuals with impaired cardiovascular function who must travel in an ambulance over rough roads, or in evacuation from a combat or disaster zone.
	Clark, et. al., 1967	The authors found evidence of cardiovascular effects, including changes in mean arterial pressures and pulmonary edemas in response to short-term vibration in male adults subjected to whole-body, x-axis sinusoidal vibrations of 1g in frequencies ranging from 4 – 12 Hz for 3 minutes.
Respiratory	**Green, et. al. , 2008**	This study included simulated rides over rough road surfaces identical to the authors' 2006 study. Subjects displayed prolonged mild hypocapnia (lower than normal levels of CO_2 in the blood stream brought on by tachypnea (elevated respiratory frequency) which the authors feel could be significant for individuals with impaired respiratory control who must travel in an ambulance over rough roads, or in evacuation from a combat or disaster zone.
	Ernsting, 1961	The author reported hyperventilation and increased oxygen consumption on exposure to high frequency vibration.
	Dupuis, 1969	The author reported decreased respiration frequency, but increased respiration volume on exposure to vibrations in the 2-10 Hz range at a weighted magnitude of 1.25 m/sec^2.
	Sharp, et. al., 1975	This study found that constant-displacement sinusoidal vibration in the 2-10 Hz range resulted in increased oxygen uptake due to hyperventilation and muscle tension. The effects were greatest at the highest frequencies.
Endocrine and metabolic	**Litta-Modignani, et. al., 1964**	The authors reported small, but significant changes to steroid levels in blood and urine samples of human subjects exposed to short term whole-body vibrations. All readings were within normal levels.
	Pushkina, 1961	This study reported hypoglycemia (low blood sugar), hypocholesterinaemia (low blood cholesterol) and low blood

		levels of ascorbic acids after exposure to vibration.
Motor processes	**Roll & Roll, 1987**	The authors found that vibration applied to the muscles of the eye influenced proper orientation of the eye relative to posture
Motor processes (cont'd)	**Eklund, 1972**	The author found a variety of adverse effects to balance due to exposure to whole-body vibration
Sensory processes	**Moseley & Griffin, 1987**	This study points to a possible link between vibration and and biodynamic eye reflex movement. Evidence is also presented vibration effects on vestibular systems which can result in instability, disorientation of body, and disruptions of vision.
Central nervous system	**Ullsperger & Seidel, 1980**	The authors found that 4 Hz whole-body vibration produced significant decreases in EEG amplitudes which may have an effect on perception thresholds.
Skeletal	**Klingenstierna & Pope, 1987**	This study found a temporary reduction in body height of around 10-20mm upon exposure to whole body vibration
Other	**Roman, 1958**	The author found that whole-body vibration tests at 25 Hz and +/- 1g to +/-10g amplitude ratings with exposures of 3 to 15 minutes produced severe chest pain and gastrointestinal bleeding at the highest settings and exposure times.
	Loeckle, 1950	The author reported traces of blood in the urine of a man with a kidney stone at 30 Hz and +/- 9g accelerations
	Gratsianskaya, 1974	The results of this study indicates menstrual disorders, internal inflammation, and abnormal childbirth in women exposed to 40-55 Hz vibration.

3.5 Human activity interference problems associated with vibration

The performance of human tasks requires the complex coordination of a variety of perceptual, motor and control processes including closed-loop control with feedback. Whole-body vibration can severely impact the proper completion of any task which requires even fairly gross perception, motor, or control skills. This is of critical importance to EMS personnel who must sometimes perform delicate life saving procedures in the back of a moving ambulance.

3.5.1 Vision problems

Anyone who has tried to read a book or a computer display in a moving vehicle can appreciate the effect of vibration on vision. blurred vision effects due to vibration exposure result from movement of perceived images on the retina of the eye. This can be due to movement of the observer, movement of that which is being observed, or a combination of both. The

severity of vibrational effects on vision is dependent on the character and amplitude of the

vibrations transmitted to the head and to the viewing distance. Vibrations below approximately

2 Hz typically do not result in any major loss of visual acuity as the eye is able to accommodate

with its own pursuit eye movement function which helps the eye follow moving subjects. As the

vibration frequency increases, the ability of the human visual system to keep pace lessens. This

starts at around 10 Hz and is very pronounced by 20 Hz. Above 20 Hz there may be resonances

present in the eye muscles which lead to even greater deficiencies. Of note, is that at frequencies

below 3 Hz, vertical vibrations of the visual target causes a greater amount of visual loss than

movement of the observer (Griffin, 1990, p168). Shown in Figure 9, is the amplitude and

frequency of vibrations below which visual acuity will be unaffected by vibration.
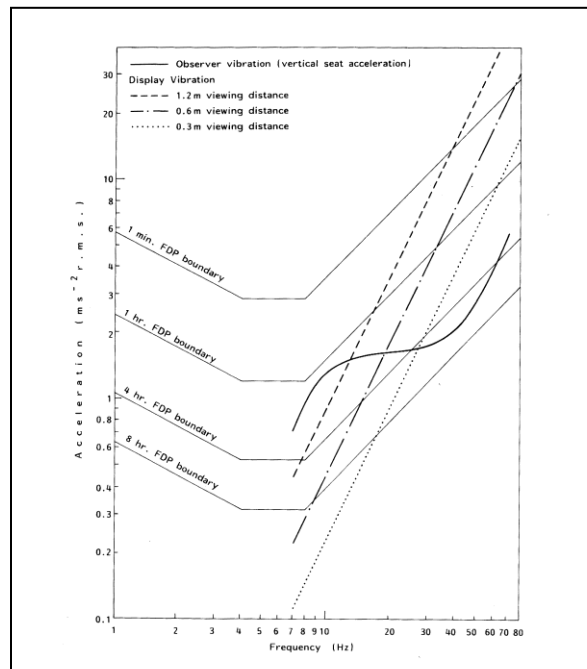
Figure 9. *Visual acuity limits for various whole-body vibration regimes from Griffin*

Figure 9. is reproduced from Griffin's *Handbook of Human Vibration* and is based on the

mean results of data from studies performed on seated individuals. Values can be determined for

various viewing distances and vibration exposures based on fatigue-decreased proficiencies

(1990, p. 130).

3.5.2 *Control and motor skill problems*

Significant errors due to whole-body vibrations can be introduced to movement and control tasks involving the fine motor movements of hands and arms. This is an important effect, since the degree of vibration-induced disturbance can become the deciding factor in the ultimate success or failure of a task. As categorized by Griffin, there are three sources of error associated with vibration-affected manual tasks: (1) vibration-correlated (or breakthrough) error, (2) input-correlated error, and (3) remnant (1990, p. 145).

Vibration-correlated error is due primarily to vibrations which are transmitted through the body to the arm and hand or to an object which may be controlled by the subject. Vibrations transmitted through a seated human body tend to reach a maximum effect at about 4-5 Hz due to the vibrational transmissibility of the body. Figure 10, reproduced from Griffin, shows the transmission of vibrations to a subject's outstretched hand (1990, p. 151). As shown in Figure 9, random vertical vibrations of a rigid seat produced the greatest amount of hand motion in the x, and z axes in the 2-6 Hz frequency range and at 4-8 Hz in the y-axis. Curves were included for an empty hand held out at 150 mm, a hand holding a 2.2 kg weight at 150 mm and an empty hand at 680 mm.

The second source of error described by Griffin is input-correlated error. In a target tracking task, such as positioning an IV needle in a particular spot on a moving patient's arm, this error is simply due to the normal limitations of the human visual and motor system to perform such a task. Successfully completing the task is dependent on the "skill" of the operator, and the speed of the target being tracked.

This error is attributable to neuromuscular lag time, tracking strategy, or a host of other

variables. Even though this error will be present in the absence of vibration, if any of the causal variables can be affected by vibration, it will play a role in this component of the total error as well (1990, p. 146).

The third and final component of task error is remnant. Literally, this is error which is leftover once input and vibration-correlated error have been accounted for. It is attributable to the inherent non-linear component of human, biological control systems which enter into any complex type of visual-motor task and degrades performance. A simple example is the natural tendency for a subject to slow down the execution of a task in order to improve accuracy. This source of error is very difficult to predict (Griffin, 1990, p. 146).
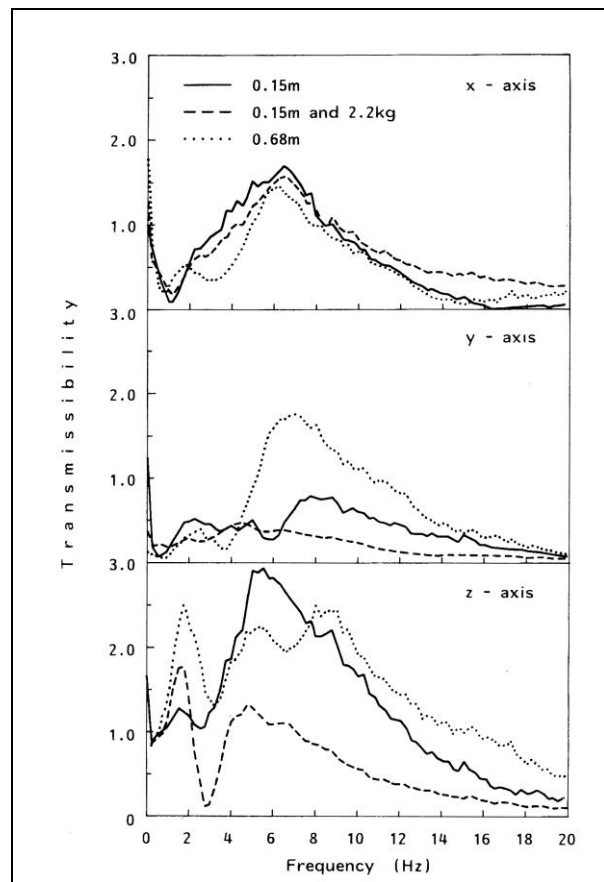
Figure 10. *Transmissibility to the hand of vertical vibrations applied to a seated subject as measured by Griffin*

Summed together, vibration-correlated (or breakthrough) error, input-correlated error, and remnant result in the total positioning error. The total error may be expressed as an r.m.s. tracking error in length dimensions. For instance, for an EMT in a moving ambulance trying to start an IV in a patient's arm, the distance between the EMT's target and where the needle actually enters the patient's arm may be considered the total error, and may be measured in mm. This kind of task can be referred to as a zero-order, or displacement controlled task, where first and second order tasks would refer to velocity and acceleration controlled operations, respectively. Higher order tasks tend to be less affected by vibration, but are, in general, more difficult to control (Griffin, 1990, p. 148).

Total error in visual motor tasks reach their peak value at 4-8 Hz, the frequency range which causes peak values of vibration-correlated error. Vibration-correlated and total error both increase with increasing acceleration amplitude. This is shown in Figure 11, reproduced from Griffin (1990, p. 153). The data for this graph shows r.m.s tracking error for a total error in a
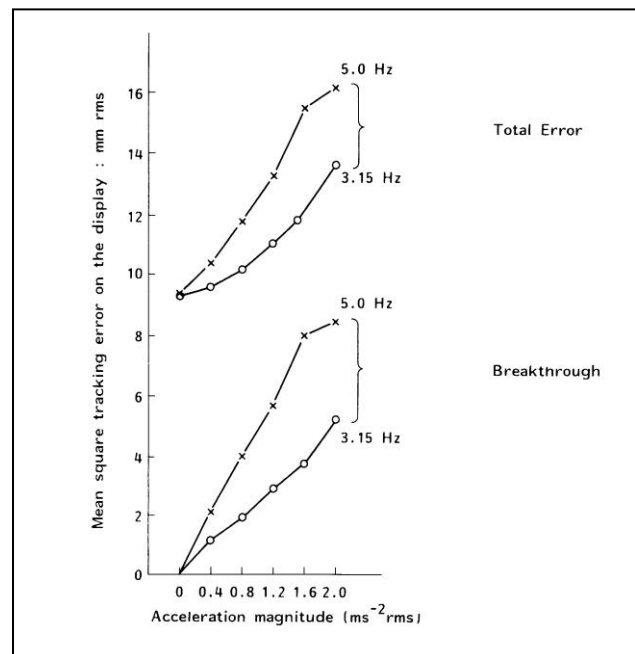
Figure 11. *Total and breakout error in visual motor tasks as a function of vibration amplitude as reported by Griffin*

tracking task performed by seated individuals subjected to sinusoidal vertical vibrations at 3.15 and 5.0 Hz. Vibration-correlated (breakthrough) and total error are shown. As a visual example of visual motor skill task degradation caused by whole-body vibration, Figure 12 illustrates a sample of handwriting legibility tests conducted by Griffin on seated individuals subjected to whole-body vibration and asked to write on a hand-held clipboard. Note the degraded performance at the higher amplitudes and at frequencies in the neighborhood of 4 Hz (1990, p. 156). Higher frequency vibrations can also cause degraded task performance at 20 Hz and above due to neuromuscular mechanisms. This is seldom an issue unless the vibration amplitude is quite high (as in a helicopter), since the biodynamics of the human body are capable of attenuating these higher frequencies (Ribot, Roll & Gauthier, 1986).
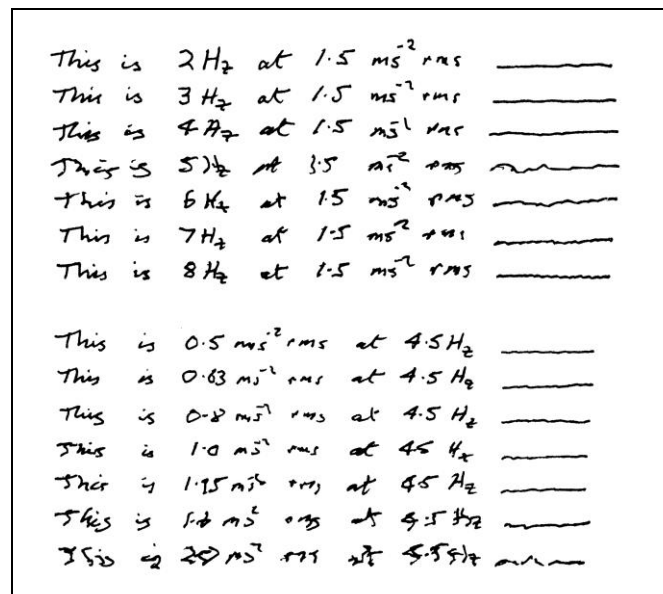
Figure 12. *Handwriting samples of individuals subjected to whole-body vibrations as presented by Griffin*

3.5.3 Speech, cognitive and combined effects problems

Whole body vibrations in the range of 5 to 20 Hz at moderate to high amplitude levels may cause impaired or difficult to understand speech. This is due to the vibration's ability to modulate airflow through the larynx, cause general increases in muscle tension and produce

direct movements of the lower jaw. The amount of speech impairment is a function of vibration frequency, amplitude, and direction, as well as body posture and the vocabulary employed (Griffin, 1990, p. 158). Cognitive effects, such as loss of simple recall or difficulty with routine central processing tasks (i.e. mental arithmetic) due to vibration exposure are generally mild and most often are attributable to the secondary effects of vibration-induced fatigue or increased task difficulty. Of critical concern to this study are combined stress effects which maximize the performance degradation properties of vibration alone. These stress effects include the combination of vibration with heat, noise, acceleration, fear, excitement, and many other environmental stressors which are common to the emergency medical profession. According to Griffin, these additional effects can have: (1) no effect, (2) an additive effect, (3) a synergistic effect which is greater than the sum of its parts and (4) an antagonistic effect which is less in total than any of the single individual components (1990, p. 164).

3.6 Summary of human effects of whole-body vibrations

Whole-body vibrations elicit a variety of physiological and task performance reduction responses and stress reactions in the human body. While direct physical evidence of the precise mechanisms by which these reactions occur is not well understood, some general observations about the nature of whole-body vibration can be made:

1. Vibration effects are both amplitude and frequency dependent, as well as dependent on vibration direction and duration. Therefore, the relative discomfort, or hazard associated with a particular vibration amplitude level must be correlated to vibration frequency, direction and duration. In general, a vibration of 10 HZ is

deemed uncomfortable by most normal adults at 5 m/sec^2 after a 16 min.

exposure, at 4 m s^{-2} after 25 min, at 3 m/sec^2 after 60 min. and so on. Tables of

various exposure limits can be found in international vibration tolerance standards

such as those published by the ISO and british Standard Organization.

2. The human body is most sensitive to vibrations in the 1-80 Hz range, but due to

   the natural frequencies of various anatomical structures and internal organs, the

   various body systems and associated physiological effects are frequency

   dependent. This is summarized in Table 7. In general, vibrations around .3 Hz

   excite motion sickness and vibrations in 4 to 10 Hz range excite body resonances.

Table 7. *Summary of resonant frequencies of body systems and their resulting
physiological effects, adapted and expanded from Bellieni, et. al., 2004, p. 210*

Resonant Frequency (Hz)	Body part, organ, or system	Physiological effect
.3	Inner ear	Motion sickness
1 – 4	Respiratory	Hyperventilation
2 – 8	Motor skills	Difficulty performing simple target tracking tasks, handwriting etc.
4 – 6	brain (cognition)	Fatigue, loss of concentration
4 – 8	Inner ear, heart	balance and sway problems
5 – 20	Speech	Difficulty speaking clearly
20 – 30	Spine	back disorders &, pain
10 – 20+	Vision	Diff. tracking objects, reading, blur

3. Vibration effects are dependent on biodynamic considerations such as the

   transmissibility of various anatomical structures, body postures, and point of

   vibration application/entry to the body.

4. Vibrations in the frequency range over 20-30 Hz typically may have a local effect

   on contacting tissues, but do not penetrate into the body due to the vibration

   attenuating features of internal body structures at higher frequencies.

3.7 Vibration effects on ambulance patient safety and comfort

In a compelling correspondence to the August 12, 1967 issue of the british Medical Journal, C. H. Cullen et. al. of Victoria Memorial Jewish Hospital of Manchester, UK recount an all-too-familiar description of the ambulance transport of an accident victim with multiple injuries. The ambulance ride of 47 minutes over good roads at an average rate of speed of 20 – 30 m.p.h., resulted, at some points, in vertical patient displacements of up to 6 in. The patient, who had previously been stabilized from cardiac arrest and secondary shock, relapsed into a shock condition during the transport. His blood pressure dropped and his skin grew clammy and cold. The patient recovered consciousness upon his arrival to the hospital, but later succumbed to his injuries. The authors commented, " It is impossible to exonerate the ambulance ride from being an important secondary factor in contributing to his death." The authors continue, "It (the patient displacement) was clearly due to the design of the ambulance suspension, which has not kept pace with that of private cars." (Cullen, Douglas & Danzinger, 1967, p. 438). Sadly, ambulance suspensions have not changed significantly in the forty years since this letter was written.

Many patients transported in ambulances are health compromised. Study of the general movement of critically ill patients within hospitals has shown that negative patient outcomes, including death, may result if adequate preparations are ignored or en-route treatment is not maintained (Waddell, 1975). In extending the research to patients being transported in ambulances, Waddell, Scott, Lees & Ledingham found a variety of cardio/respiratory effects associated with ambulance transportation due to the direct effects of transportation stimuli and the indirect effects of the inability of EMTs to provide adequate treatment due to vehicle motion

(Waddell, Scott, Lees & Ledingham, 1975). Waddell's observations are not surprising, and not unique. An ambulance is a motor vehicle, and, as has been shown, the occupants of all motor vehicles which traverse even the smoothest road surfaces, are exposed to a variety of whole-body vibrations. It is logical to assume that ambulance occupants would experience similar physiological effects of whole body vibrations as described in Table 6. In a study comparing the safety of air versus ground transport for critical cardiac patients, Schneider, et. al., found an increase of 41% in untoward events in air transport and 7% in ground transportation. The authors speculated that the significant difference in the number of events seen could be due to "physical stress, including noise, vibration and G-forces" (1988, p. 452). A variety of similar studies have been conducted on the characterization and effects of ambulance vibrations on the patients being transported within the diagnostic compartment. The effects studies are primarily epidemiological in nature, since the mechanisms which link vibratory stimuli to physiological response are not well understood. Nonetheless, the quantification of the accelerations and forces associated with ambulance transport in these characterization studies is an important component of better understanding the potential risks of such transport. Some selected effects and quantification studies are shown in Table 8. In order to provide a point of reference in interpreting the data in Table 8, it is useful to recall that the acceleration due to gravity on Earth, or 1g, is 9.8 m/sec^2, and the maximum acceleration of a Ferrari F50 moving from 0 to 100 km/hr is 7.5 m/sec^2.

Table 8. *Typical results of ambulance vibration studies*

Study Authors	Vibe. Freq. (Hz)	Peak accel. (m/sec^2)	R.M.S. accel. (m/sec^2)	Road profile description	Measurement configuration	Physiological effects
Sherwood, et. al., 1994	--	15	--	City & highway	Triaxial vector sum measurement on mannequin forehead, vehicle floor and base of	Clinical significance requires further study but vibrations exceed ISO guidelines.

					isolette	
Bellieni, et. al., 2004	5	11.8	1.3	City & highway	Vertical axis in isolette, on passenger seats, & on driver's seat	Clinical significance requires further study but vibrations exceed ISO guidelines.
Shenai, et. al., 1981	3 – 18	5.0 – 13.0	2.2 – 6.0	Highway @ 48 mph	Vertical axis on supine infant head, abdomen, thigh	Clinical significance requires further study but vibrations exceed ISO guidelines.
Silbergleit, et. al., 1991	1 – 15	3.1 – 8.1	.7 – 1.9	bumpy road, city road and highway	Triaxial vector sum measurement on standard backboard at head position	Clinical significance requires further study but vibrations exceed ISO guidelines.
Mcnab, et. al., 1995	< 50	0 – 1.7	.0 - .7	bumpy road, city road and highway	Triaxial vector sum measurement from acoustical measurements	Clinical significance requires further study but vibrations exceed ISO guidelines.
Pichard, et. al., 1970	1	.16 - .85	--	City & highway	Z-axis, head-to-toe of recumbent patient	30% of patients suffered a variety of untoward events including cardiac arrest, arrhythmias, nausea, and respiratory distress
Weber, et. al., 2009	--	--	--	City & highway, 15 min drive, Vienna, Austria	--	A significant rise in plasma catecholamine levels (indication of stress) was noted and attributed at least in part to the ambulance transport
Schneider, et. al., 1988	--	--	--	Unrecorded surface < 50 mi radius	--	• All patients studied were diagnosed with either myocardial infarction or unstable angina prior to transport. • A total of 7% of patients experienced a variety of untoward events including: arrhythmias, chest pain, hypotension, bradycardia, seizures, cardiac arrest, nausea, vomiting, equipment failure (ambulance) or IV line loss during transport
Witzel, 1999	--	--	--	Paved road	--	• Heart rate increased

				– 72 km/ hr for 13 km w/ siren		30% over slow ride within first 8 min. and remained high throughout trip • Mean arterial pressures of 122 – 130 mm Hg. • Cortisol blood level increased 60% at peak
				Paved road – 40 km/ hr for 13 km w/o siren	--	• Heart rate 30% lower than fast ride peaked within 2 minutes and returned to normal prior to end of trip • Mean arterial pressure 108 mm Hg. • Cortisol blood level increased 30% at peak

The studies described in Table 8 substantially agree on several points with regard to the health effects of vibration on ambulance patients:

1. A statistically significant increase in untoward events and increased stress can occur in critically ill patients during ground ambulance transport.

2. Direct physiological effects of whole-body vibrations in ambulances should be the subject of further study.

3. Indirect physiological effects of whole-body vibrations in ambulances due to the difficulty of EMTs maintaining adequate care in a moving vehicle are a cause for concern.

4. The whole-body, vertical axis vibrations experienced by patients during ambulance transport can be roughly be characterized as low frequency (0 – 20 Hz), with average r.m.s. amplitudes of 2 – 6 m/sec^2 in the vertical axis.

5. The vibrational loads experienced in ambulance patient compartments often exceed

the vertical vibration exposure limits for normal, healthy adults so it is likely that the

physiological effects associated with such vibration levels could adversely affect

neonates, pediatric patients and health compromised adults travelling in ambulances.

6. A smooth ambulance ride could improve patient outcomes, especially for critically ill
   or pediatric patients.

7. Vibration absorbing mattresses and/or stretchers as well as other vibration attenuating
   solutions should be sought to shield ambulance patients from road vibrations which
   cannot be absorbed by the vehicle's native suspension system.

Graphs of power spectral density and root mean square acceleration data from the Shenai,

et. al. study are typical for ambulance travel at 48 mph on a major US interstate highway.

Vertical vibration measurements were taken with an accelerometer mounted on the lower

abdominal wall on infant who was placed on a 2.5 cm thick gel mattress within a standard

transport incubator. The typical power spectral density of the vibrations encountered are shown

in Figure 13 (1981, p. 56).
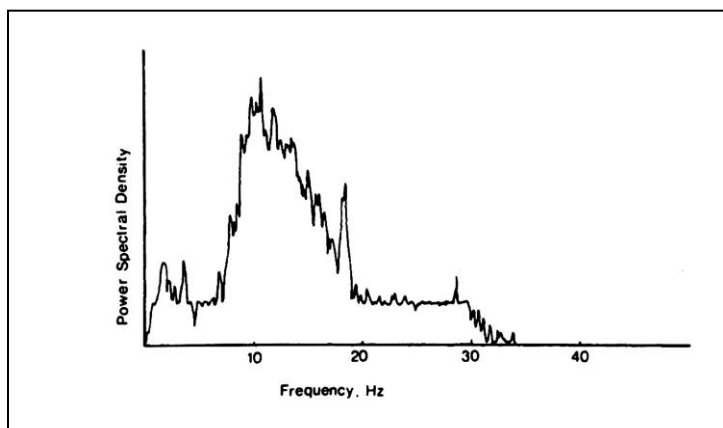
Figure 13. *Power spectral density of vertical acceleration in ambulance transport as
tested by Shenai, et. al. (1981, p56)*

The r.m.s values of vertical accelerations recorded in the same study are shown in Figure 14 (1981, p. 56).
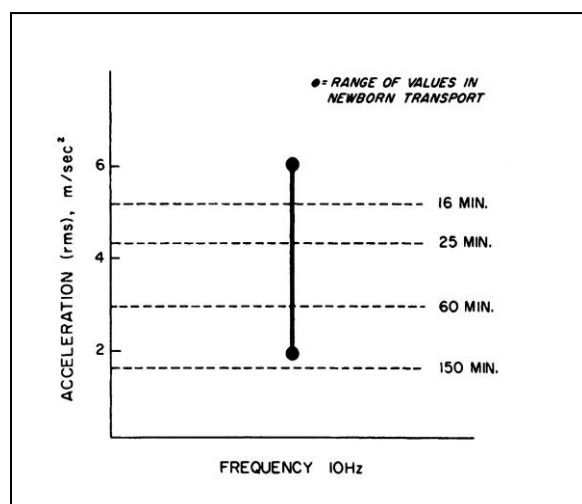
Figure 14. *Vertical r.m.s. ambulance acceleration values recorded at 10 Hz. Dotted lines indicate vibration exposure limits for normal, healthy adults. Shenai, et. al. (1981, p. 56)*

3.8 Vibration effects on ambulance crews and patient care

It has long been suspected that long-term exposures to whole-body vibrations carries with it a significant health risk. Waters, Rausche, Genaidy & Rashed (2007) have noted studies which link vehicular whole-body vibration and shock to a variety of conditions in tractor drivers, including low back disorders, premature degenerative deformations of the thoracic and lumbar spinal vertebrae, an increased risk of spinal abnormalities after 5 years of exposure, an increased prevalence of back pain in workers exposed to whole-body vibration above a threshold level, and progressive spine degeneration. Exposures were measured between $1 - 2$ m/sec^2 at $2 - 20$ Hz for various lengths of time. (p. 386). EMTs working in ambulances are exposed to similar vibrational loadings. While no specific studies exist linking ambulance vibrations to back pain in the EMT profession, it is safe to assume that their physiological response to vibration would be similar to that of individuals so exposed.

The dangers associated with travelling in the patient compartment of an ambulance

unrestrained have already been discussed (Maguire, et. al., 2002) as well as possible restraint

measures for EMTs (Johnson, et. al., 2006). One such restraint system was patented in the United

States by Clarkson under US Patent No. 4563023 (1983), and is shown in Figure 15. These kinds
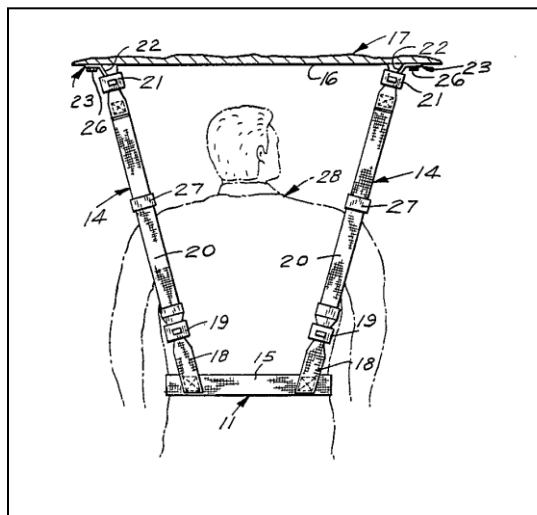
Figure 15. *US Patent No. 4,563,023 by Clarkson*

of devices are designed to limit injury as a result of trauma in the case where an EMT may be

thrown about the cabin. Based on the tasks required of EMTs, and the restrictions imposed on

their motion by the restraint, the practicality of such a device is dubious. Also, such a restraint

does not alleviate any of the hazards associated with low amplitude vibrations.

In *An Introduction to Human Factors Engineering*, Wickens, Lee, Liu, & Decker (2004),

identify the major effects on physical performance due to full-body vibrations. These include the

disruption of any task which involves eye-hand coordination, or visual requirements due to the

apparent blurring of the object to be perceived because of its vibratory motion (pp. 325-27). The

impact of this aspect of shock and vibration on the tasks normally conducted in ambulances is

intuitively obvious. What is less obvious is the role which acoustical noise (as opposed to

mechanical vibration) plays in disrupting the ability of EMTs to provide optimum care to the

critically ill ambulance patient. Acoustical noise occurs over a broad range of frequencies:

humans are capable of perceiving acoustical noise in the range of 60 to 60,000 Hz as opposed to 0 to 80 Hz for mechanical vibration. Acoustical noise is most often present at a much lower amplitude than mechanical vibration.

Typical unweighted ambulance noise levels, as recorded by Macnab, Yuenquan, Gagnon, Dora & Lazlo (1995), ranged from 80 db to 110 db, with an average of 100 db (p. 216). The sound level at which sleep disturbance normally occurs is 75 db. At 100 db, permanent hearing loss is possible after a continuous exposure of over two hours. In an ambulance environment there are certain tasks which EMTs are required to perform which require the unimpeded use of hearing. It is therefore reasonable to assume that any task which requires auditory input from an EMT, such as the assessment of breath sounds or heart sounds, can be adversely affected.

Prasad, Brown, Ausband, Cooper-Spruill, Carroll and Whitely (1994) found statistically significant differences between quiet and moving blood pressure measurements. They concluded that determining an accurate blood pressure reading would be hampered by the sound and vibration of a moving ambulance.

Brown, Gough, Bryan-Berg, and Hunt (1996) found a significant difference in the ability of medical personnel to assess breath sounds between a quiet room and a moving ambulance. They concluded that the environment of a moving ambulance is not conducive to the accurate assessment of breath sounds.

Table 9 provides a list of medical procedures routinely performed in ambulances by EMTs and paramedics which could be enhanced by reducing the vibration levels in the vehicle.

Table 9. *Medical procedures routinely performed in an ambulance*

Medical procedures commonly performed in an ambulance which are difficult due to vibration
EKG/ECG measurement
blood pressure measurement
IV starts
Pushing medications
Lung & heart sound assessment
ETT / advanced airways
Pulse oximetry measurement
D-sticks
$ETCO_2$
Inserting nasal canulas

Moving ambulance scope of service. (2009). Retrieved July 19, 2009 from EMTLife.com web forum site: http://www.emtlife.com/showthread.php?s=f5d37720248c66Dd28c2dd73ca13dD55&p=153247#post153247

This list was generated with input from EMS professionals on the EMT Life website ("Moving ambulance scope of service," July 19, 2009). The general consensus of the group was that all these procedures could be enhanced, made safer, more effective and more accurate if the noise, vibration and shock levels commonly encountered in an ambulance could be reduced ("Moving ambulance scope of service," 2009). A similar list of procedures and a need for the reduction of road-induced vibrations in ambulances was expressed to the author by EMS personnel and emergency room directors at a recent presentation given to the WPI/University of Massachusetts Emergency TransCare Medical Services (ETMS) Ambulance Team at the UMASS Medical Center in Worcester, MA on July 23, 2009 (Cotnoir & Fofana, 2009).

It is clear that the safety of both ambulance passengers and their attending medical technicians, as well as the standard of care received by the patients, could be enhanced by the
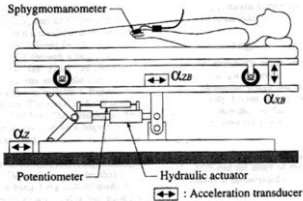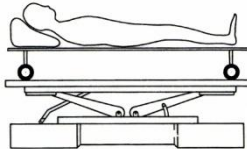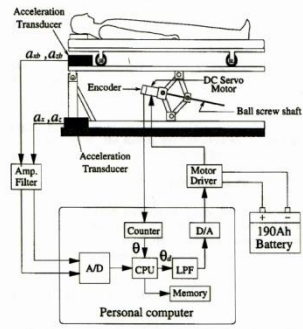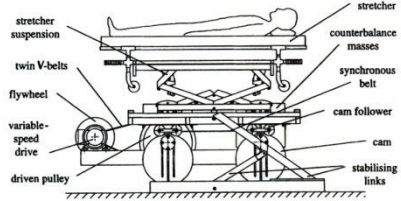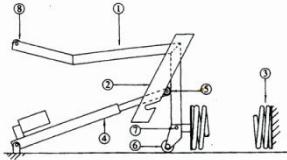
attenuation or reduction of shocks, vibrations and noise experienced inside an ambulance during emergency transport.

3.9 Current design solutions

The range of engineered solutions to reduce the shock and vibration of ambulance transport is rather meager. The design solutions include enhanced restraint systems and ergonomic design of passenger compartments (Gilad & Bryan, 2007; Best, Zivkovic, & Ryan, 1993; KKK-A-1822F, 2007; ME/48, 1999) which can mitigate injuries in a crash or jerk situation where blunt trauma against a non-compliant surface is the main concern. However, these solutions are ineffective at reducing or eliminating potentially harmful shocks or vibrations.

A variety of vibration aDsorbing stretchers and stretcher suspension systems have also been developed, as summarized in Table 10. While these can be effective at minimizing vibrations, they all suffer from similar disadvantages: high cost, high maintenance, high bulk and weight, high power consumption, and a non-universal fit.

Table 10. *Selected vibration absorbing stretchers and stretcher suspension systems for ambulances*

Study authors	Stretcher/suspension design	
Sagawa, et. al., 1997 (manually control)	This design succeeded in using pitch angle of the stretcher to help stabilize the patient's blood pressure. Success at controlling vibration was inconclusive.	
Snook & Pacifico, 1976	Double electrically controlled electric motors in concert with compression springs produced reductions of up to 66% in peak acceleration values over a normal stretcher in the 3 to 10 Hz range	
Sagawa & Inooka, 2002 (actively controlled)	The authors claim this servo-controlled electric design maintains the patient at .45 m/sec^2 +/- 1.32 m/sec^2 within a frequency range of $0 - 70$ HZ	
Henderson & Raine, 1998	In the $0 - 12$ Hz range, this servo-controlled hydraulic design reduced r.m.s. accelerations from 64% to 85% depending on road surface.	
Leyshon & Stammers, 1986	With a mattress in place, this design attenuates ambulance floor vibrations by 7 db @ 1.5 Hz and 9 db @ 4 Hz	
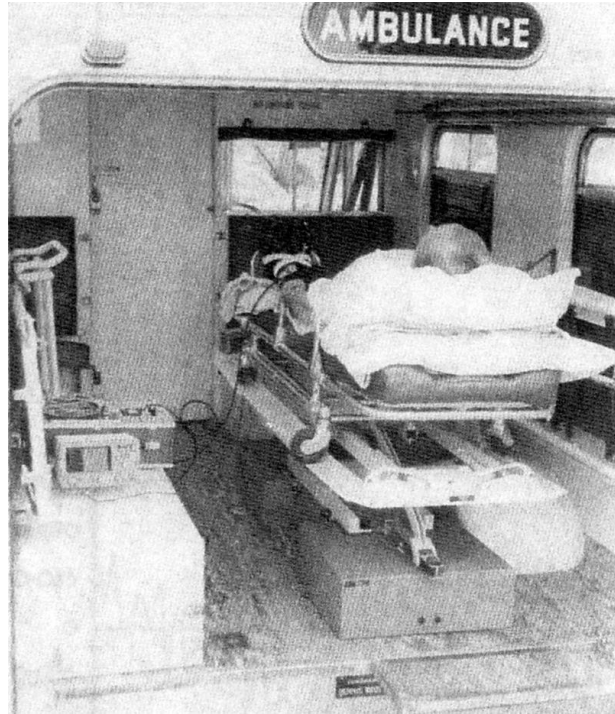
Figure 16. *Snook floating stretcher installed in an ambulance. Snook & Pacifico, 1976, p. 14.*

A typical, in-ambulance set-up for a stretcher of this type is shown in Figure 16. The bulk of the unit and extreme height off the ground highlight a couple of the disadvantages of this family of solutions.

Other solutions include modifications to the native vehicle suspension. This was attempted with the use of actively controlled electrorheological (ER) fluid dampers and tested by driving an instrumented ambulance over speed bumps (Murata & Maemori, 1999). The authors reported that the method was successful in reducing the maximum acceleration the patient was exposed to by 34% when compared to the performance of standard shock absorbers. Murata & Maemori also concluded that the system needed more improvement since the accelerations and displacements measured at the patient's head and center of gravity were greater than the displacements and accelerations recorded at the vehicle's center of gravity (p. 846). It is

undefined in the paper how the optimized ER dampers affected the ground clearance and other dimensional and operating characteristics of the ambulance studied (1999).

Stretcher gel and foam mattresses have been used frequently and do provide some remediation of vibration and shock, but no peer-reviewed studies with significant quantifiable data of their attenuation properties were found.

A vibration absorbing stretcher support was patented in the United States in by Hillberry and Mortimore under US Patent No. 6890137 (2005), and is shown in Figure 17. Vibration suppression pads are mounted below the floor of the ambulance and receive each of the wheels of the stretcher. The patent disclosure claims the design will reduced patient trauma, but there does not seem to be any accommodation for locking the wheels into the pads, so presumably any vertical acceleration of high enough magnitude to overcome the weight of the stretcher and patient would cause the stretcher to lose contact with the floor, thereby nullifying the effect of the device. No research on road tests or availability of the device was found.
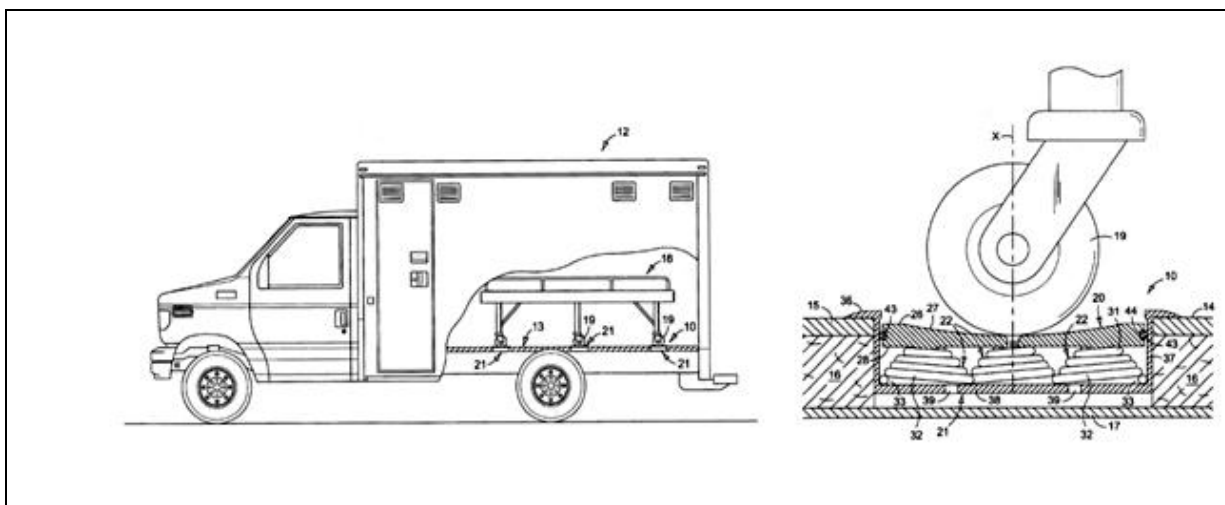
Figure 17. *US Patent No. 6,890,137 by Hillberry & Mortimore*

4.0 Methodology

The goal of this dissertation was to:

1. Experimentally determine the vibrational amplitude, frequency and energy of a typical ambulance ride, and correlate those vibrational characteristics to human physical impacts on ambulance passengers and EMT crews.

2. Use the vibrational parameters to characterize road forcing functions to simulate typical ambulance travel over the undulating surface of a variety of common road surfaces at a broad range of frequencies to verify and validate the computational models of a variety of vibration attenuation solutions.

3. Model a force field domain control system (FFDCS) embodied in a force plate design capable of working in tandem with a standard ambulance suspension system to attenuate the most harmful vibrations encountered by such a vehicle in normal service.

4.1 Experimental method

Vibration data was acquired on four, typical US-manufactured Type I or Type III ambulances from three New England emergency medical services which were driven over four different road surface types at three constant speed settings.

4.1.1 Vehicle selection

This study included the selection and acquisition of a group of ambulance vehicles for test. For the purpose of this study, the most common ambulance models were Type I and Type III configurations built on the most common US manufactured chasses and suspension systems found in local urban and rural emergency medical services. These included vehicles built on Ford E-450, F-450, F550 and Chevrolet C-4500 chasses with and without air-ride suspensions.

Two new vehicles (2008, 2009) as well as two older (2001, 2005) models were selected.

All ambulances selected were built to KKK-A-1822 star-of-life standards. A variety of

chassis and body manufacturers were represented in the selection of test vehicles for this study as

shown in Table 11.

Table 11. *Test vehicle descriptions*

Amb #	Date of test (2009)	EMS	body mfg.	Mfg. Yr. Chassis	Suspension	Type	Class	GVWR (lbs)	Tires
1	12/3	UMASS	Horton	2005 Ford F450	Standard leaf spring & shock absorber	I	1	16000	225/70 R19.5
2	12/6	Putnam, CT EMS	Lifeline	2001 Ford E450	Standard leaf spring & shock absorber	III	1	14050	225/75 R16
3	12/7	UMASS	Braun	2008 Chevy C4400	Standard leaf spring & shock absorber	I	1	16500	225/70 R19.5
4	12/13	Woodstock, C T EMS	Lifeline	2009 Ford F550	Air ride	III	5	17950	225/70 R19.5

Photographs of each vehicle tested are shown in Figure 18 (a-d) below. Detailed

specifications for the ambulances can found in Appendix A of this report.
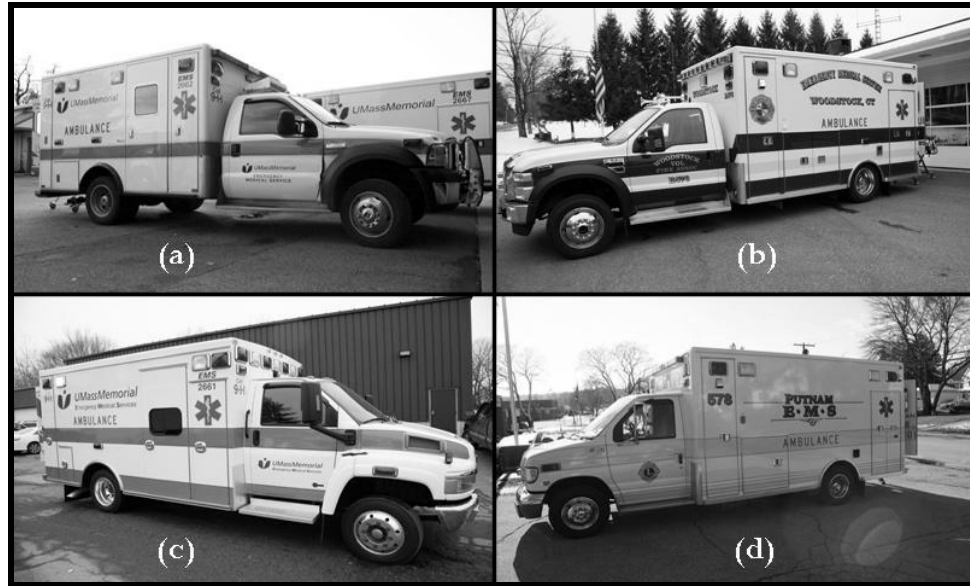
Figure 18 (a-d). *Vehicles on test in this study included (a) 2005 F-450 Type I, (b) 2009 F-550 Type I, (c) 2009 Chevrolet C-4400 Type III, and, (d) 2001 Ford E-450 Type III*

4.1.2 Road surface selection and qualitative characterization

Each instrumented ambulance test was carried out on four different common New England road surfaces, characterized as highway, secondary, city and unpaved. The road surfaces studied in this study lead to a broad spectrum of vibrational excitations. Road surfaces were visually classified as shown in Figures 19(a-d).

Figure 19. *Images of local road surface characterization including (a) unpaved roads, (b) paved secondary roads, (c) paved city streets and, (d) paved multi-lane highways*

In addition to road surface excitations associated with travel over a smooth road, random shocks due to various chance surface irregularities also occur. Some of these irregularities include potholes, frost heaves, speed bumps and severely worn or crowned pavement. All of the road surfaces tested included some or all of these random artifacts. These are shown in Figures 20 (a-d).

Road excitation data was categorized by both vehicle velocity and road surface characterization. City and rural road construction and maintenance projects are carried out under the purview of local municipalities, while pavement design and structural resurfacing projects of all controlled access highways adhere to state project development and design specifications and the American Association of State Highway Transportation Officials (AASHTO) design guidelines.
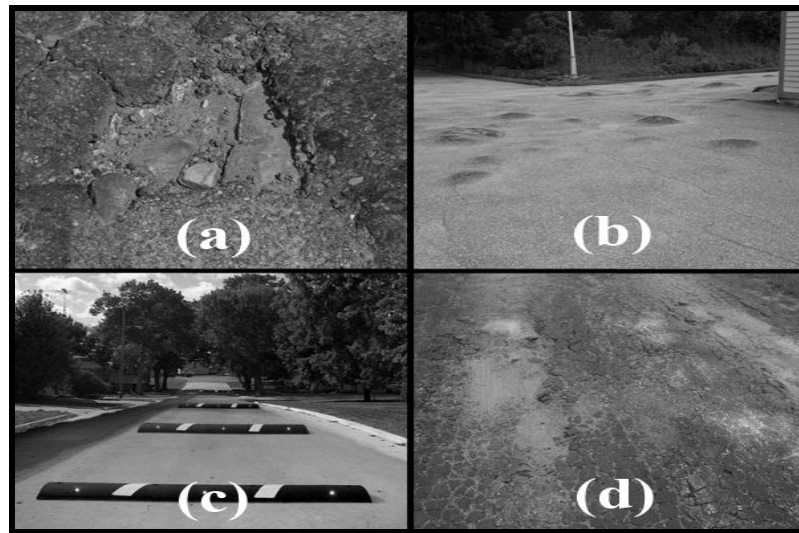
Figure 20. *Images of typical road perturbations including (a) potholes, (b) frost heaves, (c) speed bumps, and (d) severely crowned and worn pavement.*

Road construction and characterization data is shown in Table 12 (Massachusetts Highway Authority, 2006) .

Table 12. *Road type surface and vehicle velocity characterization.*

Characteristics	Unpaved Roads	Rural Paved roads	Paved city streets and parking lots	Paved Highways
Material / Construction	Dirt, stone, gravel or sand with variable methods of construction	New: 76 – 102 mm (3 - 4 in) bituminous concrete or hot-mix asphalt (HMA) on 305 mm (12 in) gravel base Old: up to 127 mm (5 in.) asphalt paving on an existing base	New: 76 – 102 mm (3 – 4 in.) bituminous concrete or hot-mix asphalt (HMA) on 305 mm (12 in.) gravel base Old: up to 127 mm (5 in.) asphalt paving on an existing concrete or cobblestone base	Flexible pavement: 3-4 courses of hot mix asphalt (HMA) placed over a granular sub-base as shown in Figures 3(a-b) Rigid pavement: plain and jointed or continuously reinforced layer of Portland cement concrete over a granular sub-base Composite pavement: 1 or more courses of hotmix asphalt (HMA) over a Portland cement base
Dimensions m (ft)	Variable; could be < 9.1 m (30 ft)	Variable; could be < 9.1 m (30 ft)	9.1 m (30 ft) wide with a cross-slope of 2 – 3%'	3.0 – 3.7 m (10-12 ft) per travel lane with 2.4 – 3.0 m (8-10 ft) shoulders and a 1.5 – 2% cross-slope
Maximum allowable speed kph (mph)	Variable	56 – 72 kph (35 – 45 mph)	24 – 56 kph (15 – 35 mph)	Over 72 kph (45 mph)

4.1.3 Ambulance experimental protocols and set-up

Extreme care was taken to ensure each ambulance tested was set-up in an identical manner. Vibration data was gathered in each of the four ambulances along a selection of roads in Central Massachusetts and Northeastern Connecticut (USA).

For the purposes of this study, a fixed protocol of vehicle speeds and road surfaces were studied as shown in Table 13 in order to gather data from a wide variety of typical road conditions and to control for normal variations in road surface and speed.

Table 13. *Road surface/speed combinations*

Road Surface	≥ 65 mph*	Speed 36-64 mph*	≤ 35 mph*
Highway	✓	✓	✓
Paved secondary road		✓	✓
Paved city street		✓	✓
Unpaved road			✓
Speed bump			✓

*Reported in English units in keeping with US convention

Ambulance drivers were familiar with all the routes, which were similar in all phases of the study. Top vehicle speeds were limited by road surface conditions as well as prevailing posted speed limits, so vibrations were not measured at all speeds for all road surfaces.

In order to ensure accurate loading of the ambulance during vibration testing, a Laerdal Nursing Anne full-body, articulated training manikin was immobilized to a standard transport stretcher (Ferno Proflex, or equivalent) as shown in Figure 21.

Figure 21. *Typical transport stretcher as used in tests (Ferno Proflex)*

The manikin was secured to the stretcher with leg, thigh and cross-chest straps as shown in Figure 22, and loaded into the ambulances prior to each test.

Figure 22. *Laerdal manikin immobilized on stretcher ready for test*

Vehicle accelerations were measured on the floor of the patient compartment in each

ambulance tested in the position and orientation shown in Figures 23 and 24 respectively.
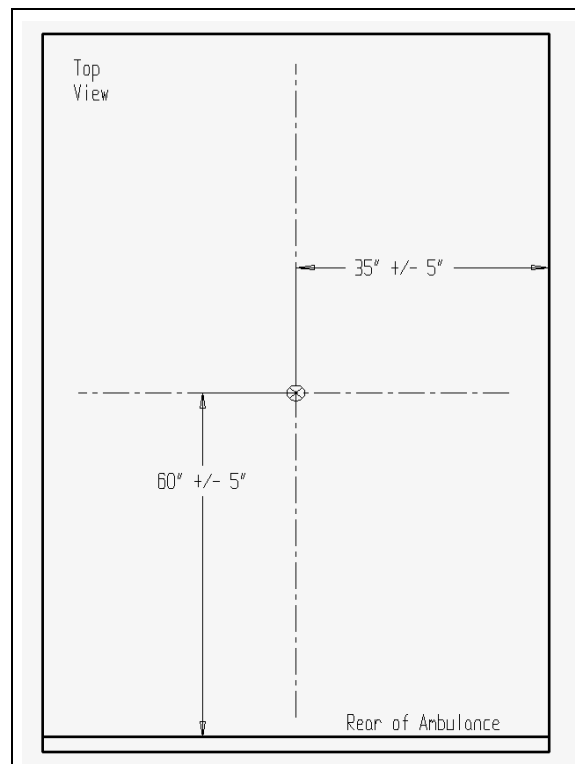
Figure 23. *Position (in inches) of acceleration recorder on patient compartment floor*
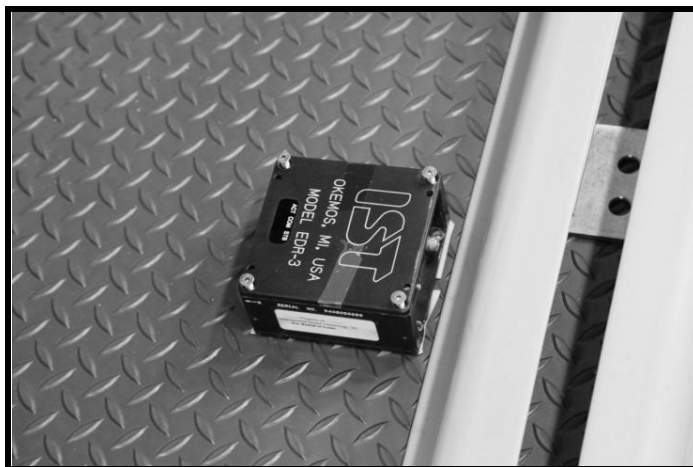
Figure 24. *Photograph of acceleration recorder on patient compartment floor*

The acceleration recorder was positioned below what would roughly correspond as the location of a patient's chest and was set-up with measurement axes oriented as shown in Figure 25.
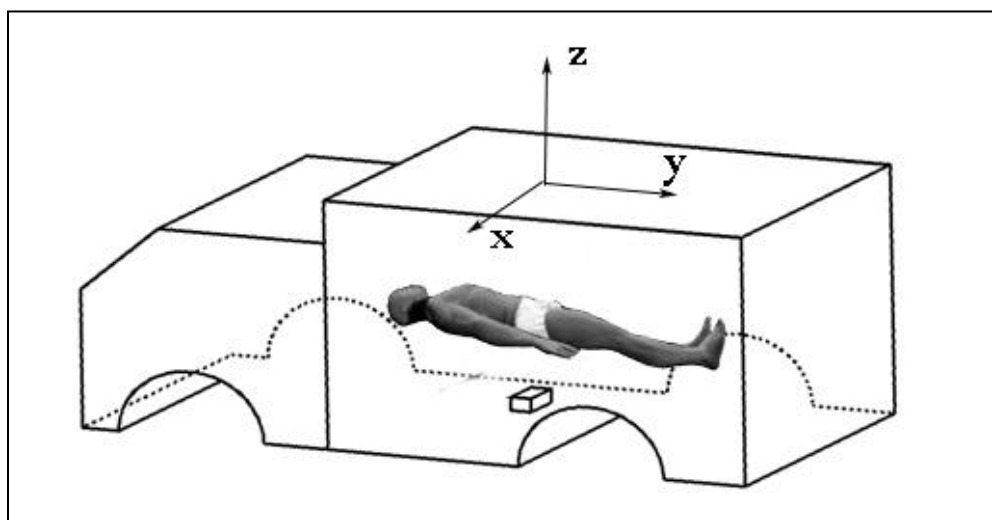
Figure 25. *Orientation of measurement axes of acceleration recorder*

The recorder axes corresponded to the axes of the vehicle and manikin as shown in Table 14.

Table 14. *Orientation of measurement axes relative to vehicle and manikin (subject)*

Sensor/recorder axes	Manikin	Vehicle
x	lateral (left-to-right)	side-to-side
y	superior-to-inferior (head-to-foot)	front-to-back
z	posterior-to-anterior (back-to-front)	floor-to-ceiling

The recorder was securely mounted to the floor of the vehicle with the use of 2" wide, .012" thick, Shurtape DF 550 double stick carpet tape. For the purposes of this study, the tape provided adequate holding power without adding any measurable damping.

4.1.4 Acceleration recorder description

Acceleration measurements were obtained using an Instrumented Sensor Technology EDR-3C-10 Shock & Vibration Sensor/Recorder. Detailed specifications and calibration data for the recorder may be found in Appendix B of this report. The compact size (37 in^3, 2 lbs.), 4 Mb of on-board memory and battery power source of the recorder allowed for portable operation. The unit was equipped with a built-in triaxial accelerometer, for simultaneous measurement of acceleration in three axes. The recorder's three piezo resistive elements provided the low frequency response (true DC) which was required to collect vibration data at the frequencies of interest to this study. The sensitivity of the accelerometer was 1.473 mV/g over a range of 11.5 g, yielding a measurement resolution of 0.23 g. A 90 Hz internal anti-aliasing filter was also employed. The analog data was digitized through a 10-bit A/D converter. In addition to the digitized readings of acceleration, the device also recorded the date and time of the measured events as part of the output data stream. Each road type/vehicle speed combination

was sampled multiple times for each ambulance type in discrete ten second intervals called

events. Approximately 70, 10-second events were recorded for each vehicle. All events were

sampled 498.8 times per second (498.8 Hz) for acceleration values. A remote trigger switch was

used to manually initiate recording of the acceleration data for each event. The start time of each

event was logged on special data sheets which were then subsequently inspected visually to

match the acceleration data to the road type/vehicle speed being tested. The sensor is shown in

Figure 26.

In addition to the sensor/recorder unit, a Toshiba Satellite L-305 laptop computer running

EDR3CCOM and IST Dynamax software was employed to set-up and calibrate the recorder, as

well as to reduce and analyze the data following collection.

Figure 26. Photograph of *IST EDR-3C-10*
Environmental shock &vibration sensor/recorder: models EDR-3, EDR-3C, EDR-3D. (2010,Jan 25) Promotional flyer from Instrumented Sensor Technology, Inc. Okemos, MI.

A wired remote toggle switch was used to enable data recording when traversing the

required road surfaces. The computer was connected to the sensor/recorder via a serial cable at

the start of each experimental run in order to download set-up parameters and arm the unit. The

device was set to auto-calibrate prior to the recording of each event. After each ambulance run

the data which was stored on the sensor/recorder was downloaded to the laptop computer for

long-term storage and analysis. The entire system set-up in a typical test ambulance is shown in

Figure 27.
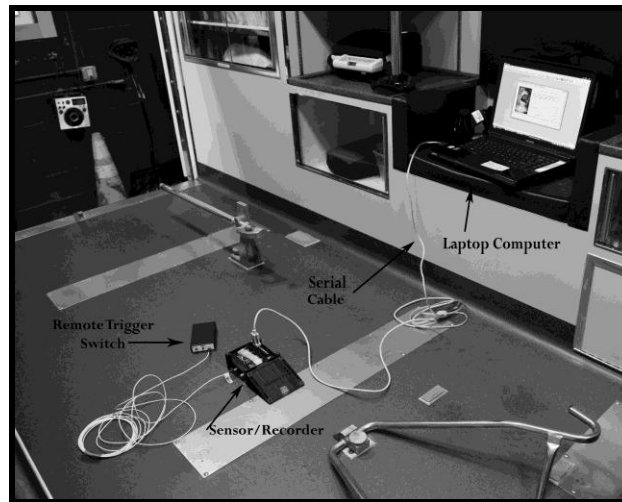
Figure 27. *Photograph of data sensor/recorder system set-up*

Figure 28 is a schematic diagram of the data recorder setup and Figure 29 is a block
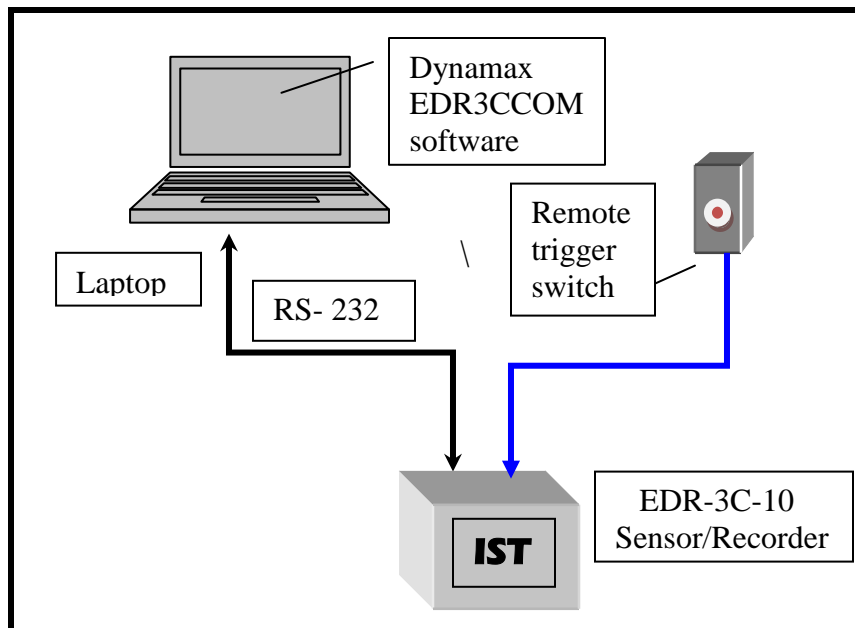
Figure 28. *Schematic diagram of data sensor/recorder system set-up*

diagram of the EDR-3C-10 sensor/recorder device.
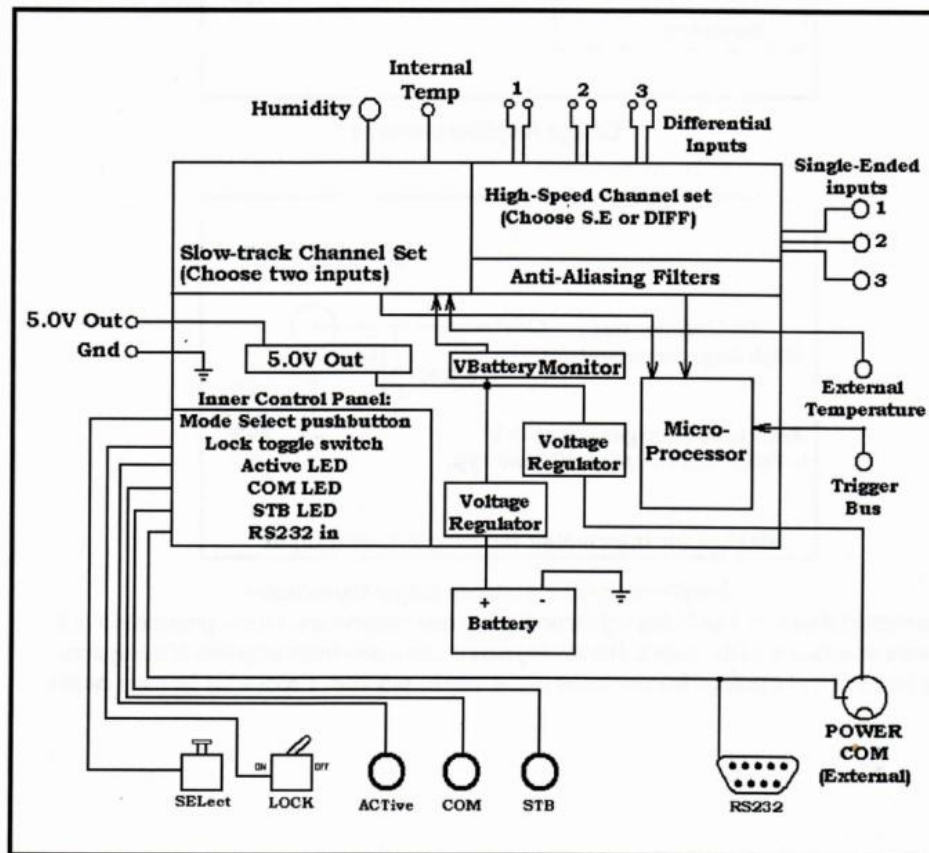
Figure 29. *Schematic block diagram of IST EDR-3C-10 sensor/recorder*
EDR-3C and, EDR-3D hardware users manual. (1999) Instrumented Sensor Technology, Inc. Okemos, MI. p. 59.

4.2 Data Acquisition

For each road surface/vehicle speed combination studied, the vibration data collected

included individual time domain accelerations in the x, y and z axes as well as the r.m.s. (root

mean square) acceleration, or triaxial vector sum of all three measured axes. Analysis of the data

with the IST proprietary Dynamax software yielded peak acceleration values in the x, y, and z

axes as well as the peak r.m.s. acceleration values.   Further analysis of the data using the

Microsoft Excel spreadsheet program was used to generate (1) mean r.m.s. acceleration values in

each measured axis, (2) mean peak accelerations in each measured axis, and, (3) mean crest factors for each recorded 10 second interval. These last three data types are International Organization for Standards (ISO) standardized measures for the characterization of vehicular vibrations in terms of its impact on human occupants. The mean peak accelerations in each measured axis provided an indication of the amplitude of vibrations due to intermittent shocks or jolts, like those encountered when travelling over potholes or other road irregularities. The r.m.s. acceleration values in each measured axis provided an indication of the amplitude of a vehicle's overall vibration level during travel over a particular road surface at a particular speed. The mean crest factors in each measured axis were calculated by dividing the mean peak acceleration of a 10 second sample by the mean r.m.s. acceleration of that sample yielding a measure of the uniformity of the accelerations experienced, which provided a good indicator of ride smoothness for purposes of comparison.

4.3 Data analysis

The data analysis included: (1) development of a base-line reference for evaluating the vibrations to which occupants of typical US ambulances are exposed using ISO standardized measures of vibration amplitude, shock amplitude, and smoothness of ride, (2) association of vehicle speed/ road surface characterization combinations with vibration amplitudes and frequency and energy content characteristics experienced in the ambulance, and (3) characterization of the nature of the road surface forcing functions for model verification and to further evaluate the performance of the FFDCS force plate model and other vibration attenuation alternatives.

4.4 FFDCS force plate model development

In the final phase of the study, a force plate model was created and analyzed. The

experimentally derived vibration forcing functions were used as model inputs in order to explore the feasibility and reliability of the force plate concept. The results of this analysis were used to recommend design considerations to guide future work in the serial fabrication of stable and reliable ambulance borne-vibration attenuation systems effective at the amplitudes and frequencies of interest.

5.0 Experimental results and discussion

5.1 Test/event description

As described earlier, each road type/vehicle speed combination was sampled multiple times for each ambulance type in discrete ten second intervals called events. Approximately 70, 10-second events were recorded for each vehicle. The event numbers of each vehicle ride test of this study categorized by road surface and vehicle speed are shown in Table 15.

Table 15. *Test/event descriptions*

Amb #	Total # events	Event[1] #'s							
		Highway			Secondary road		City street		Un-paved road
		≤35 mph	36-64 mph	≥65 mph	≤35 mph	36-64 mph	≤35 mph	36-64 mph	≤35 mph
1	64	1-3	4-6; 15-20	7-14	21-23; 27-29	24-26; 30-32	41-64	38-40	33-37
2	63	1-3	4-6; 10-15	7-9; 16-18	25-27; 50-52	31-33; 58-60;	19-24; 44-49; 61-63	28-30	34-43
3	71	1-3	4-6	7-15	16-18; 22-24	19-21	34-58	31-33	25-30
4	93	16-18	19-24; 31-35	25-30	4-6; 10-12	1-3; 13-15; 41; 43-45	7-9; 34-36; 49-58; 68-70; 77-82; 91-93	37-39; 59-67	71-76

[1]Each event represents a 10 second recording interval.

5.2 Description of ambulance vibration amplitude data

The following tables and graphs describe the results of the ambulance vibration tests conducted as part of this study. These data provided a means of characterizing and evaluating the vibrations to which occupants of typical US ambulances are exposed using ISO standardized measures of vibration amplitude, shock amplitude, and smoothness of ride as well as frequency

spectra.   Data for the study was gathered in accordance with the accepted vibration measurement methods outlined in ISO 2631-1, 1997 (International Organization for Standardization 1997 ISO 2631-1, 1997) and BS 6841 (British Standards Institution 1987 BS 6841, 1987). Acceleration information was obtained for 4 axes (x, y, z, and resultant), with both most severe axis data and total vibration (triaxial sum) values reported. Both ISO and British vibration standards require the vibration amplitude data to be calculated using a vibration dose value (VDV) which provides an acceleration value weighted for the frequency, the amplitude and the length of exposure to the vibration under investigation. Since the goal of this study was not to determine vibration exposure limits, but to characterize the actual vibrations experienced in order to provide design inputs for vibration attenuation, only un-weighted vibration values were reported . Furhtermore, concentration was placed on vibrations in the vertical axis, which for the purposes of this study was consistently referred to as the z-axis. The amplitude values reported in this study are defined below.

The un-weighted **mean r.m.s. acceleration** is the root mean square average of all the 10 second interval recordings for a specific road surface/vehicle speed combination for a particular ambulance. For a set of discrete values, The r.m.s. value is calculated by taking square root of the sum of the squares of each discrete value divided by the number of values in the set. For example, the mean r.m.s. acceleration value for highway travel of ambulance #1 at speeds of 65 mph and above was calculated by averaging the calculated r.m.s. acceleration values from all the events recorded at 65 mph and above on a highway road surface. The r.m.s. value applies to the total measurement bandwidth, or half the sample frequency. The 90 Hz low pass filter used on the sensor had the effect of damping the high frequency energy in the input signals. Energy that was damped by the low pass filter and energy beyond the total measurement bandwidth of the

sensor were therefore not included in the r.m.s. value. The r.m.s. value is the ISO standard measurement for the amplitude of a vehicle's overall vibration level.

The un-weighted **maximum peak acceleration** is the absolute value of the single greatest positive acceleration sample point from all the 10 second interval recordings for a specific road surface/vehicle speed combination, for a particular ambulance. The maximum peak accelerations in each measured axis provided an indication of the largest amplitude vibrations due to intermittent shocks or jolts, like those encountered when travelling over potholes or other road irregularities. This value represented the amplitude of the accelerations produced by traversing the very worst jolts a particular road surface/speed combination had to offer.

The un-weighted **mean peak acceleration** is the arithmetic average of the maximum peak acceleration values from all the 10 second interval recordings for a specific road surface/vehicle speed combination for a particular ambulance. For example, the mean peak acceleration for highway travel of ambulance #1 at speeds of 65 mph and above was calculated by averaging the maximum peak acceleration values from all the events recorded at 65 mph and above on a highway road surface. The mean peak accelerations in each measured axis provided an indication of the average amplitude of vibrations due to intermittent shocks in keeping with ISO measurement guidelines, and was useful for the comparison of data gathered for this study with other similar work. In this study, the mean peak acceleration was typically smaller in amplitude than the maximum peak acceleration discussed earlier, but was useful in providing an average amplitude of all the accelerations produced by intermittent road perturbations experienced for a specific vehicle/road surface/speed combination.

In a similar fashion, the un-weighted **mean crest factor** in each measured axis was calculated by dividing the mean peak acceleration of each 10 second sample by the mean r.m.s.

acceleration of that sample and then averaging over all the events recorded for that particular ambulance/road surface/ vehicle speed combination. This yielded a dimensionless ISO standard measure of the uniformity of the accelerations experienced, which provided a good indicator of ride smoothness.

Accelerations in the x, y and z-axes were all collected, but for the purposes of this study, and in keeping with ISO standardized procedures for the measurement of vehicular vibration amplitude, only the vertical z-axis values, most severe axis values, and the resultant values were reported here.

Raw vibration amplitude data is presented in graphical and tabular format in Appendix C of this study. The data includes Z-axis, worst axis and resultant, tri-axial accelerations for overall vibrations (mean r.m.s.), shock accelerations (maximum peak and mean peak) and a measure of vibration uniformity as expressed by the mean crest factor. These values are all reported for each ambulance in units of meters per second squared and are categorized by vehicle speed and road surface traversed.

5.3 Characterization of ambulance vibration amplitude data

Characterization of the ambulance vibration amplitude data is summarized for vertical, z-axis vibrations in the following tables and charts.

5.3.1. Characterization of ambulance vibration amplitude data by vehicle

The average, overall vibration amplitudes, average peak vibration amplitudes and vibration amplitude uniformity experienced in each ambulance, as expressed by the mean r.m.s., mean peak and crest factor values, respectively, are listed in Table 16 and shown graphically in

Figure 30.

Table 16. *Vibration amplitude data characterized by vehicle*

Overall amplitude of vibrations z-axis					Amplitude of bumps and shocks z-axis					Uniformity of vibration amplitudes z-axis				
Mean r.m.s. (m/sec^2)					Mean peak (m/sec^2)					Mean crest factor				
For ambulance #1, all speeds, all road surfaces														
$\bar{x}$	Min	Max	*s*	*n*	$\bar{x}$	Min	Max	s	*n*	$\bar{x}$	Min	Max	s	*n*
1.15	0.60	2.41	.55	64	6.08	3.44	13.56	3.2	64	5.61	4.17	6.80	0.76	64
For ambulance 2, all speeds, all road surfaces														
$\bar{x}$	Min	Max	*s*	*n*	$\bar{x}$	Min	Max	s	*n*	$\bar{x}$	Min	Max	s	*n*
0.83	0.62	1.05	0.16	63	3.88	2.88	5.36	0.96	63	4.84	3.95	6.06	0.73	63
For ambulance #3, all speeds, all road surfaces														
$\bar{x}$	Min	Max	*s*	*n*	$\bar{x}$	Min	Max	s	*n*	$\bar{x}$	Min	Max	s	*n*
1.34	0.71	2.55	0.56	71	7.03	3.90	15.45	3.64	71	5.42	4.20	7.70	1.10	71
For ambulance #4, all speeds, all road surfaces														
$\bar{x}$	Min	Max	*s*	*n*	$\bar{x}$	Min	Max	s	*n*	$\bar{x}$	Min	Max	s	*n*
0.64	0.46	0.96	0.16	93	3.20	1.87	4.40	0.86	93	5.32	4.37	6.98	0.92	93

Figure 30 describes the overall and shock z-axis vibrations measured, as well as the z-axis crest factor for each ambulance tested. As evidenced by the graph, ambulances 1 & 3, which were driven over Worcester roads, experienced higher average and peak accelerations and slightly higher crest factors. The measured mean Worcester r.m.s. vibration values exceeded the respective Connecticut values by 39% and 109%, while the average peak Worcester values exceeded the Connecticut values by 57% and 120%, respectively. Because there were no significant variations in measured vibrations between ambulances for tests conducted on the same type of road surface at the same speed (see data in Appendix A), it is logical to conclude

that the differences between ambulances seen in this graph were most likely due to differences in either driver or road surface. For the purposes of this study, the significance of any differences between ambulance vibrations was not tested statistically.
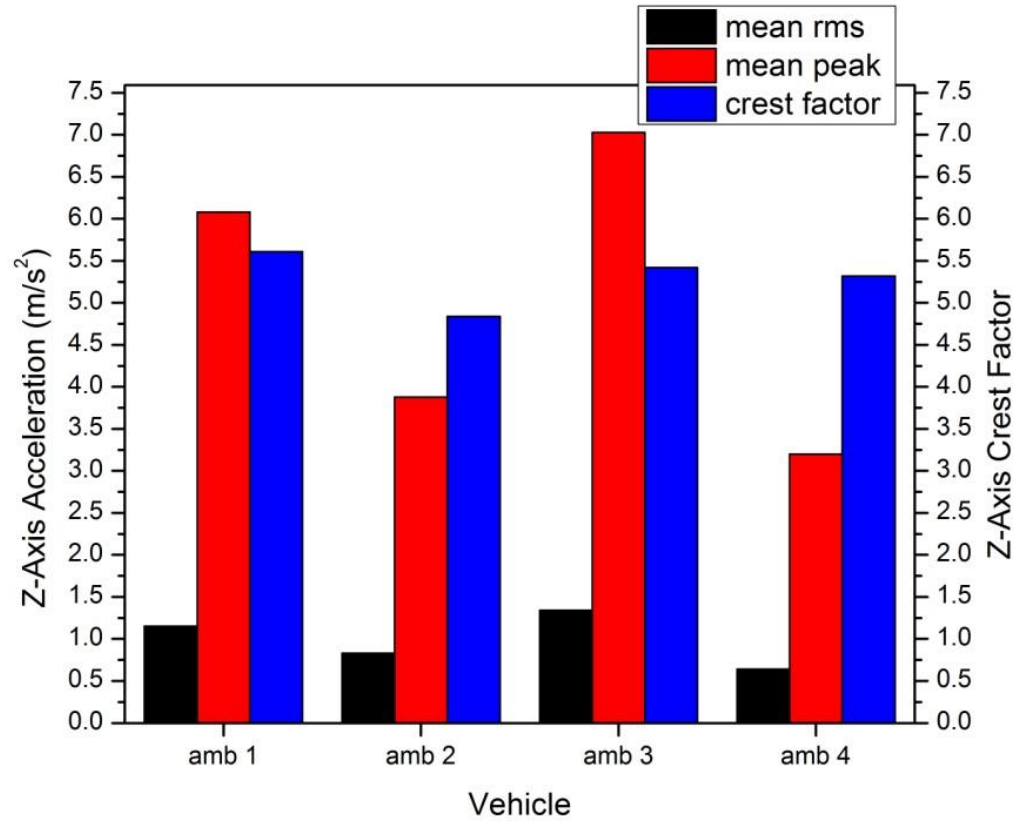
Figure 30. *Graph of z-axis mean r.m.s. acceleration, mean peak acceleration and crest factor for each ambulance at all speeds and road surfaces*

5.3.2 Characterization of ambulance vibration amplitude data by road surface

The average, overall vibration amplitudes, average peak vibration amplitudes and vibration amplitude uniformity experienced in each ambulance, characterized by road surface traversed, and expressed by the mean r.m.s., mean peak and crest factor values, respectively, are listed in Table 17. The data is shown graphically in Figure 31.

Table 17. *Vibration amplitude data characterized by road surface*

Overall amplitude of vibrations z-axis					Amplitude of bumps and shocks z-axis					Uniformity of vibration amplitudes z-axis				
Mean r.m.s. (m/sec^2)					Mean peak (m/sec^2)					Mean crest factor				
For all speeds, all ambulances, highway travel														
$\bar{x}$	Min	Max	s	n	$\bar{x}$	Min	Max	s	n	$\bar{x}$	Min	Max	s	n
0.89	0.59	1.63	0.31	73	4.28	3.07	7.25	1.20	73	5.20	4.04	6.98	0.99	73
For all speeds, all ambulances, secondary road travel														
$\bar{x}$	Min	Max	s	n	$\bar{x}$	Min	Max	s	n	$\bar{x}$	Min	Max	s	n
0.93	0.50	1.34	0.28	49	4.65	2.50	6.42	1.40	49	5.18	4.20	6.06	0.56	49
For all speeds, all ambulances, city street travel														
$\bar{x}$	Min	Max	s	n	$\bar{x}$	Min	Max	s	n	$\bar{x}$	Min	Max	s	n
0.90	0.60	1.29	0.26	110	4.90	2.92	8.03	1.71	110	5.71	4.47	7.70	1.00	110
For all speeds, all ambulances, unpaved road travel														
$\bar{x}$	Min	Max	s	n	$\bar{x}$	Min	Max	s	n	$\bar{x}$	Min	Max	s	n
1.54	0.46	2.55	1.09	27	8.44	1.87	15.45	7.06	27	4.97	3.95	5.99	0.96	27

Figure 31 describes the overall and shock z-axis vibrations measured, as well as the z-axis crest factor calculated, for each road surface tested. Not surprisingly, the graph indicates that the relatively smooth highway surfaces produced the lowest average and peak accelerations while unpaved roads produced the highest. Secondary roads and city streets produced slightly higher average and peak accelerations than highway surfaces, but lower than unpaved roads. Vibration uniformity as evidenced by the crest factors was roughly equal for all road surfaces.. For the purposes of this study, the significance of any vibrational differences between road surfaces was not tested statistically.

Figure 31. *Graph of z-axis mean r.m.s. acceleration, mean peak acceleration and crest factor for each road surface for all ambulances at all speeds*

5.3.3 Characterization of ambulance vibration amplitude data by vehicle speed

The average, overall vibration amplitudes, average peak vibration amplitudes and

vibration amplitude uniformity experienced in each ambulance, characterized by vehicle speed,

and expressed by the mean r.m.s., mean peak and crest factor values, respectively, are listed in

Table 18. The data is shown graphically in Figure 32.

Table 18. *Vibration amplitude data characterized by vehicle speed*

Overall amplitude of vibrations z-axis					Amplitude of bumps and shocks z-axis					Uniformity of vibration amplitudes z-axis				
Mean r.m.s. (m/sec^2)					Mean peak (m/sec^2)					Mean crest factor				
For all road types, all ambulances, speed ≤ 35 mph														
$\bar{x}$	Min	Max	s	*n*	$\bar{x}$	Min	Max	s	*n*	$\bar{x}$	Min	Max	s	*N*
0.94	0.46	2.55	0.62	151	5.18	1.87	15.45	3.78	151	5.50	3.95	6.98	0.73	151
For all road types, all ambulances, speed 36 – 64 mph														
$\bar{x}$	Min	Max	s	*n*	$\bar{x}$	Min	Max	s	*n*	$\bar{x}$	Min	Max	s	*n*
0.99	0.60	1.34	0.26	57	4.92	2.62	8.03	1.68	57	5.33	4.16	7.70	1.06	57
For all road types, all ambulances, speed ≥ 65 mph														
$\bar{x}$	Min	Max	s	*n*	$\bar{x}$	Min	Max	s	*n*	$\bar{x}$	Min	Max	s	*n*
1.18	0.96	1.63	0.31	29	4.90	3.50	7.25	1.63	29	4.40	4.04	4.79	.35	29

Figure 32 describes the overall and shock z-axis vibrations measured, as well as the z-axis crest factor calculated, for each speed range tested. For this study, all road surface vibration was averaged together. As such, the data show no evidence to suggest that when a variety of typical road surfaces are traversed, there is a significant effect on ambulance vibration based on vehicle speed. This is not surprising, since the most vibration prone road surfaces were the unpaved roads and city streets. The poor condition and posted speed limits of these road surfaces limited the ambulance drivers to keep their speed below 35 MPH. This skewed the vibration values up for the lowest speed range since the worst roads were traversed at the lowest speeds..

Figures33 (a-b) graphically describe the variation in mean r.m.s. and mean peak z-axis vibration respectively at different speeds when only travel over smooth highway surfaces is
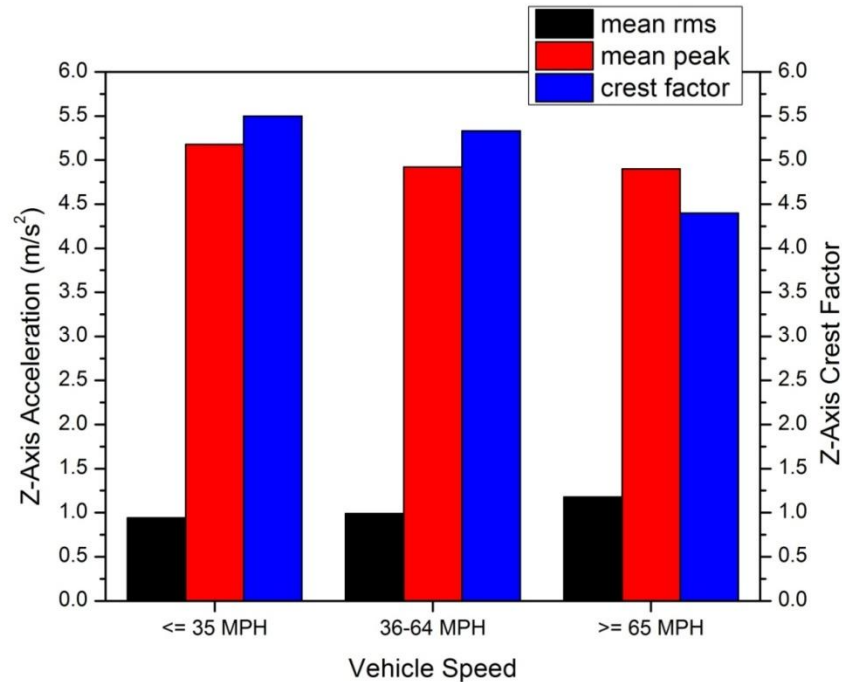
Figure 32. *Graph of z-axis mean r.m.s. acceleration, mean peak acceleration and crest factor for each vehicle speed setting for all ambulances on all road surfaces*

considered. Figure 33(a) would seem to indicate that on a highway road surface, there is an increase in mean z-axis vibration associated with an increase in vehicle speed. The trend is not so evident in the mean peak data shown in Figure 33(b).
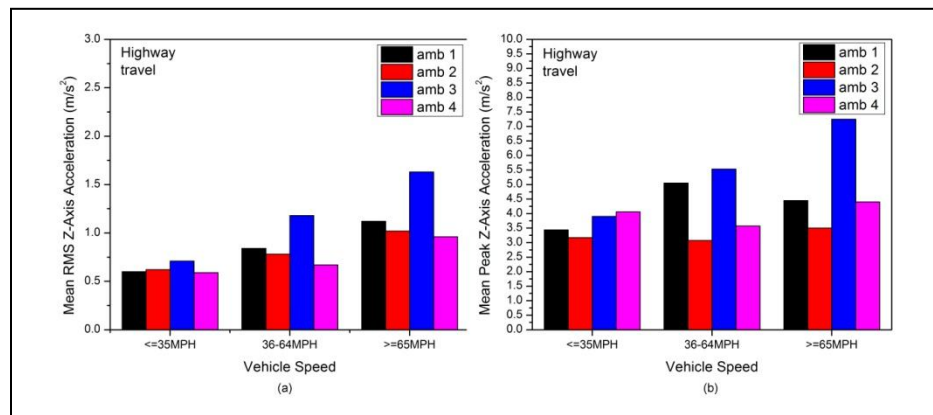
Figure 33. *Graph of (a) z-axis mean r.m.s. acceleration and (b) mean peak acceleration by ambulance for each speed range tested*

Figures 33 (a-b) would seem to indicate that there is more sensitivity to random events,

such as pot holes and other road irregularities, in the peak data than in the mean r.m.s. data. For the purposes of this study, the significance of any vibrational differences between vehicle speeds was not tested statistically.
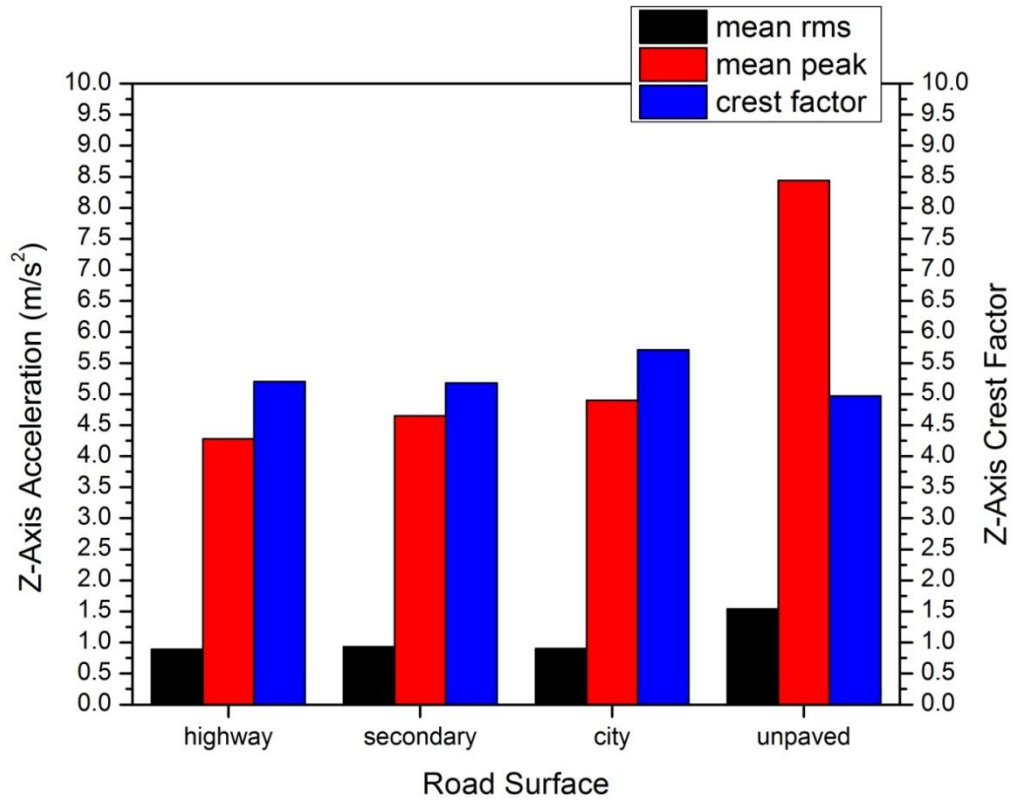
5.3.4 Characterization of ambulance vibration amplitude summary

The average overall z-axis vibration amplitudes encountered in the ambulances tested for this study varied from .46 to 2.55 m/sec^2 with a mean value of .99 m/sec^2. The average resultant-axis measurements varied from .66 to 2.94 m/sec^2 with a mean value of 1.33 m/sec^2. As a means of comparison, this is about twice the average vibration one might feel while riding in a typical passenger car (Paddan & Griffin, 2002).

The z-axis vibration amplitudes associated with sharp jolts, like those which were caused by encountering speed bumps, frost heaves, or pot holes ranged from 4.16 to 15.45 m/sec^2 with a mean value of 5.00 m/sec^2. The resultant-axis measurements averaged 5.64 m/sec^2, varying from 2.88 to 16.08 m/sec^2.

The average crest factors averaged 5.08 and 4.16 for the z-axis and resultant-axis measurements respectively. The crest factor is most useful in comparing vibration responses in terms of uniformity. A non-uniform response is typically due to impacts, non-periodic events and random noise. A high crest factor would indicate the presence of these forcing elements and help further characterize the vibration amplitudes and frequencies.

Since the vibration literature uses both z-axis and resultant-axis data, both data were reported here in order to make comparisons with other studies in the field more meaningful.

Table 19 summarizes the characterization of z-axis vibrations on all road surfaces for all ambulances at all speeds and Table 20 summarizes the characterization of resultant-axis vibrations on all road surfaces for all ambulances at all speeds.

Table 19. *Summary of z-axis* vibration *amplitude data*

Overall amplitude of vibrations z-axis			Amplitude of bumps and shocks z-axis			Uniformity of vibration amplitudes z-axis		
Mean r.m.s. (m/sec^2)			Mean peak (m/sec^2)			Mean crest factor		
For all speeds tested, all ambulances, all road surfaces								
$\overline{x}$	**Min**	**Max**	$\overline{x}$	**Min**	**Max**	$\overline{x}$	**Min**	**Max**
0.99	0.46	2.55	5.00	4.16	15.45	5.08	4.16	7.70

Table 20. *Summary of resultant-axis* vibration *amplitude data*

Overall amplitude of vibrations resultant axis			Amplitude of bumps and shocks resultant-axis			Uniformity of vibration amplitudes resultant-axis		
Mean r.m.s. $(m\ sec^{-2})$			Mean peak $(m\ sec^{-2})$			Mean crest factor		
For all speeds tested, all ambulances, all road surfaces								
$\overline{x}$	**Min**	**Max**	$\overline{x}$	**Min**	**Max**	$\overline{x}$	**Min**	**Max**
1.33	0.66	2.94	5.64	2.66	16.08	4.16	3.08	6.07

The data in Tables 19 and 20, shown graphically in Figures 34 – 36, characterize the overall, peak and uniformity of ambulance vibrations measured in both the vertical and resultant axes.
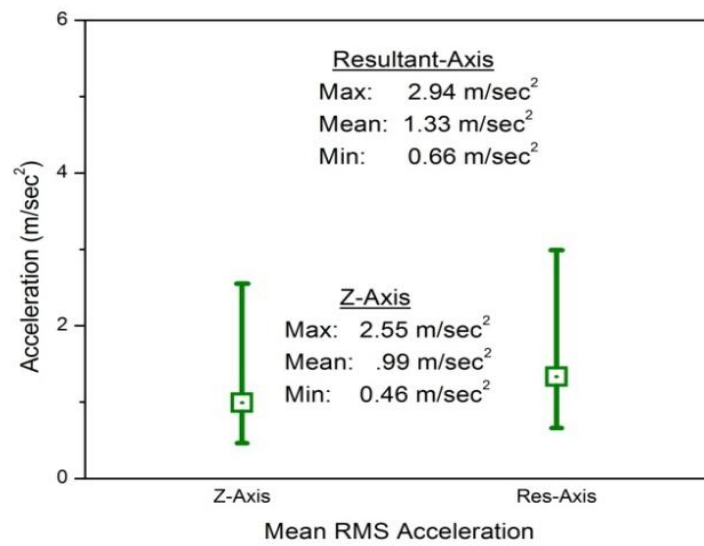
Figure 34. *Graph of overall amplitude of z-axis and resultant-axis mean r.m.s. acceleration*
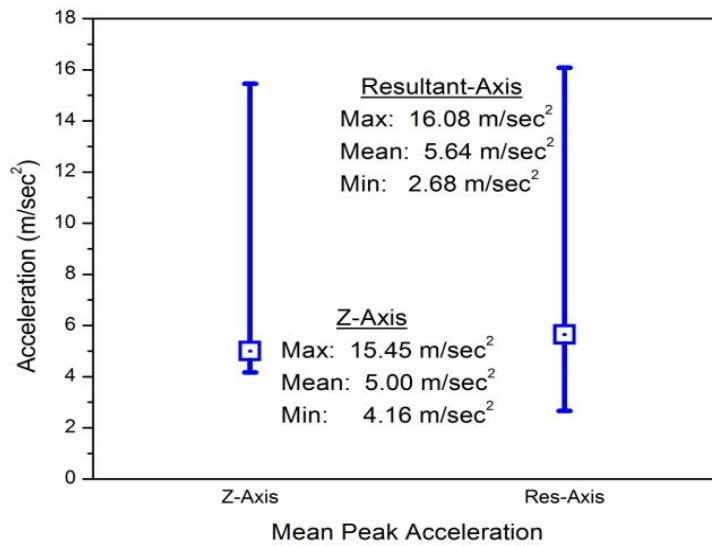
Figure 35. *Graph of shock amplitude of z-axis and resultant-axis mean peak acceleration*
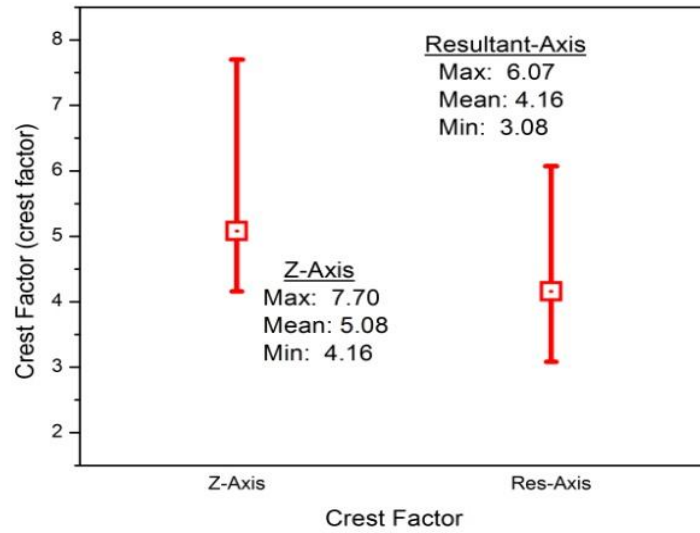
Figure 36. *Graph of uniformity of z-axis and resultant-axis crest factors*

5.3.5 Comparison of ambulance vibration amplitude to other studies

Ambulance vibration data which has been reported in the literature suffers from a high degree of variability. This is due in large part to the great variability in the type of ambulances studied, variations in driver skill, differences in local road and speed conditions, the specification of test equipment used, experimental procedures employed, and data reporting techniques.

Nonetheless, as shown in Table 21, and graphically in Figure 37, the vibration amplitude data gathered for this study was in general agreement with the majority of other studies which were researched for both maximum peak and mean r.m.s. ambulance vibration amplitudes. Road profile descriptions and measurement configurations were included to make comparisons more meaningful.

Table 21. *Comparison of vibration amplitude data to other studies*

Study Authors	Max Peak accel. (m/sec^2)	Mean R.M.S. accel. (m/sec^2)	Road profile description	Measurement configuration
Cotnoir, 2010	16.08	1.78	Highway, Secondary Roads, City Streets & Unpaved roads	Triaxial vector sum (Resultant Axis)
	15.45	1.04		Vertical axis on compartment floor
Sherwood, et. al., 1994	15	--	City & highway	Triaxial vector sum measurement on mannequin forehead, vehicle floor and base of isolette
Bellieni, et. al., 2004	11.8	1.3	City & highway	Vertical axis in isolette, on passenger seats, & on driver's seat
Shenai, et. al., 1981	5.0 – 13.0	2.2 – 6.0	Highway @ 48 mph	Vertical axis on supine infant head, abdomen, thigh
Silbergleit, et. al., 1991	3.1 – 8.1	.7 – 1.9	bumpy road, city road and highway	Triaxial vector sum measurement on standard backboard at head position
Mcnab, et. al., 1995	0 – 1.7	.0 - .7	bumpy road, city road and highway	Triaxial vector sum measurement from acoustical measurements
Pichard, et. al., 1970	.16 - .85	--	City & highway	Z-axis, head-to-toe of recumbent patient
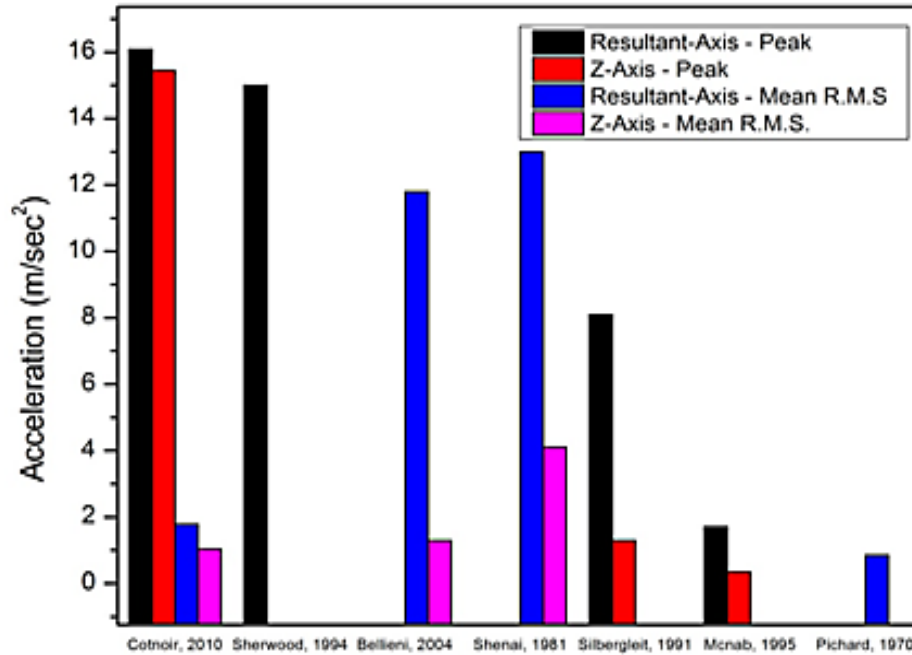
Figure 37. *Comparison of vibration amplitudes to other studies*

5.4 Data analysis

A goal of this study was to experimentally determine the vibrational amplitude, frequency and energy of a typical ambulance ride, and correlate those vibrational characteristics to human physical impacts on ambulance passengers and EMT crews. In order to fully characterize the vibrational data frequency and energy content information was first extracted.

5.4.1 Frequency/energy content analysis

Instrumented Sensor Technology Dynamax software was used to collect and analyze the ambulance vibration data. The software collected and statistically reduced the vibration amplitude data as a time domain function. The Dynamax software was also used to calculate the power spectral density (PSD) for events of interest. The PSD function was used to display the data in the frequency domain as a function of power versus frequency. The PSD graph identifies the frequencies at which the majority of the vibrational energy is concentrated. A classic Fast-Fourier Transform (FFT) using rectangular spectral windowing was utilized for this analysis. Figure 38 shows a typical multi-axis vibration time history and PSD graph for a 10 second measurement event, in this case, ambulance #3, driven at ,<= 35 MPH on an unpaved road surface. Additional sample time domain and frequency domain graphs from various ambulances, road surfaces and vehicle speeds are included in Appendix C of this dissertation. While minor differences in the PSD graphs were observed in the data collected, every test run, regardless of vehicle, road surface or speed selected, exhibited the peaks in the .12 to 6 Hz frequency spectrum. Z-axis vibration energy in all the ambulances tested was clearly concentrated in the sub 6 Hz spectrum and encompassed the highest amplitude peaks within the critical sub 10 Hz. part of the spectrum which has the largest ramifications for human health and comfort. Since the
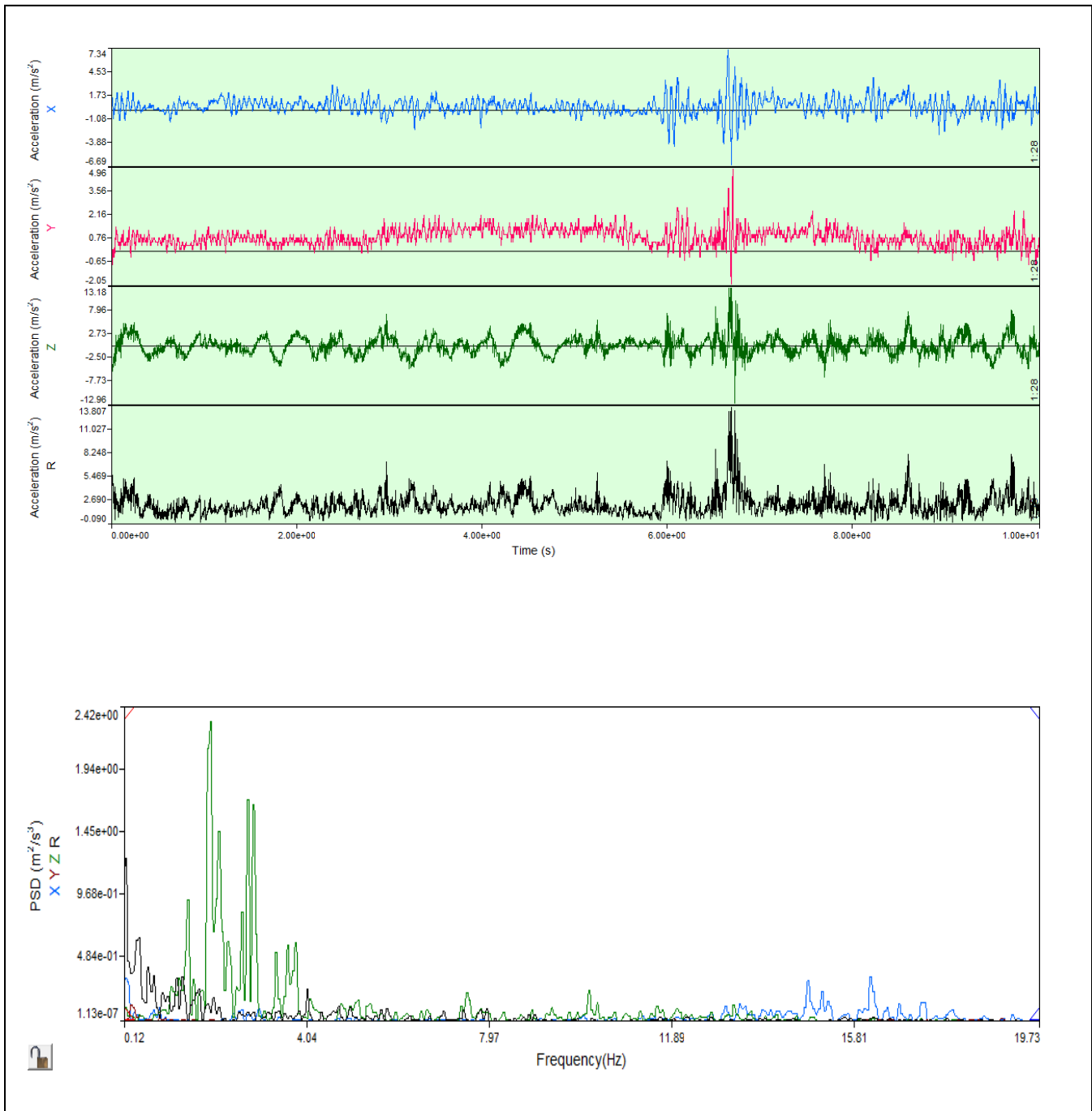
Figure 38. *Graph of multi-axis vibration time history and power spectral density, Amb. #3,*
>=65 MPH, Highway surface

z-axis data was most critical to this analysis, Figure 39 shows a typical multi-axis vibration time

history and PSD graph for a 10 second measurement event, in this case, ambulance #3, driven at

,>=65 MPH on an highway road surface.
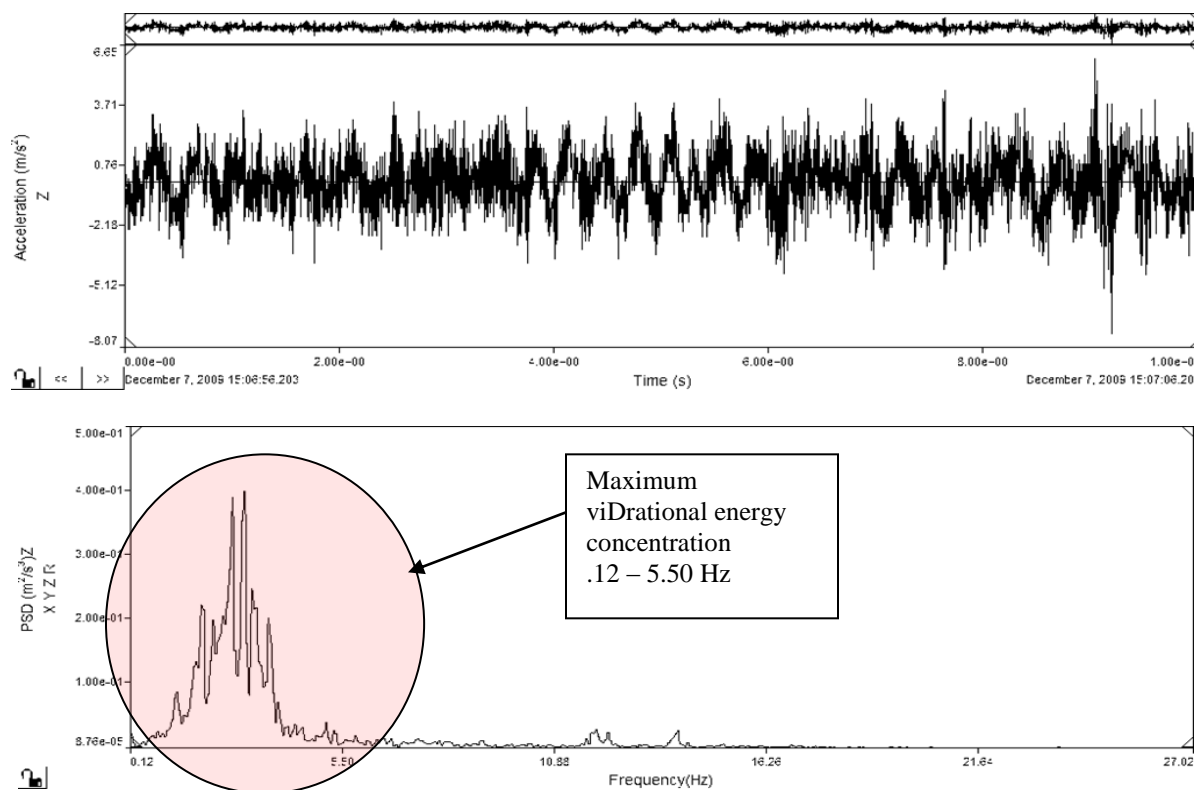
Figure 39. *Graph of z-axis vibration time history and power spectral density, Amb. #3, >=65 MPH, Highway surface*

5.4.2 *Analysis of patient safety, comfort and care*

Effects on patient safety

This study has shown that the average vertical vibrations experienced in ambulance patient compartments during normal travel vary from .46 to 2.55 m/sec^2 at frequencies from .1 to 6 Hz. As shown in Table 5, the majority of major anatomical structures in the human body resonate at the same frequencies as vibrations measured in the ambulance tests associated with this study. This leads to physiological effects manifesting themselves in the associated body systems which could have negative safety ramifications for health-compromised ambulance patietnts. Some of those vibration-induced effects and the frequencies at which those effects

occur is listed in Table 7. This is shown graphically in Figure 40, superimposed on the PSD

graph of the z-axis vibrations associated with ambulance #3 travelling at a speed of >=65 MPH

on a highway road surface.
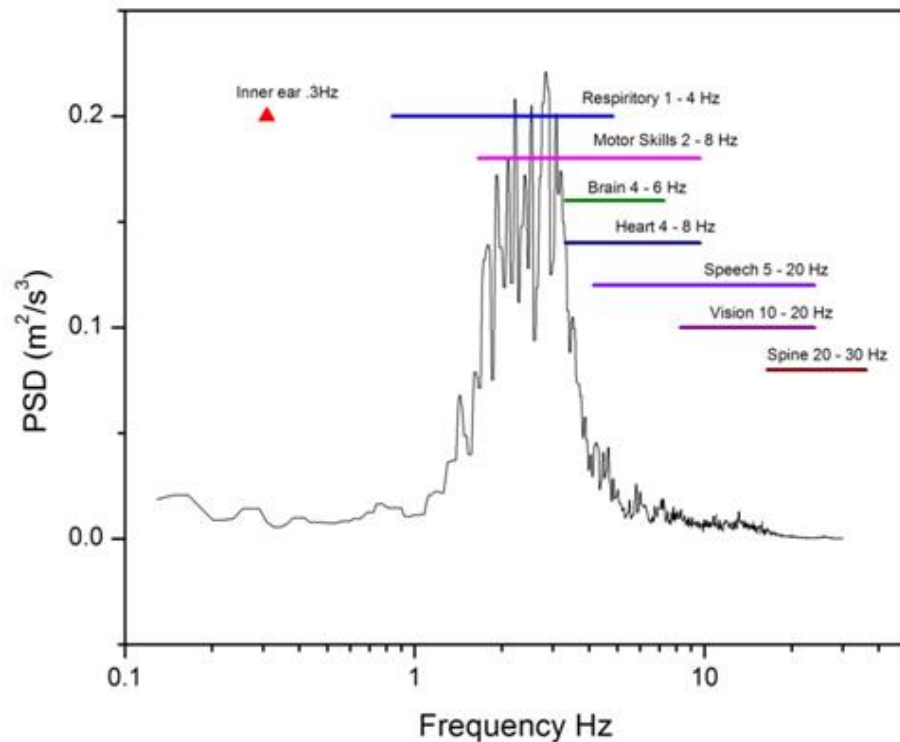
Figure 40. *Physiological effects of ambulance whole-body vibration frequencies superimposed on PSD graph of z-axis power spectral density, Amb. #3, >=65 MPH, Highway surface*

Effects on patient comfort

Effects of motor vehicle ride comfort are difficult to quantify since individual thresholds

of vibration perception vary from person to person. Some of the mitigating factors which affect

an individual's perception of vibration include body position, single- versus multiple-frequency

input, presence or absence of aural or visual inputs and duration of exposure to name just a few.

There is no universally accepted standard to judge the comfort of ride-induced vibration. Most

studies agree that the human body is most sensitive to vertical acceleration in the 4 – 8 Hz range,

so, some guidelines do exist (Gillespie, 1992). Wong (2008) provides some approximate values

of likely human qualitative responses to various levels of motor vehicle vibration. These are shown graphically in Figure 41, onto which has been superimposed the average z-axis vibration encountered in the ambulances measured in this study. From this graph we can observe that the average z-axis vibration amplitudes measured in this study would fall into a range which most individuals would agree is fairly uncomfortable. It should be noted that this represents a conservative estimate. When vibrations occur in multiple directions, the total value of frequency-weighted r.m.s. accelerations are most commonly used in determining comfort levels (Wong, 2008). A lower z-axis value was used here.
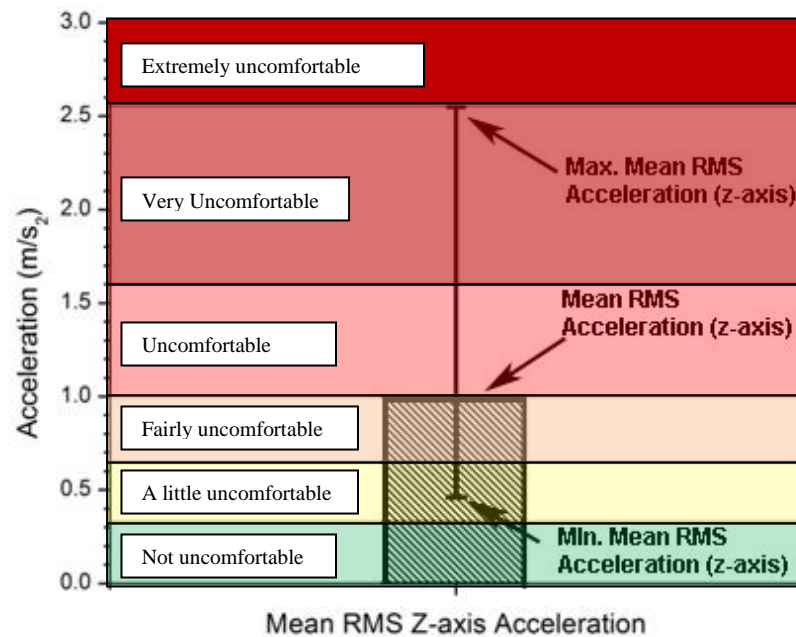
Figure 41. *Human comfort response to vibration amplitude superimposed on a graph of the mean r.m.s. z-axis accelerations measured in this study. Comfort values adapted from Wong, 2009, p. 474.*

Several studies have produced graphs of human comfort tolerance limits for vertical vibration which are frequency weighted. The results of two of these studies, the SAE J6a recommended human tolerance limits to ride vibration SAE, (SAEJ670e, 1978) and the

International Standard ISO 2631-1978(E), recommendations for the evaluation of human

exposure to whole-body vibration, are plotted in Figure 42. The SAE and ISO recommendations

represent the least and most tolerant of ride vibration values respectively. Any vibration

amplitude above the plotted red or black line would indicate a vibration amplitude which could

be considered uncomfortable. Superimposed on this graph are yellow and red areas which

represent the mean and peak z-axis vibration amplitudes measured as part of this study in the .12

to 6 Hz frequency range. The majority of mean r.m.s. acceleration values measured exceed all

the SAE tolerance limits and several of the ISO limits between 2 and 6 Hz. The mean peak

acceleration values exceeded both limits.
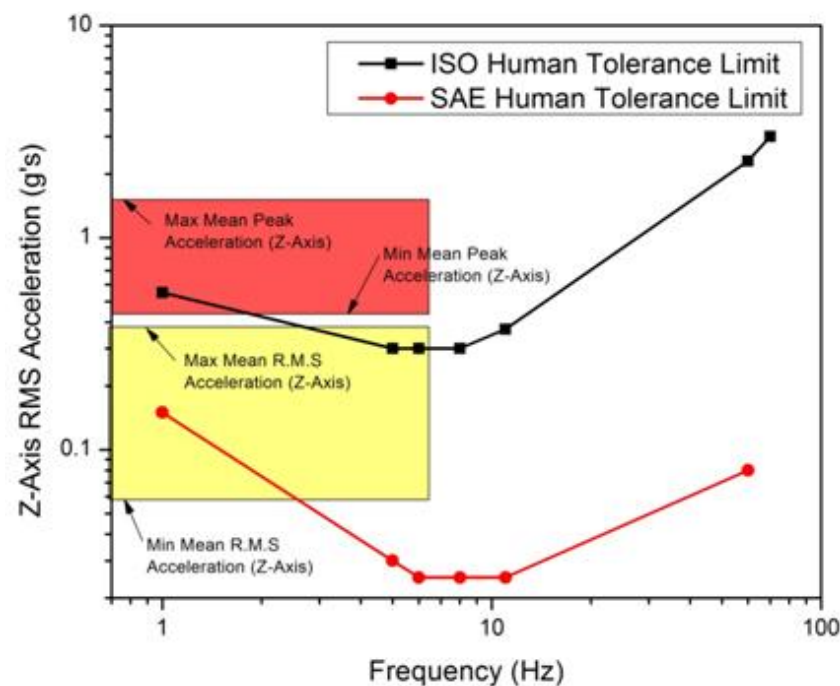
Figure 42. Human tolerance limits for vertical vibration with *the mean r.m.s. and peak z-axis*
accelerations measured in this study superimposed. Human tolerance values adapted
from Gillespie, 1992, p. 183

.

Effects on patient care

It has been established that significant errors due to whole-body vibrations can be

introduced to movement and visual control tasks involving the fine motor movements of hands

and arms. This is an important effect, since the degree of vibration-induced disturbance can

become the deciding factor in the ultimate success or failure of a task. This was important to this

study since so many ambulance-based patient-care procedures rely on the eye-hand coordination

of the emergency medical personal.

Plotted on Figure 43 is average eye-hand tracking error versus vibration amplitude

measured when test individuals were asked to perform a simple zero-order pursuit tracking task

while being exposed to first 3.5 and then 5.0 Hz excitations. The work was conducted by Lewis

and Griffin (1978).
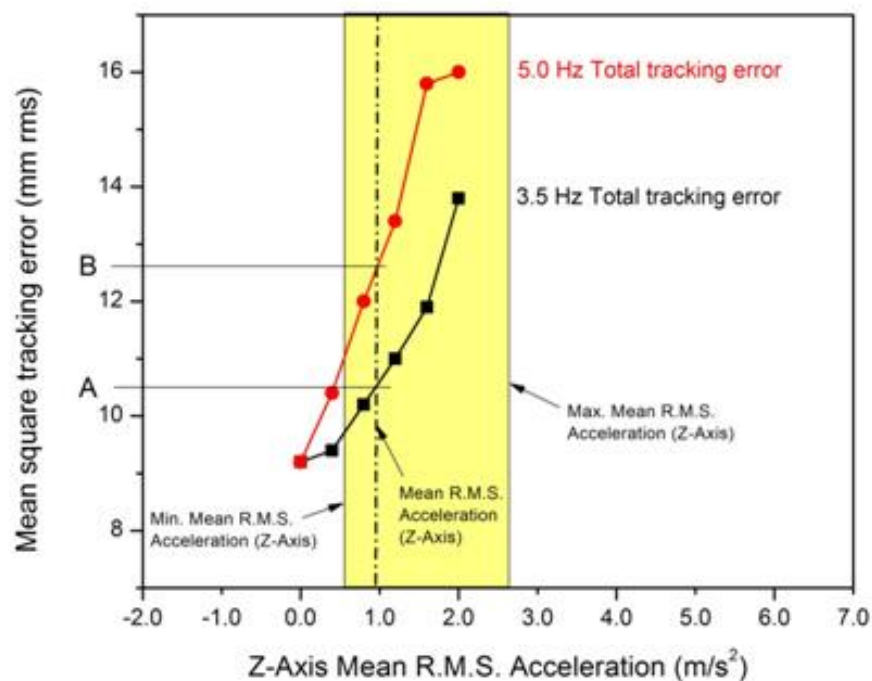
Figure 43. *Average tracking error associated with whole body vibration with the mean r.m.s. z-axis accelerations measured in this study superimposed. Tracking error values adapted from Griffin, 1990, p. 153.*

.

Superimposed on this graph is a yellow area which represents the mean r.m.s. z-axis

vibration amplitudes measured as part of this ambulance study in the .12 to 6 Hz frequency

range. The dotted vertical line represents the average value of the overall vibration. The left and

right edges of the box represent the minimum and maximum r.m.s. values. The intersections of

the dotted line with the Lewis and Griffin data for 3.5 Hz and 5.0 Hz excitations correspond to

total positioning errors at points A and B of approximately 10.5 mm at 3.5 Hz and 12.5 mm at

5.0 Hz, respectively. It should be noted that only overall vibration data was used in this

illustration, and that peak vibration data would be more severe.   As a practical matter, an error

of 10.5 to 12.5 mm is a significant impediment to the successful performance of various patient

care procedures commonly performed in emergency vehicle transport. This includes the

administration of IV medicines, airway management, various sticks and insertion of nasal

cannulas.

Plotted on Figure 44 are the results of a study which documents the interference of

whole-body vibration on the ability of individuals to hold cups of liquids without spilling. The

study was conducted by Whitham and Griffin (1978). The red line on the graph indicates the

vibration amplitude required for twenty-five percent of the test group to spill the liquid in

conical paper cups they were holding in a single hand. It should be noted that spillage of the

liquid was attributed to three major factors (1) the vertical vibration excitation transmitted to the

hand, (2) the cross-axis coupling of the vibration which caused horizontal motion of the hand,

and, (3) the excitation of the fluid in the cup at its natural resonance frequency. These three

factors were at a maximum at 4 Hz for the system which was studied.

Superimposed on this graph is a yellow area which represents the mean r.m.s. z-axis

vibration amplitudes measured as part of this ambulance study in the .12 to 6 Hz frequency

range. The dotted horizontal line represents the average value of the overall vibration. The

bottom and top edges of the box represent the minimum and maximum r.m.s. values. It can be

seen from the graph that spillage would have occurred in the ambulance compartments tested as

the level and frequency of vibration measured in those ambulances correspond to the amplitudes

and spectra associated with such an occurrence.
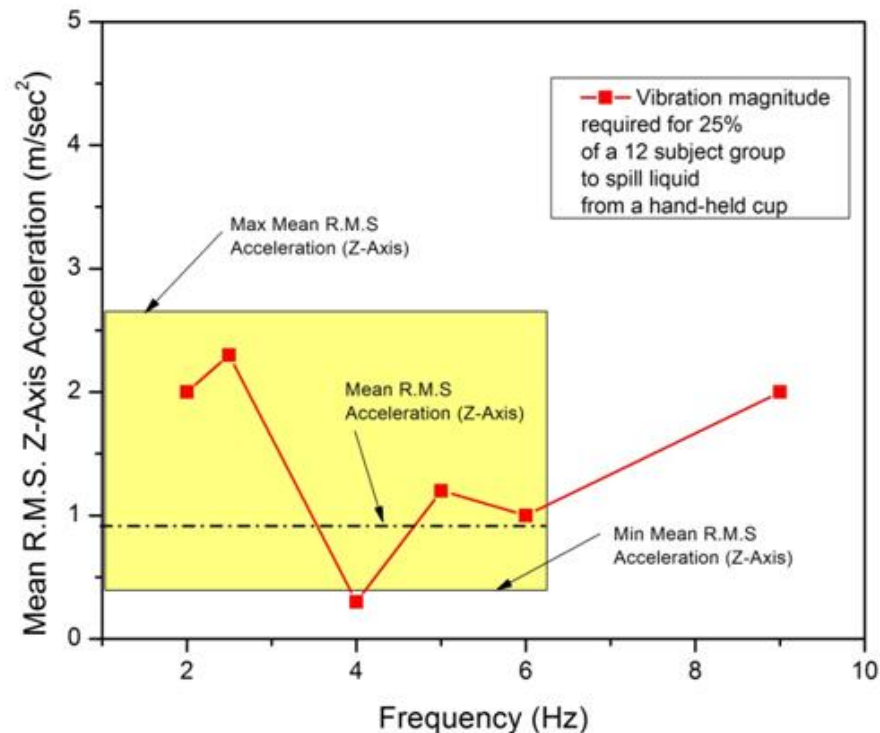
Figure 44. *Amplitude of z-axis vibration required for 25% of a group of 12 subjects to spill liquid from a hand-held cup with the mean r.m.s. z-axis accelerations measured in this stud superimposed. Spill data adapted from Griffin, 1990, p. 154.*

The ramifications of this finding for ambulance patient care are quite profound. The data

obviously suggest that the performance of simple motor tasks like holding a cup of water without

spilling it are difficult in a vibration environment like that found in the back of a moving

ambulance. Once again, the major amplitudes and frequencies encountered in ambulance

transport correspond to major effects associated with human motor control. beyond that,

however, the results at 4 Hz point to the importance of considering the natural frequency of any

system or devices which emergency service personal may be holding within the moving vehicle.

An otherwise benign, or even life-saving object may become a dangerous projectile if excited at

a particular frequency. Also this particular analysis clearly underscores the importance of considering cross-axis coupling effects which can amplify and obscure the dynamic effect of vertical vibratory excitation which is present in the ambulance compartment. A simple vertical jolt from a pothole could result in a lateral or fore-aft motion of a person or object in an unexpected way.

Figure 45 is plot of average percentage reading error of individuals subjected to vibrational excitations where both the subject and the display are in simultaneous motion. The study, carried out by Moseley and Griffin (1986), utilized 1.1 mm high characters at a viewing distance of 750 mm.

Superimposed on this graph is a yellow area that represents the mean r.m.s. z-axis vibration amplitudes which were measured from .46 to 2.55 m/sec^2 in the .12 to 6 Hz frequency spectrum. As shown on the graph, the range of reading errors corresponding to this vibration environment varied from a low of 30 percent at 1.0 m/sec^2 and 4 Hz to a maximum of almost 80 percent at 2.5 m/sec^2 and .4 Hz. These values all reside well within the envelope of vibration excitation experienced in the ambulance vibration tests of this study.

There are numerous negative implications of reading deficits on mobile patient care from decreased reading accuracy associated with interpreting medicine labels, equipment read-outs, medical devices, and the like. Even at the lowest vibration levels, errors are in the order of 30 missed characters out of 100. There is a similar vibration effect leading to increased reading times as well.
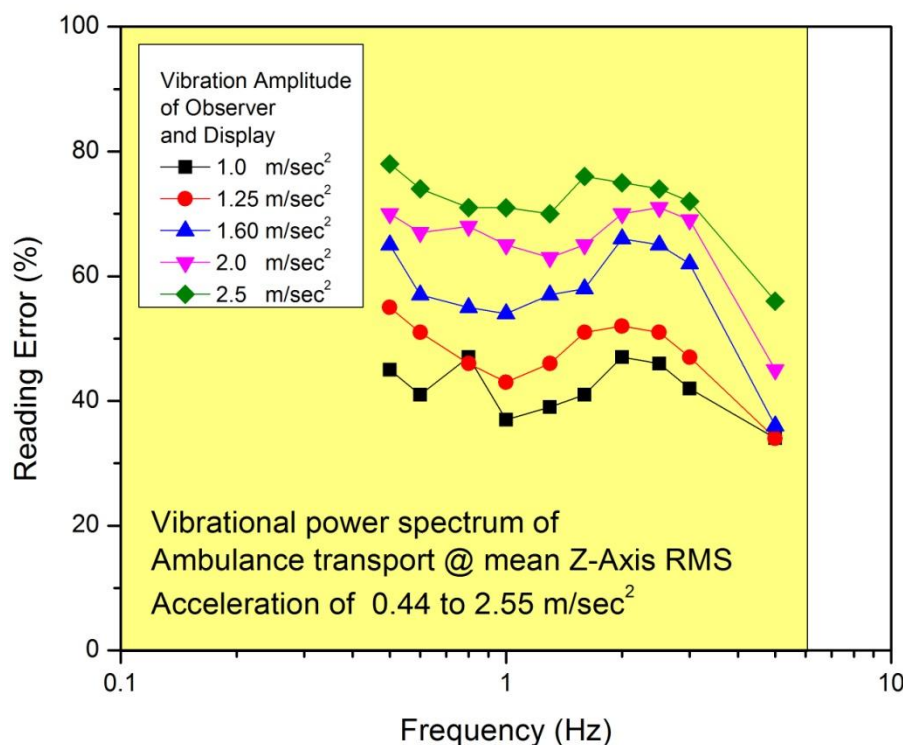
Figure 45. *Vibration spectrum of z-axis excitation and associated reading errors for simultaneous motion of observer and display with r.m.s. z-axis accelerations measured in this study superimposed. Data adapted from Griffin, 1990, p. 139.*

Figure 46 is an illustration of how writing legibility can be affected by various vibration amplitudes and frequencies. This is an excellent example of how complex hand-arm motor functions are disrupted by vibration due to the large displacements of that particular biodynamic system in the 4-8 Hz frequency spectrum. The superimposed PSD graph and histogram of mean r.m.s. z-axis vibration amplitudes measured in this study serves to further demonstrate the significant effect the measured vibration spectrum of ambulance travel has on the disruption of fine motor function. The associated negative effects on patient care include any medical procedure which involves fine motor control for emergency personnel to perform. It also limits or even precludes the use of certain sensitive medical diagnostic or life-saving devices such as

electrocardiograms (ECGs) or defibrillators which may require the ambulance to stop, and pull over prior to use.
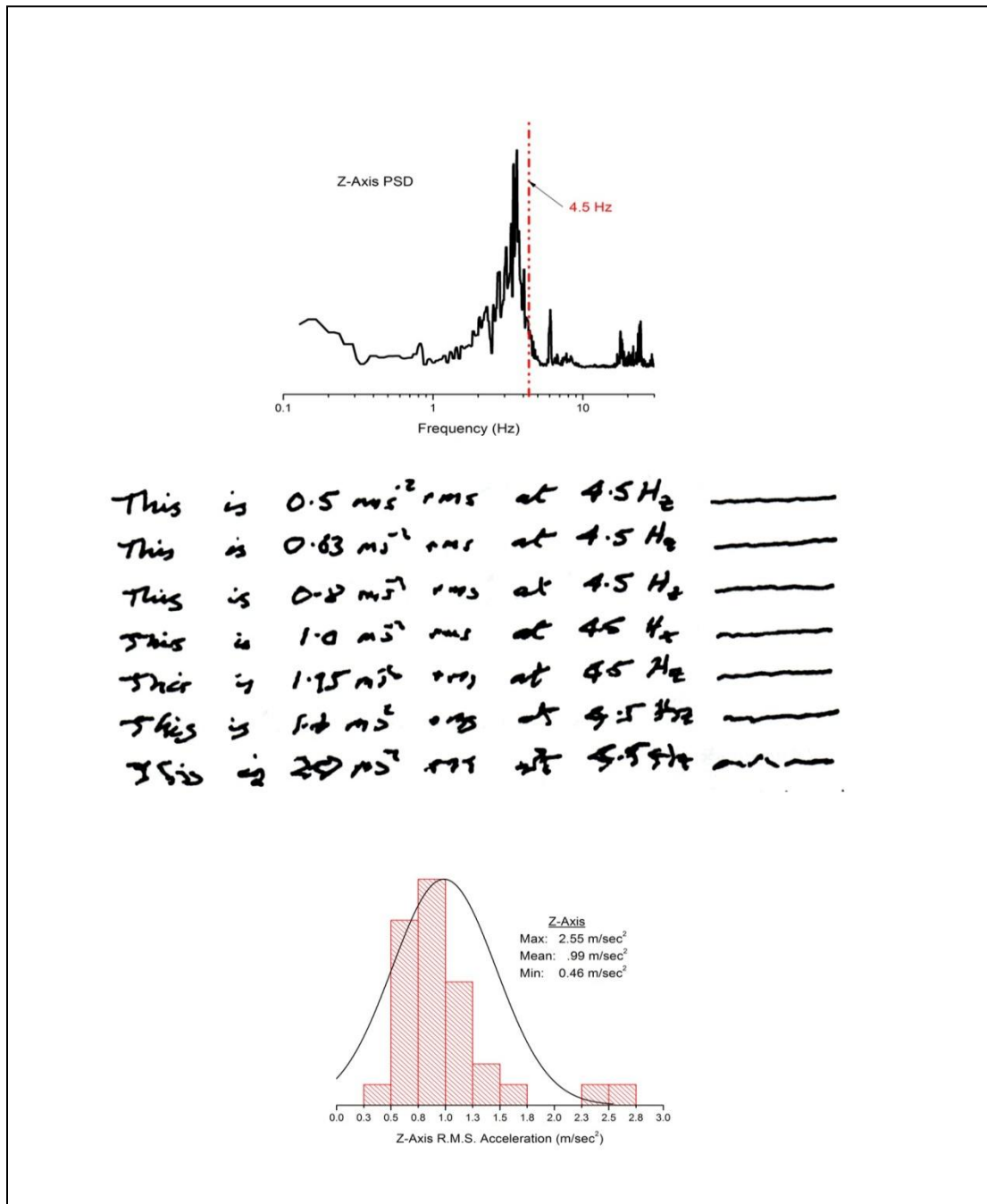
Figure 46. *Amplitude and frequency of ambulance vibration and examples of associated handwriting performance. Data adapted from Griffin, 1990, p. 139.*

5.5 Ride model development

A second goal of this study was to use the vibrational parameters described in section 5.3 to characterize road forcing functions to simulate typical ambulance travel over the undulating surface of a variety of common road surfaces at a broad range of frequencies to later verify and validate the computational model(s) of various potential vibration attenuation solutions.

The vibrations which are most crucial to this study, in terms of improving the safety, comfort, and care, are those which are in the low frequency ranges below 20 Hz, with special attention paid to the 1-10 Hz range, to which the human physiology is most vulnerable. Vehicle vibrations are typically categorized by frequency as "ride" (low frequency) and "noise" (high frequency). Even though noise is admittedly present even in low frequency excitations, ride is of paramount interest here, since it involves vibration in the frequency range of 0 to 25 Hz.(Gillespie, 1992, p. 125). An analytical vehicle ride model was developed in order to study the ride of a typical ambulance. An initial, generalized model of the ambulance is shown in Figure 47. It is a seven-degree-of-freedom (7-DOF) model which includes the pitch, roll and bounce of the body as well as the bounce of the two front wheels and the bounce and roll of the solid rear axle. The sprung mass is taken to be the mass of the entire body, while the unsprung mass includes the wheels and steering arms (Wong, 2008, p. 475).

The generalized 7-DOF model can be simplified to examining just one quarter of the vehicle, if it is necessary to consider only the major vertical motions of the vehicle (Wong, 2008, p. 476). This kind of model is often used in the initial phases of new suspension designs (Margolis & Asgari, 1991, p. 4).
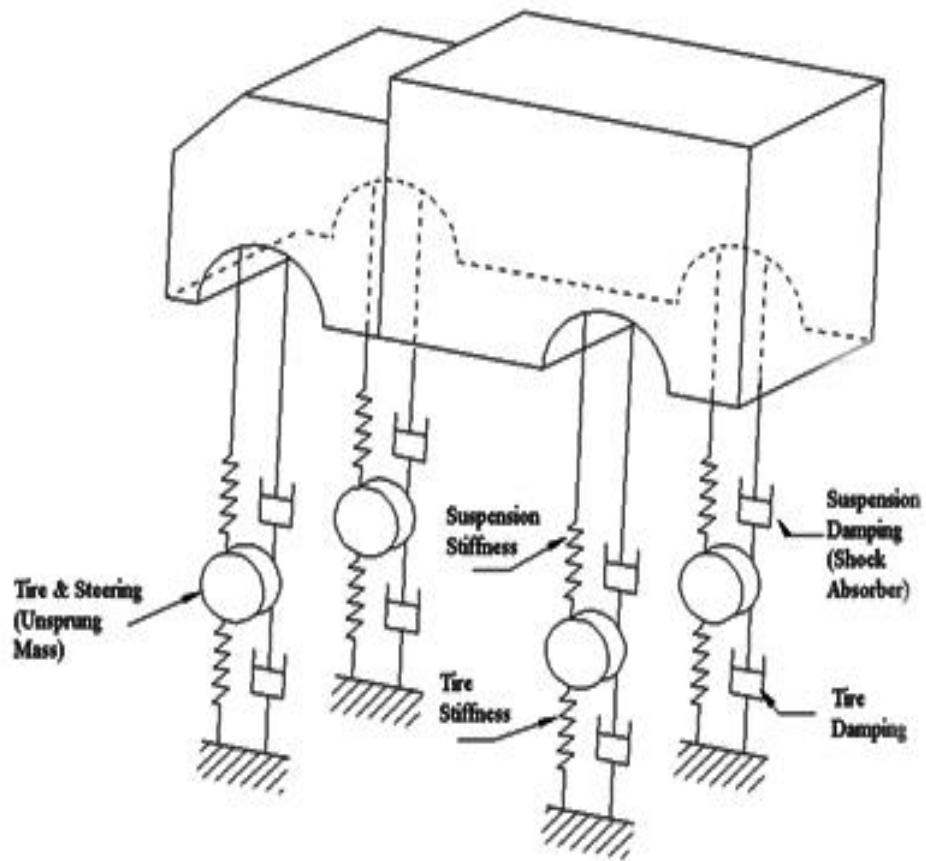
Figure 47. *7 degree-of-freedom ambulance ride model*

Because this model is used to represent one quarter of a vehicle, assuming that the front and rear tires can be uncoupled, it is often referred to as a "quarter car" model. It is shown graphically in Figure 48.

The quarter car model is considered an accurate model for the study of the essential features associated with passenger discomfort (vibration, vertical acceleration), road holding, and working space (Gobbi and Mastinu, 2001; Wong, 2008; Gillespie, 1992).
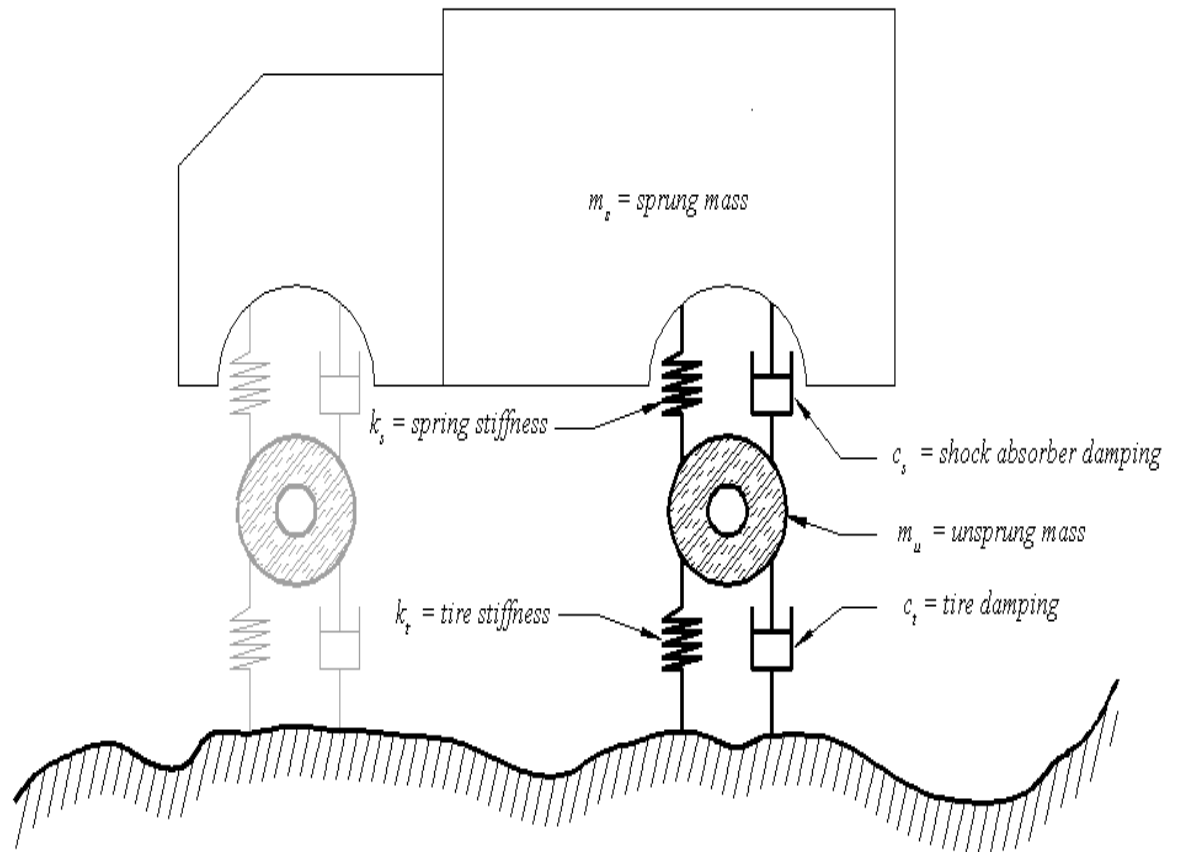
Figure 48. *quarter-car ambulance ride model*

The quarter car model is commonly studied with a single- or two- DOF analysis. A two-DOF model, as shown in Figure 48, assumes the tires are massless springs, but takes into account both the sprung and unsprung masses. This approach is considered adequate for analysis of systems experiencing excitations up to 30 to 50 Hz. (Genta, 1997, p. 392).
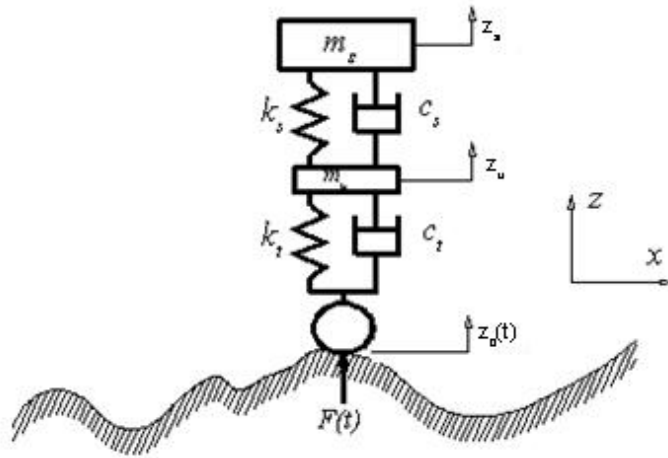
Figure 49. *2-DOF quarter car ride model of ambulance*

Figure 49 shows the two-DOF quarter car model, where:

m_s = sprung mass
m_u = unsprung mass
k_s = suspension stiffness
c_s = shock absorber damping
k_t = tire stiffness
c_t = tire damping
$z_g(t)$ = vertical displacement of tire at ground contact point
z_u = vertical displacement of unsprung mass, starting at equilibrium position
z_s = vertical displacement of sprung mass, starting at equilibrium position
$F(t)$ = excitation force acting on wheels due to profile of road surface

The single-DOF (SDOF) model used for this study, as shown in Figure 50, assumes the tires are rigid bodies and the only mass which is considered is the sprung mass of the vehicle. This is a suitable choice for studying the ambulance vibration in this study based on the following assumptions:

1. The vehicle vibrations of interest are only in the vertical direction.

2. The stiffness and damping effects of the tire can be neglected

3. The tire has good traction and never leaves the road surface (tire hop is not an issue).

4. The frequencies of interest to analyze are low, typically below 10 Hz, and in the

   neighborhood of the natural frequency of the sprung mass.
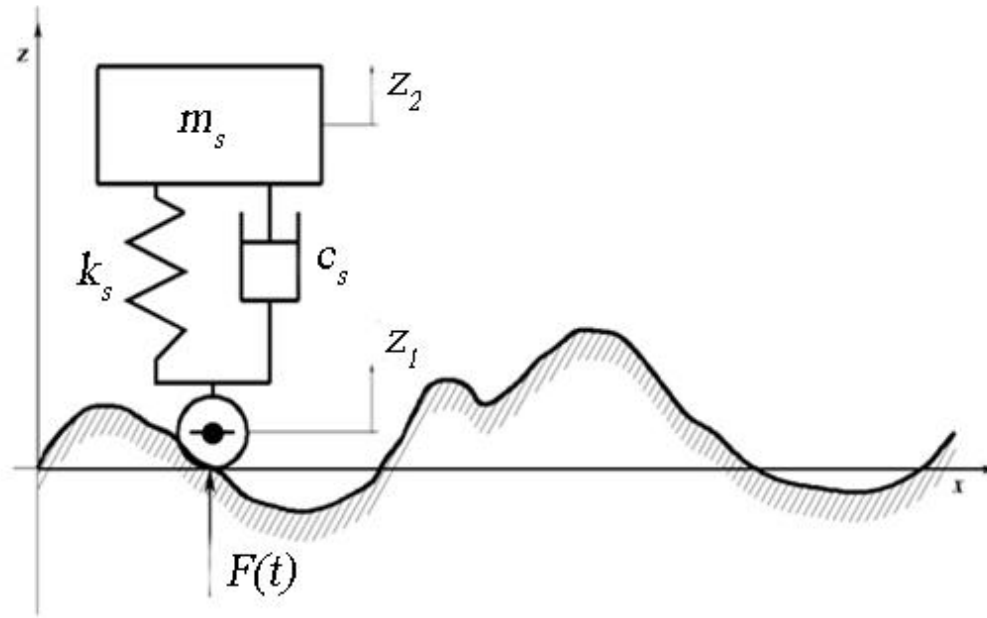
Figure 50. *SDOF quarter car ride model of ambulance*

For the SDOF quarter car model:

m_s = sprung mass
k_s = suspension stiffness (leaf springs)
c_s = shock absorber damping
z_1 = vertical displacement of tire at ground contact point
z_2 = vertical displacement of sprung mass, starting at equilibrium position
$F(t)$ = excitation force function acting on wheel due to profile of road surface

Model parameter values for the vehicles discussed in this study are shown in Table 22.

Table 22. *Ambulance quarter-car model parameters*

Parameter	SI Units
m_s – sprung mass	2137 kg
m_u – unsprung mass	50 kg
k_s = suspension stiffness	110 kN/m
k_t = tire stiffness	200 kN/m
c_t = tire damping	353 N·s/m
c_s = shock absorber damping	1500 N· s/m

Following the standard method of quarter vehicle ride model analysis for forced vibrations, such as those utilized by many researchers in the field, (Gobbi & Mastinu, 2001; Sun, Zhang, & Barak, 2002; Wong, 1993; Gillespie, 1992), an equation of motion for the sprung mass is attained from the derivation of Newton's Second Law.

$$F = ma \tag{5.1}$$

The free body diagram of the SDOF model is shown in Figure 51.
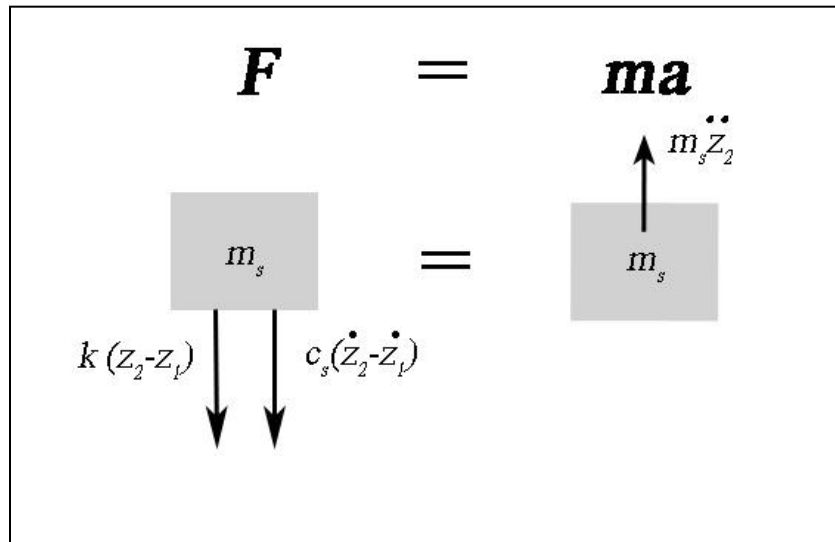
Figure 51. *Free body diagram of the sprung mass of the SDOF quarter car model*

The equation of motion for the system becomes:

$$m_s \ddot{z}_s + c_s(\dot{z}_2 + \dot{z}_1) + k_s(z_2 - z_1) = 0 \tag{5.2}$$

We can define the terms z, $\dot{z}$, $\ddot{z}$, such that they represent the relative displacements, velocities and accelerations, respectively, between the sprung vehicle mass and the tire at the road surface, thus:

$$z = z_2 - z_1 \tag{5.3}$$

$$\dot{z} = \dot{z}_2 - \dot{z}_1 \tag{5.4}$$

$$\ddot{z} = \ddot{z}_2 - \ddot{z}_1 \tag{5.5}$$

$$\ddot{z} + \ddot{z}_1 = \ddot{z}_2 \tag{5.6}$$

Substituting equations 5.3 – 5.6 into equation 5.2, and rearranging, yields the equation of motion in terms of the forcing function input determined experimentally in this study:

$$m_s \ddot{z} + c_s \dot{z} + k_s z = -m\ddot{z}_1 \tag{5.7}$$

Therefore, the forcing function may then be defined as:

$$F(t) = -m\ddot{z}_1 \tag{5.8}$$

Since the ambulance sprung mass, suspension stiffness and shock absorber damping constants were known (as shown in Table 24), measured values of acceleration, along with calculated velocities and displacements of the sprung mass were substituted into equation 5.7. In this way, the forcing function input force, $m\ddot{z}_1$, was calculated with respect to time for a representative sample of the ambulances, road surfaces, and vehicle speeds tested in this study.

A library of forcing functions, was created for the test cases shown in Table 23. Each file contained 30 seconds of data and roughly 5000 data points in time units of secs and force units of Newtons. The files were stored in Microsoft Excel CSV (comma separated values) format.

Graphical results of the dynamic modeling of ambulance 1 is shown in Figures 52 – 55 for highway travel at speeds between 36 and 64 MPH. The graphical output for the balance of

the library of forcing functions may be found in Appendix E of this dissertation.

Table 23. *F(t) Forcing function cases developed*

Ambualnce	Road Surface	Speed	File name
1	Highway	<= 35 MPH	forcing _hw_under35_amb1
1	Highway	36 - 64 MPH	forcing _hw_36-64_amb1
1	Highway	>= 65 MPH	forcing _hw_over 65_amb1
1	Secondary Road	<= 35 MPH	forcing_sec_under35_amb1
1	City Street	<= 35 MPH	forcing_city_under35_amb1
1	Unpaved Road	<= 35 MPH	forcing_unpaved_under35_amb1

Figures 52(a–c) graphically describe the motion of the vehicle sprung mass for ambulance 1 for a thirty second time interval as it traversed a highway road surface in the 36-64 MPH speed range.

(a)　　　　　　　　　(b)　　　　　　　　　(c)
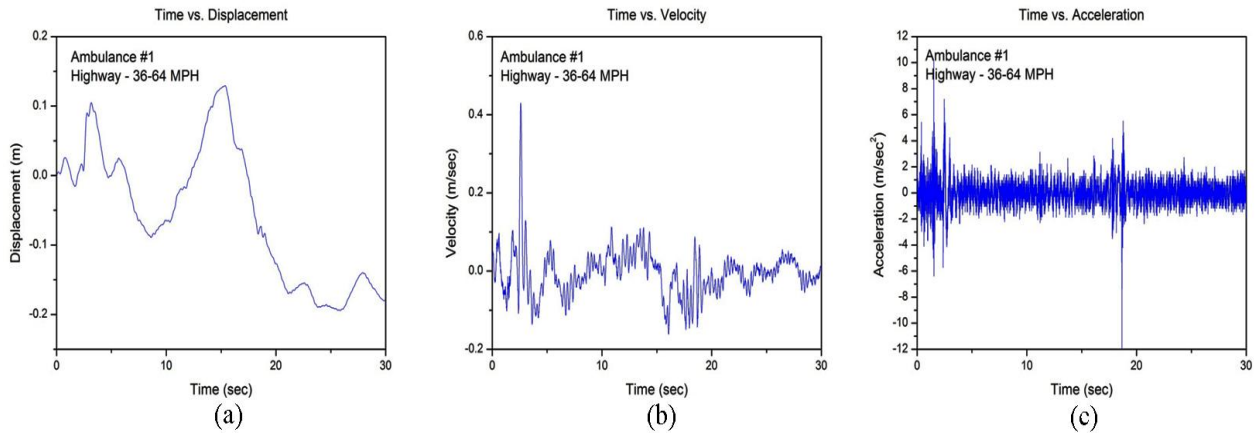
Figure 52. *The sprung mass (a) z-axis displacement, (b)z-axis velocity and (c) z-axis acceleration time history graphs for ambulance 1 for travel on a highway road surface.*

The vibration spectra for this case is shown in the PSD curve in Figure 52. In addition to the characterizations already put forward, it is well worth noting here, that even a brief perusal of the ambulance amplitude and spectral data will show a combination of both deterministic and random stationary signals emanating from the vehicles' engines and drive trains as well as non-stationary vibrations excited by the forcing functions attributable to road surfaces – especially in

the bandwidth of .1 to 20 Hz which involve the excitation of resonances and harmonics which have human physiological implications. The low frequency peaks in the spectra shown in Figure 53 are most certainly due to road induced vibration and contain periodic and quasi-periodic deterministic elements as well as random components of both a continuous and transient nature.
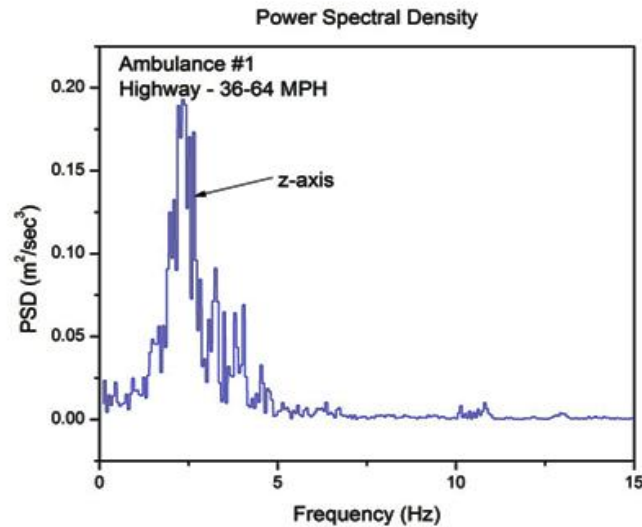
Figure 53. *Z-axis power spectral density graph for ambulance 1 for travel on a highway road surface.*

The forcing function for this case is shown in Figure 54. The noise in the signal is evident. It is highly instructive to consider one additional analysis, the phase portrait, achieved by plotting
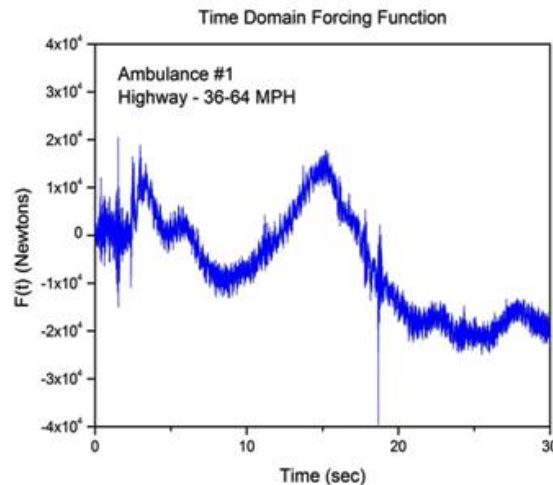
Figure 54. *Time domain road forcing function in the vertical z-axis for ambulance 1 for travel on a highway road surface.*

the sprung mass velocity vs. displacement. This is found in Figure 55.
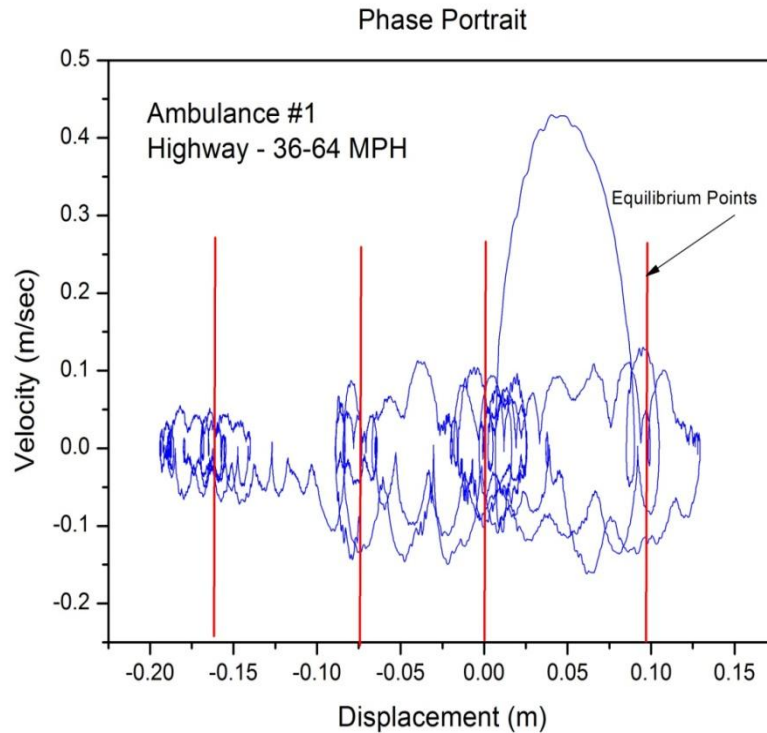
Figure 55. *Phase portrait plot for ambulance 1 for travel on a highway road surface.*

The phase portrait shown in Figure 55 indicates inherent stability in the system, yet it also includes the presence of at least four equilibrium points (denoted by vertical red lines in the graph).   The multiple equilibrium points allow us to conclude that non-linearities must exist in the system.   As verified by this study's empirical tests, the accelerations experienced in the ambulance patient compartment were unsustainable. It can only be concluded that the current ambulance suspension system is inherently incapable of producing the level of vibration isolation required – especially in the critical low frequency sprectrum. There were frequency elements in the output which were not present in the input signal. This was borne out by the fact that the same low frequency z-axis peaks appeared in every test run regardless of speed or road surface.

The presence of the aforementioned non-linearities as well as the deterministic suggests that vibration attenuation in addition to what is currently provided on modern ambulances should be provided. Due to design constraints inherent in current designs, a supplimentary system of isolation is a logical alternative. Whatever the solution, some non-linear damping and non-linear restoring force will be required along with control elements to offset both the deterministic and stochastic elements of the random (white noise) components present in the road excitations.

5.6 Force plate model and design

The third and final goal of this study was to model a force field domain control system (FFDCS) embodied in a force plate design capable of working in tandem with a standard ambulance suspension system to attenuate the most harmful vibrations encountered by such a vehicle in normal service.

This study has shown a standard ambulance chassis, possessing the suspension parameters similar to the test vehicles used, is incapable of adequately and reliably attenuating some of the road excitations commonly encountered by the vehicle. These excitations have also been shown to potentially have a negative effect on patient safety, care and comfort.

The suspension stiffness required to support the typcial 4309 kg payload of the ambulance patient compartment is currently borne by a dependent rear suspension comprised of a solid axle and two multi-leaf, single-stage leaf springs with a ground rating of 4286 kg (9450 lbs) (2008 Ford Trucks body builders layout book, 2007, p58) . The rating is a function of leaf spring design parameters including length of the spring, thickness of the spring, and the width of the spring. The vertical spring rate of leaf spring/solid axle rear suspension systems is high in order to carry the high payloads associated with a Type I or Type III ambulance. More compliant, independent designs would not provide the necessary stiffness.

All ambulances manufactured in the United States must comply to the 2007 federal specification for the star-of-life ambulance, KKK-A-1822F which is promulgated by the U. S. General Services Administration (2007). This standard "identifies the minimum requirements for new automotive Emergency Medical Services (EMS) ambulances (except military field ambulances) built on Original Equipment Manufacturers Chassis (OEM) that are prepared by the OEM for use as an ambulance" (2007, p. 1). The important requirements salient to this study include those listed in Table 24.

Table 24. *Selected federal Star-of-Life standard ambulance requirements*

Requirement	Description
3.4.4 Vehicle Performance	"The ambulance shall provide a smooth, stable ride. When available from the OEM, automatic vehicle stability control (AVSC) shall be furnished."
3.4.5 Speed	"The vehicle shall be capable of a sustained speed of not less than 65 mph over dry, hard surfaced level roads, at sea level, and passing speeds of 70 mph when tested under normal ambient conditions."
3.4.10.6 Floor height	"The finished floor (loading) height shall be a maximum of 34"."
3.5.2 Payload capacity	For dual rear wheeled, modular ambulances (Type I or III) 1750 lbs. / 794 kg minimum
3.6.5.6 Suspension	"Vehicle shall be equipped with laterally matched sets (front and rear) of spring, torsion, or air-suspensioin system components. Components shall have a rated capacity in excess of the load imposed on each member. Only corrections permitted by the OEM to compensate for lean due to normal spring tolerance variations are permitted. Correction of lean due to imbalance is not permitted."
3.6.5.7 Spring stops	"Stops or bumpers must be supplied to prevent the wheel and axles from striking the engine, oil pan, fenders, and body under all conditions of operation."
3.6.5.8 Shock absorbers	"Shock absorbers, double-acting type, heaviest duty available from OEM for model offered, shall be furnished on the front and rear axles."

Figure 56 is a drawing of a typical ambulance chassis (Ford F-550 Super Duty) showing the critical distance from the ground to the top of the chassis, which, at 33 in. (838.2 mm), only provides 1 in. of working space to get to a 34 in. (863.6 mm) finished floor loading height specified in paragraph 3.4.10.6 of KKK-A-1822F.
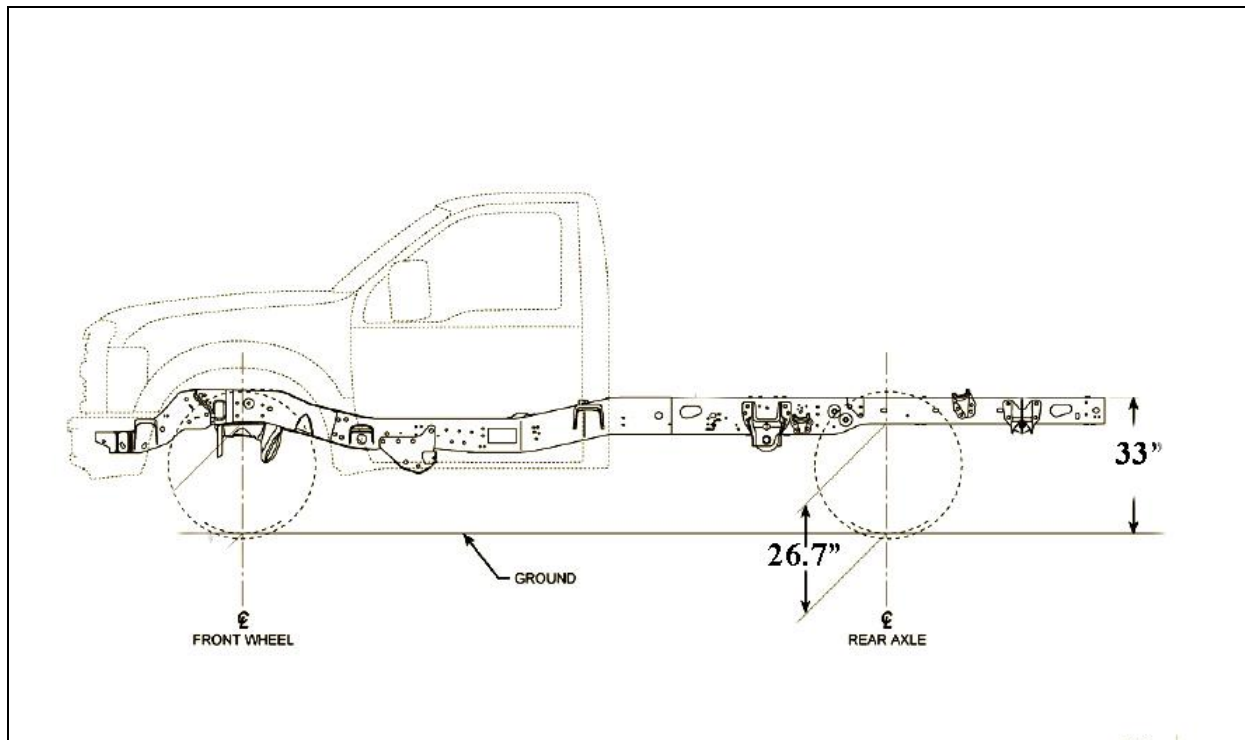
Figure 56. *Ground height of Ford 2009 F550 Super Duty Chassis*

When payload and floor design constraints are considered, the choices available to the suspension designer eliminate many of the options which provide the smoothest and most compliant rides: namely those independent systems which lack stiffness or the air suspension systems which require a generous amount of working space between the axle and body floor.

One possible solution to controlling ambulance vibrations is a secondary vibration attenuation system to augment the standard ambulance suspension system which could operate within the design space required. The force plate could be fit within the existing structure of a

typical chassis as shown in Figure 57.
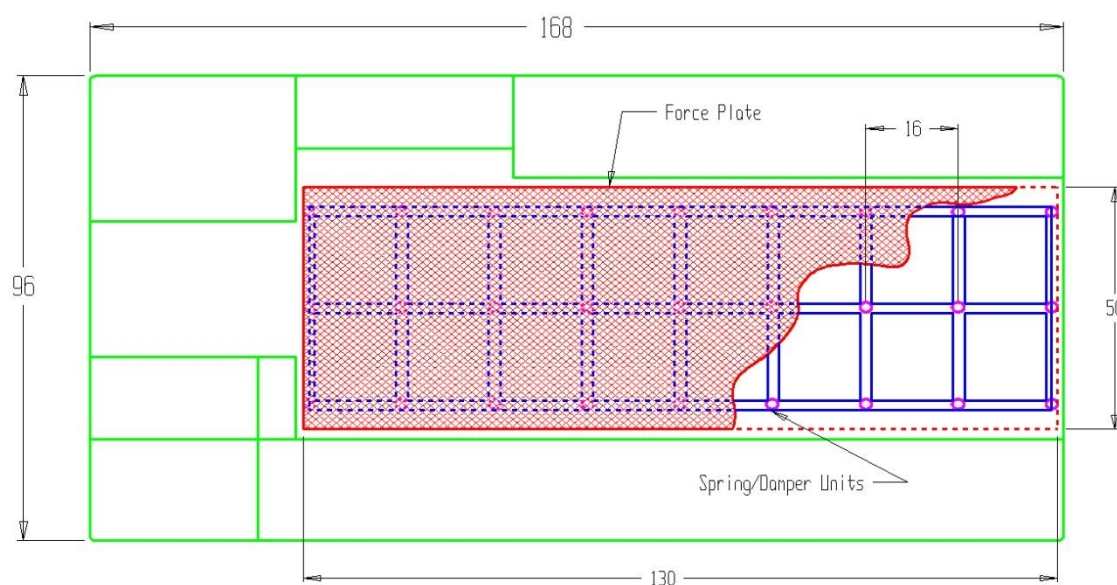
Figure 57. *Top view of force plate fitted into the interior of a 167 in. ambulance compartment*

Such a secondary vibration attenuation system could use a combination of passive and active components to control the acceleration forces within the patient compartment of the ambulance, creating a field devoid of provocative excitation forces, hence the name, force field domain control system (FFDCS). The FFDCS could lead to a safer, more comfortable patient environment where medical interventions could be carried out with greater precision and effectiveness.

In its simplest form, the FFDCS concept could be embodied in a force plate mounted to the existing floor of a standard ambulance patient compartment. It would consist of two, thin plates which would sandwich active hydraulic and passive spring/damper elements to attenuate vibrations and shocks in response to the accelerations produced by road irregularities. The concept of operation is illustrated in Figure 58.
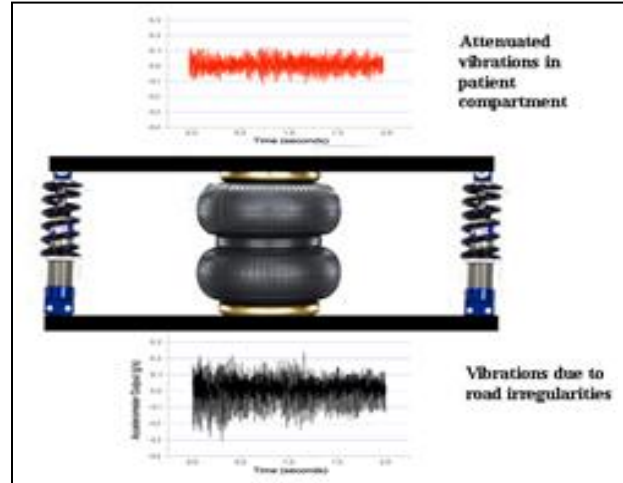
Figure 58. *Force plate concept of operation*

Figure 59 illustrates a force plate fitted in a 167" ambulance compartment.
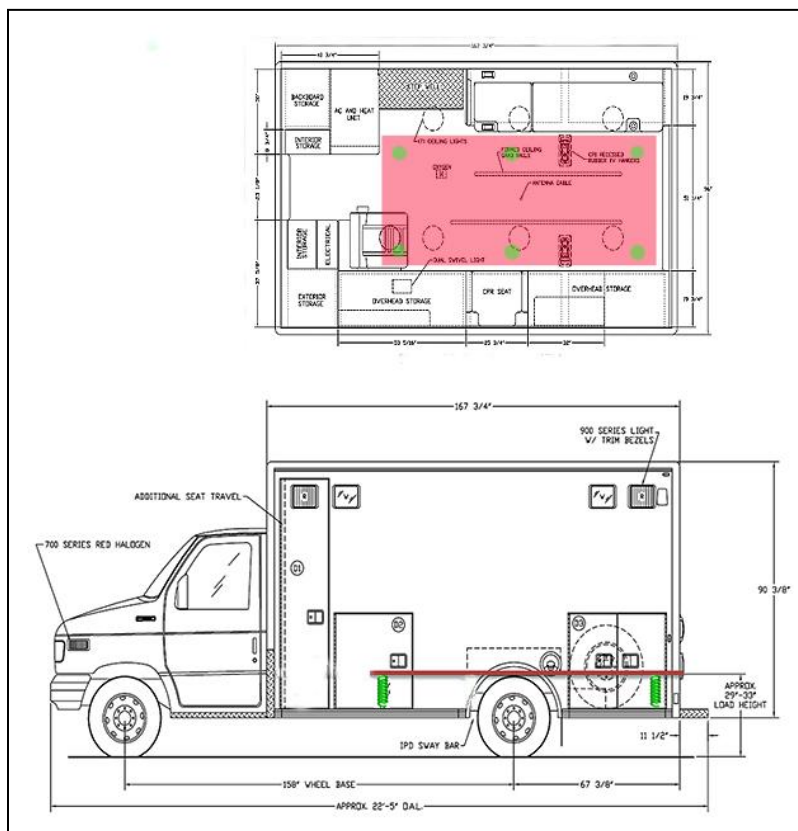
Figure 59. *Force plate shown fitted in a 167" ambulance patient compartment*

The force plate concept can be used to demonstrate the development of a control law for effective automatic control of an ambulance force attenuator. The force plate as conceived in this study utilizes both active and passive elements for spring and damping. The system was modelled in order to develop a control law which can be used in futue work to determine if reliable and stable control of such a system is feasible and to identify the stiffness, damping coefficients as well as the intensity parameter of the stochastic elements of control. The control system block diagram is shown in Figure 60. Active spring/damper hydraulic, pneumatic or electric actuators, (hydraulic units are shown in Figure 60 for illustrative purposes only), could be used to effect plate displacement through microprocessor control based on a wide variety of possible input singles. These could include: the position, velocity or acceleration of the vehicle's sprung or unsprung mass, or both, manual actuation from the dashboard, pre-stored or possibly real-time road condition information.
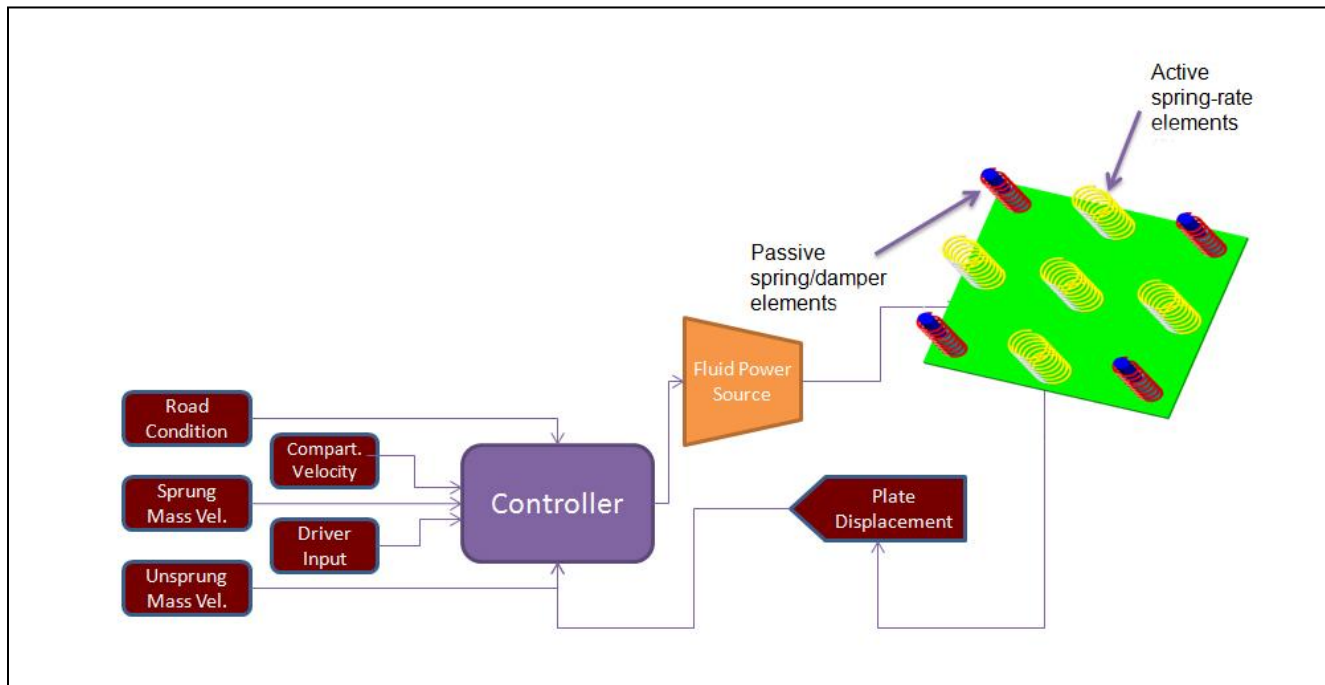
Figure 60. Control block diagram of force plate

A generalized model of an ambulance with a force plate installed is depicted in Figure 61.
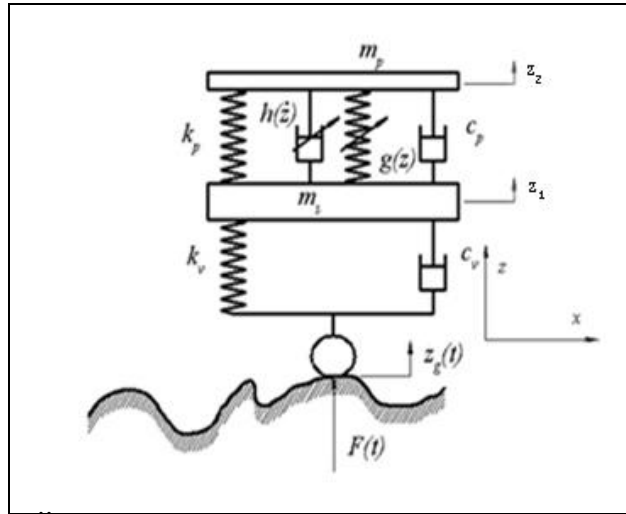
Figure 61. *FFDCS force plate vibration model*

In this model, the native ambulance suspension model has been reduced to the single

DOF system described in section 5.5 of this study with the force plate model imposed on top of

it. So for the vehicle and force plate we have:

m_s = sprung mass of vehicle
m_p = mass of force plate and supported load
k_v = stock vehicle stiffness
c_v = stock vehicle damping
k_p = passive stiffness of force plate
$g(z)$ = active stiffness of force plate
$h(\dot{z})$= active damping of force plate
c_p = passive damping of force plate
$z_g(t)$ = vertical displacement of tire at ground contact point
z_1 = vertical displacement of ambulance, starting at equilibrium position
z_2 = vertical velocity of force plate mass, starting at equilibrium position
$F(t)$ = excitation force acting on wheels due to profile of road surface

If just the force plate is considered, the resulting equation of motion is of the form

$$m_p\ddot{z}_2 + c_p\left(1 + g(\dot{z}_1,\dot{z}_2)\right)(\dot{z}_2 - \dot{z}_1) + k_p(1 + h(z_1,z_2))(z_2 - z_1) \tag{5.9}$$

$$= u(z_1,z_2,\mu + \sigma_0\gamma(t))$$

Where:

$g(\dot{z}_1, \dot{z}_2) = $ non-linear damping function
$h(z_1, z_2) = $ non-linear restoring force
$u(z_1, z_2, \mu + \sigma_0 \gamma(t)) = $ control law
$\mu = $ deterministic bifurcation parameter
$\sigma_0 = $ noise intensity parameter
$\gamma(t) = $ stochastic noise function

z can be defined as:

$$z = z_2 - z_1, \quad z_2 > z_1$$

While, the natural frequency and the damping ratio of the system can be given

as:

$$\omega_n = \sqrt{\frac{k_p}{m_p}}, \quad \xi = \frac{c_p}{2\sqrt{m_p k_p}}$$

Using these definitions and substituting them into Equation 5.9, yields the complete

equation of motion for our force plate model:

$$\ddot{z}(t) + 2\xi \omega_n \big(1 + g(z, \dot{z})\big)\dot{z}(t) + \omega_n{}^2\big(1 + h(z)\big)z(t) \quad (5.10)$$

$$= -\ddot{z}_1(t) + \frac{\omega_n{}^2}{k} u\big(z(t), z(t - \tau), \dot{z}(t), \mu + \sigma_0 \gamma(t)\big)$$

The control law for the force plate is simply the right-hand side of Equation 5.10, or:

$$-\ddot{z}_1(t) + \frac{\omega_n{}^2}{k} u(z(t), z(t-\tau), \dot{z}(t), \mu + \sigma_0\gamma(t))$$

(5.11)

Where:

$-\ddot{z}_1(\text{t}) = $ ambulance vertical forcing function
$z(\text{t}) = $ ambulance vertical displacement
$z(\text{t}-\tau) = $ ambulance vertical displacement with time delay, τ
$\dot{z}(t) = $ ambulance vertical velocity
$\mu = $ deterministic bifurcation parameter
$\sigma_0\gamma(t) = $ stochastic noise term

The model can now be used to determine the dynamic design parameters to create a workable, safe force plate. The ambulance displacements, velocities and accelerations for any of the vehicle, road surface and speed combinations which were measured for this study can be used to design the plate for service in a variety of environments.

The presence of the time delay term in Equation 5.11 will require its dimensional reduction into finite dimensional nonlinear, stochastic differential equations. This reduction process can be accomplished by using the mathematics outlined in papers dealing with the stability of time delay systems as described by Fofana and others (Fofana & Ryoba, 2000; Fofana, M. S., 2002; Fofana, M. S., 2003; Fofana, Ee, & Jawahir, 2003; Fofana & Ryoba, 2003). These papers provide the methodology to locate and interpret the damping, stiffness, stochastic, and time delay parameters necessary to design a force plate to provide a safer and more comfortable vibration environment within an ambulance patient compartment.

6.0 Conclusions and future work

6.1 Conclusions

As a result of this dissertation:

1. The vibrational amplitude, frequency and energy of a typical ambulance ride, were experimentally determined and related to the corresponding human physical impacts on ambulance passengers and EMT crews.

2. The experimentally derived vibration data were used to characterize road forcing functions that simulate typical ambulance travel over the undulating surface of a variety of common road surfaces and to create a mathematical model of a vibration attenuation solution.

3. The design of a force plate capable of working in tandem with a standard ambulance suspension system to attenuate the most harmful vibrations encountered by such a vehicle in normal service was used as an example in order to demonstrate the utility of the model in the design process

This study uniquely characterized, quantitatively the vibration amplitude, frequency and energy of the accelerations experienced in a typical ambulance. Average vertical vibration amplitudes of .46 to 2.55 m/sec^2 were recorded in the patient compartment of four ambulances over four road surfaces at three speed settings. Power spectrum analysis of the data revealed that the vibration energy and resulting vertical acceleration forces were concentrated in the .1 to 6 Hz range.

These average acceleration forces could have potentially negative medical implications to patients with a variety of compromised health conditions. They were in excess of what is considered to be a normal human comfort level for vibration, and most definitely were in a

vibration spectrum which could present impediments to performance for the medical team on-board. The vibration levels measured all had ramifications for the safety, comfort and care of ambulance patients.

Phase portrait analysis combined with the power spectrum data revealed the presence of nonlinearities, stochastic fluctuations and time delays inherent in the data. A unique analytical model was developed that accommodates these non-linearities, random events (both transient and continuous) and time delays.

The example of a force field domain control system embodied in a force plate and its associated control system was used a test case for the model. A sample control law equation was developed for the force plate concept. The ambulance displacements, velocities and accelerations for any of the vehicle, road surface and speed combinations which were measured for this study can be used to verify, validate and realize a wide variety of active vibration isolation systems for ambulances. This is done by using the model to calculate parameters necessary for the stable control of systems to significantly improve ambulance ride comfort and enhance all aspects of mobile patient care. This could take the form of a vibration absorbing force plate fit over the existing ambulance floor, or any number of other vibration absorbing or active vibration cancelling devices.

6.2 Future work

1. A more detailed and encompassing design effort should further analyze the technical and economic feasibility of the FFDCS force plate concept. A full set of functional requirements should be developed. Design inputs from a Quality Function Deployment analysis, a dimensional study of working space

requirements, material selection and processing as well as a human factors and failure modes and effects analysis should be conducted.

2. A marketing study to judge the viability of a ambulance vibration attenuation system should be completed. The $360,000,000 US market is split among 24 major ambulance builders in North America who are all upfit manufacturers. There are 45,000 ambulances currently in service in the US, and they answer about half a million 911 calls each day. This could indicate a significant retrofit market.

3. In addition to abating vibrations in the ambulance interior, it is possible to employ this research model to improve the design and performance of any medical or life-saving equipment which must be used in a mobile environment, including a whole host of vibration-resistant health monitoring systems.

4. A more complete ambulance vibration design methodology could be undertaken to expand the usefulness of the model created by this study. This methodology could determine the effect of dynamic system parameters (damping, stiffness, time delay, stochastic, etc.) on the overall system reliability computed by measuring the Floquet Index and moment Lyapunov exponent against both deterministic and stochastic road disturbances. The resulting computations could then be used to establish the criteria for the stability index and sustainable control of the system for future determination of improved methods of road disturbance isolation.

5. A variety of non-vibration design parameters should be investigated, such as alternate solutions. These could include:

    a. Vibration isolating stretchers and mattresses

    b. Alternative stock suspensions for ambulances

c. Vibration absorbing materials

d. Active vibration cancelling devices

e. Smaller, lower payload ambulance design which could utilize softer suspensions

The broader significance of this work lies in enhancing the patient-centered care associated with ambulance travel by improving patient comfort and safety through the assessment and administration of mobile medical interventions with improved precision, accuracy and safety.

7.0   References

2008 Ford Trucks body builders layout book. (2007). *2008 Dimensional data E-350/450 super duty cutaway 158" wheelbase (DRW)*. .

Amman, S., Pielemeier, B., Snyder, D., & Toting, F. (2001, April 30). *Road vibration investigation using the ford vehicle vibration simulator.* 2001-01-1572 presented at the SAE Noise and Vibration Conference and Exposition, Traverse City, Michigan: Society of Automotive Engineers.

Andrew, M., M, D., Yuenquan, C., Faith, G., Biraj, B., & Charles, L. (1995). Vibration and noise in pediatric emergency transport vehicles: A potential cause of morbidity? *Aviation, Space and Environmental Medicine, 66*(3), 212-219.

B. G. Kao, & P. R. Perumalswami. (1997, April 8). *A hybrid road loads prediction method with full vehicle dynamic simulation.* 971513 presented at the X International Conference on Vehicle Structural Mechanics and CAE, Troy, Michigan: Society of Automotive Engineers.

Barak, P. (1991, September 16). *Magic numbers in design of supensions for passenger cars.* Presented at the Passenger Car Meeting and Exposition, Nashville, TN: Society of Automotive Engineers.

Bellieni, C. V., Pinto, I., Stacchini, N., Cordelli, D. M., & Bagnoli, F. (2004). *Minerva Pediatrics, 56*(2), 207-212.

Best, G., Zivkovic, G., Ryan, G., &. (1993). Development of an effective ambulance patient restraint. *Society of Automotive Engineers Australasia Journal, 53*(1), 17-21.

Brauer, R. L. (1994). *Safety and health for engineers.* New York, New York: John Wiley and Sons, Inc.

British Standards Institution 1987 BS 6841. (1987). Measurement and evaluation of human exposure to whole body vibration.

Brown, L. H., Gough, J. E., Bryan-Berg, D. M., & Hunt, R. C. (1996). Assessment of breath sounds during ambulance transport. *Annals of Emergency Medicine, 29*(2).

Brown, T. L., Mear, S. T., Moore, N. E., Kannapan, S. M., Marshek, K. M., Cuderman, J. et al. (1992, September 28). *An experimental procedure for estimating ride qulatiy for passive and semi-active suspension automobiles.* 922141 presented at the SAE Worldwide Passenger Car Conference and Exposition, Dearborn, Michigan: Society of Automotive Engineers.

Capt, J. G. C., USAF, M., Capt, J. D. W., USAF, M., William, B. H., Jr., M, D. et al. (1967). Initial cardiovascular response to low frequency whole body vibration in humans and animals. *Aerospace Medicine, 38*(5), 464-467.

Clarkson, L. (1986). *Ambulance safety stablizer harness for para-medics* (USPatent 4563023). .

Cotnoir, P., & Fofana, M. (2009, July 23). *Ambulance vibration suppression via force field domain control.* Presented at the WPI/University of Massachusetts Emergency TransCare Medical Services (ETMS) Ambulance Team, University of Massachusetts Medical Center, Worcester, MA.

Cullen, C. H., Douglas, W. K., & Danzinger, A. M. (1967). Mortality of the ambulance ride. *British Medical Journal, August 12,* 438.

Davis, J. (2003). The bleeding edge. *Wired, 11(05),* 12.

Dupuis, H. (1969). Zur physiologischen beanspruchung des menschen durch mechanische schwingungen. *Fortschritt Berichte, VDI-Z 1*(7).

Eklund, G. (1972). General features of vibration-induced effects on balance. *Upsala Journal of*

Medical Science, 77, 112-124.

Elling, R. (1989). Dispelling myths on ambulance accidents. *JEMS, 14*(7), 60-64.

Ernsting, J. (1961). *Respiratory effects of whole-body vibration. IAM Report 179* (Institute of
    Aviation Medicine). . Farnborough.

Fofana, M. S., and Ryba, P. B., (2000) . On the numerical solutions of machine-tool chatter with multiple
    delays, *ASME International Mechanical Engineering Congress and Exposition Symposium on
    Manufacturing Engineering*, MED-11, 149-155.

Fofana, M. S., (2002). Aspects of stable and unstable machining by Hopf bifurcation, *Journal of
    Applied Mathematical Modelling,* vol. 26, 953-973.

Fofana, M. S., (2003). Delay dynamical systems and applications to machine-tool chatter, *Chaos,
    Solitons & Fractals*, , vol. 17, 731-747.

Fofana, M. S., Ee, K. C., and Jawahir, I. S., (2003). Machining stability in turning operation
    when cutting with a progressively worn tool insert, *Wear Journal* vol. 255, 1395-1403.

Fofana, M. S. and Ryba, P. B., (2003), Parametric stability of nonlinear time delay equations,
    International Journal of Non-linear Mechanics, vol. 39, 79-91.

Genta, G. (1997). *Motor vehicle dynamics: Modeling and simulation.* River Edge, NJ: World
    Scientific Publishing Co. Pte. Ltd.

Gilad, I., & Bryan, E. (2007). Ergonomic evaluation of the ambulance interior to reduce
    paramedic discomfort and posture stress. *Human Factors, 49*(6), 1019-1032.

Gillespie, T. D. (1992). *Fundamentals of vehicle dynamics.* Warrendale, PA: Society of
    Automotive Engineers.

Gobbi, M., & Mastinu, G. (2001). Analytical description and optimization of the dynamic
    behavior of passively suspended road vehicles. *Journal of Sound and Vibration, 245*(3),
    457-481.

Gobbi, M., Levi, F., & Mastinu, G. (2006). Multi-objective stochastic optimisation of the suspension system of road vehicles. *Journal of Sound and Vibration, 298*(2006), 1055-1072.

Goldman, D., & Gierke, H. (1960). *The effect of shock and vibration on man* (N0. '60-3, lecture and review series). Bethesda, Maryland: Naval Medical Research Institute.

Gratsianskaya, L. N., Eroshenko, E. A., & Libertovich, A. P. (1974). Influence of high-frequency vibration on the genital region in females. *Gigina Truda i Professional'nye Zabolevanija, 19*(8), 7-10.

Green, D. A., Golding, J. F., Aulukh, M., Faldon, M. C., Murphy, K. G., Bronstein, A. M. et al. (2008). Adaptation of ventilation to 'buffeting' in vehicles. *Clin. Auton. Res., 2008.*

Griffin, M. J. (1990). *Handbook of human vibration.* New York, New York: Harcourt Brace Jovanovich.

Griffin, M. J. (1998). A comparison of standardized methods for predicting the hazards of whole-body vibration and repeated shocks. *Journal of Sound and Vibration, 215*(4), 883-914.

Henderson, R. J., & Raine, J. K. (1998). A two-degree-of-freedom ambulance stretcher suspension. part 3: Laboratory and road test performance. *Proc Instn Mech Engrs, 212*(Part D: Journal of Automobile Engineering), 401-407.

Hillberry, D., & Mortimore, C. (2005). *Ambulance stretcher support to reduce patient trauma* (US Patent 6890137). .

Huang, Y., & Griffin, M. J. (2008). Nonlinear dual-axis biodynamic response of the semi-supine human body during longitudinal horizontal whole-body vibration. *Journal of Sound and Vibration, 312*(2008), 273-295.

Huang, Y., & Griffin, M. J. (2008a). Nonlinear dual-axis biodynamic response of the semi-

supine human body during vertical whole-body vibration. *Journal of Sound and Vibration, 312*(2008).

Huang, Y., & Griffin, M. J. (2009). Nonlinearity in apparent mass an dtransmissibility of hte supine human body during vertical whole-body vibration. *Journal of Sound and Vibration, 324*(2009), 429-452.

International Organization for Standardization 1997 ISO 2631-1. (1997). Mechanical Vibration and shock - evaluation of human exposure to whole-body vibration. Part 1: Gerneral requirements.

Johnson, T. D., Lindholm, D., & Dowd, M. (2006). Child and provider restraints in ambulances: Knowledge, opinions, and behaviors of emergency medical services providers. *Acad Emerg Med, 13*(8), 886-92.

Kahn, C., Pirrallo, R., & Kuhn, E. (2001). Characteristics of fatal ambulance crashes in the United States: An 11 year retrospective analysis. *Prehospital Emergency Care, 5*(3), 941-948.

KKK-A-1822F, F. S. f. t. S.-o.-L. A. (2007). U.S. general services administration. .

Kroemer, K., & Grandjean, E. (1997). *Fitting the task to the humans, 5th ed.*. New York, New York: Taylor and Francis.

Levick, N., & Grzebieta, R. (2008a). *Development of proposed crash test procedures for ambulance vehicles.* Paper number 07-0074, Objective Safety LLC, USA.

Levick, N., & Grzebieta, R. (2008b). To evaluate crashworthiness and passive safety design and testing standards for USA and Australian ambulance vehicles. *Annals of Emergency Medicine, 51*(4), 540.

Levick, N., & Swanson, J. (2005). An optimal solution for enhancing ambulance safety:

Implementing a driver performance feedback and monitoring device in ground

emergency medical service vehicles. In *49th Annual Proceedings - Association for the

Advancement of Automotive Medicine Sept 12-14 2005* (pp. 35-50). Boston, MA United

States: Association for the Advancement of Automotive Medicine, Barrington, IL United

States.

Levick, N., & Swanson, J. (2005). An optimal solution for enhancing ambulance safety:

Implementing a driver performance feedback and monitoring device in ground

emergency medical service vehicles. Unpublished manuscript.

Lewis, C.H. and Griffin, M.J. (1978). Predicting the effectgs of dual-frequency vertical vibration

on continuous manual control performance. *Ergonomics* 21:637-650.

Leyshon, D. R., & Stammer, C. W. (1986). Development and performance of an ambulance

stretcher suspension. *Proc. Instn Mech Engrs, 200*(Part D: Journal of Transport

Engineering), 249-257.

Life Line Emergency Vehicles. (2004). 167" ESD superliner 72" headroom [Dwg. No.

E4SE16772]. .

Litta-Modignani, R., Blivaiss, B. B., Magid, E. B., & Priede, I. (1964). Effects of whole-body

vibration of humans on plasma an durinary coricosteroid levels. *Aerosapce Medicine, 35,*

662-667.

Loeckle, W. E. (1950). The physiological effects of mechanical vibration. In *German aviation in

world war two* (US Government Printing Office, pp. Vol 2 & pp. 716-722). . Washington,

DC.

Lundstrum, R., Holmlund, P., & Lindberg, L. (1998). Absorbtion of energy during vertical

whole-body vibration exposure. *Journal of Biomechanics, 31*(1998), 317-326.

Macnab, M. D., Yuenquan, C., Gagnon, F., Bora, B., & Lazlo, C. (1995). Vibration and noise in pediatric emergency transport vehicles: A potential cause of morbidity? *Aviation, Space and Environmental Medicine, 66*(3), 212-219.

Maguire, B., Hunting, K., Smith, G., & Levick, N. (2002). Occupational fatalities in emergency medical services: A hidden crisis. *Annals of Emergency Medicine, 40*(6), 625-632.

Mansfield, N. J. (2006). *Literture review on low frequency vibration comfort* (Loughborough University, p. 104). Loughborough, U.K.: Collaboration in research and development of new curriculum in sound and vibration.

Margolis, D., & Asgari, J. (1991, September 16). *Multipurpose models of vehicle dynamics for controller design.* Presented at the Passenger Car Meeting and Exposition, Nashville, TN: Society of Automotive Engineers.

Massashusetts Highway Authority. (2006). *Massachusetts highway project development and design guide guide.* . Boston, MA United States.

Matsumoto, Y., & Griffin, M. (1998). Dynamic response of the standing human body exposed to vertical vibration: Influence of posture and vibration magnitude. *Journal of Sound and Vibration, 212*(1), 85-107.

ME/48, S. F. A. R. S. (1999). Joint Standards Austrialia/Standards New Zealand ASN/ZS. .

Miwa, T. (1969). Evaluation methods for vibration effect: Part 9 respsonse to sinusoidal vibration at lying posture. *Industrial Health, 7,* 116-126.

Miwa, T. (1975). Mechanical impedance of human body in various postures. *Industrial Health, 7,* 3-22.

Miwa, T. (1982). Slow vertex potentials evoked by whole-body impulsive vibrations in recumbant men. *J. Acoust. Soc. AM., 72*(1), 214-221.

Moseley, M.J., & Griffin, M.J. (1986). Effects of display vibration and whole-body vibration on visual performance. *Ergonomics*. *29*: 977-983.

Moseley, M. J., & Griffin, M. J. (1987). Whole-body vibration and visual performance: An examination of spatial filtering and time-dependency. *Ergonomics, 30,* 613-626.

Moving ambulance scope of service. (2009) (EMTLife.Com Web Forum). Retrieved 19 July 2009, from: http://www.emtlife.com/showthread.php?s=f5d37720248c66bd28c2dd 73ca13db55&p=153247#post153247.

Murata, Y., & Maemori, K. (1999). Optimum design of ER dampers for ambulances. *JSME International Journal, Series C, 42*(4), 838-846.

Paddan, G. S., & Griffin, M. J. (2002). Evaluation of whole-body vibration in vehicles. *Journal of Sound and Vibration, 253*(1), 195-213.

Papagiannakis, A. T. (1997, November 17). *The need for a new pavement roughness index; RIDE.* 973267 presented at the SAE International Truck and Bus Meeting and Exposition, Cleveland, Ohio: Society of Automotive Engineers.

Parsons, K. C., & Griffin, M. J. (1983, June 6). *Methods for predicting passenger vibration discomfort.* 831029 presented at the Passenger Car Meeting, Dearborn, Michigan: Society of Automotive Engineers.

Paschold, H. (2008). Whole-body vibration. *Professional Safety, 53*(6), 52-57.

Pesterev, A. V., Bergman, L. A., & Tan, C. A. (2004). A novel approach to the calculation of pothole-induced contact forces in mDOF vehicle models. *Journal of Sound and Vibration, 275*(2004), 127-149.

Pichard, E., Poisvert, M., Hurtaud, J. P., Ivanoff, S., & Cara, M. (1970). Les accelerations et les vibrations dans la pathologie liee au transport sanitaire. *Revue Des Corps de Sante, 11,*

611-635.

Prasad, N. H., Brown, L. H., Ausband, S. C., Cooper-Spruill, O., Carroll, & Whitely, T. W. (1994). Prehospital blood pressures: Inaccuracies caused by ambulance noise? *Am J Emerg Med., Nov 12*(6), 617-20.

Proudfoot, S. L., Romano, N. T., Bobick, T. G., & Moore, P. H. (2003). Ambulance crash-related injuries among emergency medical services workers - United States, 1991-2002. *Journal of the American Medical Association, 289,* 1628-1629.

Pushkina, N. N. (1961). Some blood indices in subjects undergoing the effect of gener (total) vibration. *Gigiena Truda I Professional'nye Zabolevanija, 6*(2006), 29-32.

Randall, J., Matthews, R., & Stiles, M. (1997). Reesonant frequencies of standing humans. *Ergonomics, 40*(9), 879-886.

Ribot, E., Roll, J. P., & Gauthier, G. M. (1986). Comparative effects of whole-body vibration on sensorimotor performance achieved with a mini-stick nad a macro-stick in force and position control modes. *Aviation, Space and Environmental Medicine, 57,* 792-799.

Roll, J. P., & Roll, R. (1987). Extraocular proprioception, body postural references an dthe spatial docing of retinal infromation. *Agressologie, 28,* 905-912.

Roman, J. (1958). *Effects of severe whole-body vibration on mice and methods of protection from vibration injury. WADC Technical Report 58-107* (Wright Air Development Centre No. ASTIA Document No. Ad 151070). . Wright-Patterson Air Force Base, Ohio.

Rui, Y., Saleem, Y., & Zhou, J. H. (1997). Road load simulation using effective road profile. *S.A.E. Transactions, 106*(2), 2236.

SafetyLine Institute. (2007, Jan). *Occupational health & safety practitioner reading. Human vibration: Basic characteristics.* (Government of Western Australia, Department of

Consumer and Employment Protection). . Perth, Western Australia.

Sagawa, K., & Inooka, H. (1997). On an ambulance stretcher suspension concerned with the reduction of patient's blood pressure. *Proc. Instn Mech Engrs, 211*(Part H: Journal Engineering in Medicine), 199-208.

Sagawa, K., & Inooka, H. (2002). Ride quality evaluation of an actively-controlled stretcher for an ambulance. *Proc. Instn Mech Engrs, 216*(Part H: Engineering in Medicine), 247-256.

Schneider, S., Borok, Z., Heller, M., Paris, P., & Stewart, R. (1988). Critical cardiac transport - air versus ground. *Amer J Emerg Med, 6*(5), 449-452.

Sharp, G. R., Patrick, G. A., & Withey, W. R. (1974). The respiratory and metabolic effects of constant amplitude whole-body vibration in man. In *Vibration and combined stresses in advanced systems. Vol. Paper B-15: AGARD conference proceedings 145*.

Shenai, J. P., Johnson, G. E., & Varney, R. V. (1981). Mechanical vibration in neonatal transport. *Pediatrics, 68,* 55 - 57.

Sherwood, H. B., Donze, A., & Giebe, J. (1994). Mechanical vibration in ambulance transport. *Journal of Obstetric, Gynecologic, and Neonatal Nursing, 23*(6), 457-463.

Siedel, J., & Greenlaw, J. (1998). Use of restraints in ambulances: A state survey. *Pediatr Emerg Care, 14*(3), 221-3.

Silbergleit, R., Dedrick, D. K., MD, Richard, E. B., & MD. (1991). Forces acting during air and ground transport on patients stabilized by standard immobilization techniques. *Annals of Emergency Medicine, 20*(8), 875-877.

Snook, R., & Pacifico, R. (1976). Ambulance ride: Fixed or floating stretcher? *British Medical Journal, 2,* 405-407.

Stephens, D. G. (1977, September 26). *Passenger vibration in transportation vehicles.* AMD -

vol. 24 presented at the The Design Engineering Technical Conference, Chicago, Illinois: ASME.

Sterud, T., Ekeberg, O., & Hem, E. (2006). Health status in the ambulance services: A systematic review. *BMC Health Services Research, 6*(82), 1-10.

Tamboli, J., & Joshi, S. (1999). Optimum design of a passive suspension system of a vehicle sujected to actual random road excitations. *Journal of Sound and Vibration, 219*(2), 193-205.

Uchikune, M. (2002). Physiological and psychological effects of high speed driving on young male volunteers. *Journal of Ocuupational Health, 44*(4), 203-206.

Vibration Injury Network. (2001). *Review of methods for evaluating human exposure to whole-body vibration.* Appendix w4A to final report, The Institute of Sound and Vibration Research.

Waddell, G. (1975). Movement of critically ill patients within hospital. *British Medical Journal, 2,* 417-419.

Waddell, G., Scott, P. D. R., Lees, N. W., & Ledingham, I. (1975). *British Medical Journal, 1,* 386-389.

Wambold, J. C. (1997, August 4). *Vehicle ride quality -measurement and analysis.* Presented at the SAE West Coast International Meeting, Universal City, California, USA: Society of Automotive Engineers.

Wang, H., Fairbanks, R., Shah, M., Abo, B., & Yearly, D. (2008). Tort claims and adverse events in emergency medical services. *Annals of Emergency Medicine, 52*(3), 256-262.

Wasserman, D. (1996). An overview of occupational whole-body and hand-arm vibration. *Applied Occupational Environmental Hygiene, 11*(4), 266-270.

Waters, T., Rauche, C., Genaidy, A., & Rashed, T. (2007). A new framework for evaluating potential risk of back disorders due to whole body vibration and repeated mechanical shock. *Ergonomics, 50*(3), 379-395.

Weber, U., Reitinger, A., Szusz, R., Hellmich, C., Steiniechner, B., Hager, H. et al. (2009). Emergency ambulance transport induces stress in patients with acute coronary syndrome. *Emerg. Med. J., 26*(2009), 524-528.

Whitham, E.M. and Griffin, M.J. (1977). *Interference with drinking due to whole-body vibration.* Proceedings of the United Kingdom Informal Group on Human Response to Vibration Meeting, National Institute of Agricultural Engineering, Sisoe, Bedfordshire, 18-20 September 1978.

Wickens, C., Lee, J., Liu, Y., & Becker, S. (2004). *Introduction to human factors engineering, 2nd e.*. Upper Saddle River, NJ: Pearson Prentice Hall.

Wilke, H., Neef, P., Caimi, M., Hoogland, T., & Claes, L. (1999). New in vivo measurements of pressures in the intervertebral disc in daily life. *Spine, 24*(8), 755-762.

Wong, J. Y. (2008). *Theory of ground vehicles.* Warrendale, PA: John Wiley and Sons, Inc.

Yue, Z., & Mester, J. (2007). *Studies in Applied Mathematics, 119,* 111-125.

Yue, Z., & Mester, J. (2007a). On the cardiovascular effects of whole-body vibration Part I. Longitudinal effects: Hydrodynamic analysis. *Studies in Applied Mathematics, 119,* 95-109.

Appendix A

Selected test ambulance & chassis specifications

Ambulance #1	
Ambulance mfg.	Horton Emergency Vehicles Co.
Date of mfg.	Oct. 2005
Ambulance type/model	F453-ICT 4x4
Chassis mfg.	Ford Motor Co.
Chassis model / yr.	F450 / 2006
Vechicle type	I
Vehicle class	1
Chassis GVWR	16000 Lbs.
Allowable. Payload per KKK-A-1822	4199 Lbs.
Tires	225/70 R19.5
Options	

Ambulance #2	
Ambulance mfg.	Life Line Emergency Vehicles
Date of mfg.	May 2001
Ambulance type/model	Type III Superliner – Floor Plan A
Chassis mfg.	Ford Motor Co.
Chassis model / yr.	E450 Super Duty
Vechicle type	III
Vehicle class	1
Chassis GVWR	14050 Lbs.
Allowable. Payload per KKK-A-1822	3390 Lbs.
Tires	225/75 R16
Options	Automatic tire chains

Ambulance #3	
Ambulance mfg.	Braun Industries, Inc.
Date of mfg.	October 2009
Ambulance type/model	Chief XL
Chassis mfg.	General Motors Corporation
Chassis model / yr.	Chevy C-4500 / 2008
Vechicle type	III
Vehicle class	5
Chassis GVWR	16500 Lbs.
Allowable. Payload per KKK-A-1822	3434 Lbs.
Tires	225/70 R19.5
Options	

Ambulance #4	
Ambulance mfg.	Life Line Emergency Vehicles
Date of mfg.	August 2009
Ambulance type/model	Type I Superliner – Floor Plan A
Chassis mfg.	Ford Motor Co.
Chassis model / yr.	Ford F-550 / 2009
Vechicle type	I
Vehicle class	1
Chassis GVWR	17950 Lbs.
Allowable. Payload per KKK-A-1822	4470 Lbs.
Tires	225/70 R19.5
Options	Air ride suspension

2006 SUPER DUTY F-250/350/450/550
STANDARD POWERTRAIN/CHASSIS EQUIPMENT SPECIFICATIONS

F-450 Chassis Cab

		4x2	4x4
DRIVE:			
POWERTRAIN:		Refer To The Ordering Guide For 50 States Usage	
Engine[1]	— Type	6.8L (415 CID) 3V SEFI V-10	
Transmission	— Type	Heavy-Duty Manual	
	— Speeds	6-Speed Overdrive	
Clutch Diameter		11.9" (13" With 6.0L V-8 Diesel)	
Transfer Case	— Type	—	Part-Time, 2-Speed
	— Low/High Gear Ratio	—	2.72:1/1.00:1
AXLES:			
Front Axle	— Type	Monobeam, Dana Super 60	
	— Capacity (Rating @ Ground)	7000 lbs.	
	— Hubs Type	—	Manual Locking
Rear Axle	— Type—Full-Floating	Dana	
	— Capacity (Rating @ Ground)	12,000 lbs.	
BRAKES:			
Front/Rear Disc	— Type	Dual-Piston Pin-Slider Calipers, Bolt-on Adapters, Wrap-around Tie Bars	
	— Rotor Diameter—Front/Rear	14.53"/15.35"	
Power Assist Unit	— Type	Hydro Boost	
	— Effective Diameter	1.56" Power Piston	
Anti-Lock System		4-Wheel (3-Channel)	
Parking Brake (Rear Brakes)		9.5" Drum-In-Hat (Foot-Operated, Hand Release)	
ELECTRICAL:			
Alternator	— Rating	110 Amperes, 1650 Watt	
Battery	— Type	Maintenance-Free	
	— Rating	78 Amp-hr., 750 CCA (Dual 78 Amp-hr., 750 CCA With 6.0L V-8 Diesel)	
Harnesses	— Type	7 Blunt Cut and Labeled Wires With Relays For Backup Lamps, Running Lamps and Battery Feed	
FUEL TANK:	— Capacity	40.0 Gal. (151 L) (Filler Hose Thru Hole In Frame Siderail)	
STEERING:	— Type	Power, Ford XR-50 (Includes Steering Damper)	
	— Ratio	18.0:1	
SUSPENSION:			
Frame	— Type	Ladder Type, 36,000 psi Steel With Front Blocker Beam	
	— Section Modulus (cu. in.)	10.1; 17.2 With 188.8" WB and 200.8" WB Regular Cab	
Springs, Front	— Type	Coil, Assigned Rating	
	— Rating @ Ground (min.)	Refer to page 29 for usage and ratings	
Springs, Rear	— Type	Leaf, Single-Stage Constant Rate Main and Auxiliary	
	— Rating @ Ground (min.)	Refer to page 29 for usage and ratings	
Shock Absorbers	— Gas-Type	1.38"	
Stabilizer Bar		Front and Rear	
TIRES:	— Type	Steel-Belted Radial, All-Season, BSW	
	— Size	Six, 225/70Rx19.5F	
WHEELS:	— Type and Size	Six, 10-Hole Disc, 19.5" x 6" Steel	

SPRING SPECIFICATIONS — REAR LEAF

Super Duty Series/Model	Combined Rating @ Ground (lbs.)	Number of Leaves	Total Thickness @ Pad (in.)	Overall Length (in.)	Width (in.)	Deflection Rate (lbs. per in./ spring)[1] [2]	Rating Each @ Pad (lbs. per spring)
Main Leaf & Auxiliary Spring (Including Spacer)							
F-250 Pickup[3]	7000	6	4.18	58.1	3.00	330/650/1290	3133
F-350 SRW Pickup[4]	7000	6	4.18	58.1	3.00	330/650/1290	3133
F-350 DRW Pickup	9000	6	4.37	58.1	3.00	457/902/1422	4024
F-350 SRW Chassis Cab	7280	10	4.76	55.6	3.00	617/1342	3271
F-350 DRW Chassis Cab	9750	12	5.80	55.6	3.00	1014/1644	5305
F-450 Chassis Cab	12,000	11	6.75 (Includes Top Plate)	55.6	3.00	1253/2179	5324
F-550 Chassis Cab	13,660	11	6.75 (Includes Top Plate)	55.6	3.00	1256/2129	6150
Main Leaf Only							
F-250 Pickup	6100	5	2.66	58.1	3.00	334/776	2695
F-350 SRW Pickup[5]	7000	5	2.66	58.1	3.00	330/650	3133

(1) Pickup and Box Delete models include two-stage, variable rate springs. Chassis Cab models include single-stage, constant rate springs.
(2) Lists first stage/second stage/third stage as applicable.
(3) Auxiliary rear spring available and included with Camper Package, Heavy Service Suspension Package, Snow Plow Prep Package and Heavy Service Package For Pickup Box Delete only at Job# 1. Auxiliary rear spring available and included with Camper Package and Heavy Service Package For Pickup Box Delete only at Job# 2.
(4) Auxiliary rear spring will be deleted as standard and included with Camper Package and Heavy Service Package For Pickup Box Delete only at Job# 2.
(5) Standard and available at Job# 2

2006 SUPER DUTY F-250/350/450/550

WEIGHT RATINGS

F-450 DRW Chassis Cab - GVWR/Payload/Spring & GAWR (Front Assigned)/Base Curb Weight

Cab Style/ Drive/WB (in.)	Engine/ Transmission Std./Opt.	Maximum GVWR (lbs.) Std./Opt.	Maximum Payload (lbs.)[1] Std./Opt.	Spring/GAWR (lbs.)[2] Front (lbs.)	Rear (lbs.)	Base Curb Weight Front (lbs.)	Rear (Lbs.)	Total (lbs.)
Regular Cab 4x2 - 140.8	6.8L/Manual	16,000/15,000	9500/8500	4800	12,000	3610	2806	6416
	6.0L/Manual	16,000/15,000	9100/8100	5200	12,000	4090	2758	6848
Regular Cab 4x2 - 164.8	6.8L/Manual	16,000/15,000	9400/8400	5600	12,000	3727	2791	6518
	6.0L/Manual	16,000/15,000	9000/8000	6000	12,000	4213	2742	6955
Regular Cab 4x2 - 188.8	6.8L/Manual	16,000/15,000	9100/8100	6500	12,000	3895	2901	6796
	6.0L/Manual	16,000/15,000	8700/7700	6500	12,000	4355	2875	7230
Regular Cab 4x2 - 200.8	6.8L/Manual	16,000/15,000	9100/8100	6000	12,000	3936	2884	6820
	6.0L/Manual	16,000/15,000	8700/7700	6500	12,000	4425	2831	7256
Regular Cab 4x4 - 140.8	6.8L/Manual	16,000/15,000	9200/8200	5200	12,000	3888	2863	6751
	6.0L/Manual	16,000/15,000	8800/7800	5600	12,000	4334	2821	7155
Regular Cab 4x4 - 164.8	6.8L/Manual	16,000/15,000	9100/8100	5600	12,000	4026	2833	6859
	6.0L/Manual	16,000/15,000	8700/7700	6000	12,000	4476	2786	7262
Regular Cab 4x4 - 188.8	6.8L/Manual	16,000/15,000	8800/7800	6500	12,000	4182	2943	7125
	6.0L/Manual	16,000/15,000	8400/7400	6500	12,000	4633	2921	7554
Regular Cab 4x4 - 200.8	6.8L/Manual	16,000/15,000	8800/7800	6500	12,000	4242	2915	7157
	6.0L/Manual	16,000/15,000	8400/7400	6500	12,000	4696	2865	7561
SuperCab 4x2 - 161.8	6.8L/Manual	16,000/15,000	9100/8100	5200	12,000	3825	2959	6784
	6.0L/Manual	16,000/15,000	8700/7700	5600	12,000	4311	2910	7221
SuperCab 4x4 - 161.8	6.8L/Manual	16,000/15,000	8800/7800	5200	12,000	4123	2998	7121
	6.0L/Manual	16,000/15,000	8400/7400	6000	12,000	4574	2950	7524
Crew Cab 4x2 - 176.2	6.8L/Manual	16,000/15,000	8900/7900	5200	12,000	3967	3033	7000
	6.0L/Manual	16,000/15,000	8500/7500	5600	12,000	4454	2980	7434
Crew Cab 4x2 - 200.2	6.8L/Manual	16,000/15,000	8800/7800	6000	12,000	4093	3008	7101
	6.0L/Manual	16,000/15,000	8400/7400	6500	12,000	4582	2955	7537
Crew Cab 4x4 - 176.2	6.8L/Manual	16,000/15,000	8600/7600	5600	12,000	4259	3078	7337
	6.0L/Manual	16,000/15,000	8200/7200	6000	12,000	4711	3030	7741
Crew Cab 4x4 - 200.2	6.8L/Manual	16,000/15,000	8500/7500	6000	12,000	4395	3043	7438
	6.0L/Manual	16,000/15,000	8100/7100	6500	12,000	4849	2993	7842

(1) Load rating represents maximum allowable weight of people, cargo and body equipment and is reduced by optional equipment weight.
(2) Gross Axle Weight Rating is determined by the rated capacity of the minimum component of the axle system (axle, computer-selected springs, wheels, tires) of a specific vehicle. Front and rear GAWR's will, in all cases, sum to a number equal to or greater than the GVWR for the particular vehicle. Maximum loaded vehicle (including passengers, equipment and payload) cannot exceed the GVW rating or GAWR (front or rear).

NOTE: Refer to page 21 for Standard Powertrain/Chassis Equipment Specifications. Refer to Option/Payload Worksheet on pages 35-39 for optional equipment weights.
NOTE: Front spring/GAWR on Chassis Cab models is assigned or specifically selected. Refer to page 32, "Chassis Cab - Optional Front Spring/GAWR Availability", for specific front spring/GAWR upgrades included in available option packages.

2006 SUPER DUTY F-250/350/450/550

TECHNICAL SPECIFICATIONS

Suspensions
FRAME SPECIFICATIONS

Cab Style	Super Duty Series/Model	Wheelbase (in.)	No. Of Crossmembers	Maximum Side Rail Section (Height x Width X Thickness) (in.)[1]	Section Modulus (cu. in.)[2]	Yield Strength (psi)
Regular Cab	F-250-350 Pickup/Box Delete	137.0	5	6.87 x 2.36 x .264	6.7	36,000
	F-350 Chassis Cab	140.8	6	7.50 x 2.74 x .280	8.7	36,000
		164.8	7	7.50 x 2.74 x .280	8.7	36,000
	F-450-550 Chassis Cab (16,000/17,950 lb. GVWR Only)	140.8	6	7.50 x 2.74 x .320	10.1	36,000
		164.8	7	7.50 x 2.74 x .320	10.1	36,000
		188.8	8	7.50 x 2.74 x .60	17.2[3]	36,000
		200.8	9	7.50 x 2.74 x .60	17.2[3]	36,000
	F-550 (19,000 lb. GVWR Only)	164.8	7	7.50 x 2.74 x .60	17.2[3]	36,000
		200.8	9	7.50 x 2.74 x .60	17.2[3]	36,000
SuperCab	F-250-350 Pickup	141.8	6	6.87 x 2.36 x .264	6.7	36,000
	F-250-350 Pickup/Box Delete	158.0	6	6.87 x 2.36 x .264	6.7	36,000
	F-350 Chassis Cab	161.8	7	7.50 x 2.74 x .280	8.7	36,000
	F-450-550 Chassis Cab	161.8	7	7.50 x 2.74 x .320	10.1	36,000
Crew Cab	F-250-350 Pickup	156.2	7	6.87 x 2.36 x .264	6.7	36,000
	F-250-350 Pickup/Box Delete	172.4	7	6.87 x 2.36 x .264	6.7	36,000
	F-350 Chassis Cab	176.2	7	7.50 x 2.74 x .280	8.7	36,000
	F-450-550 Chassis Cab	176.2	7	7.50 x 2.74 x .320	10.1	36,000
		200.2	8	7.50 x 2.74 x .320	10.1	36,000

(1) Measured to inside of metal.
(2) Cross-sectional modulus calculated at back of cab, to inside of metal.
(3) Calculated at back of cab, through the reinforced section - 17.2 SM at upper flange, 13.3 SM at lower flange.

SHOCK ABSORBER SPECIFICATIONS

Super Duty Model	Wheelbase (in.)	Usage	Front No. Used	Front Piston Dia. (in.)	Front Type	Rear[1] No. Used	Rear Piston Dia. (in.)	Rear Type
Pickup/Chassis Cab	All	Std.	2	1.38	Gas-Pressurized	2	1.38	Gas-Pressurized
Pickup	All	Opt.[2]	2	1.38	Gas-Pressurized	2	1.38	Gas-Pressurized

(1) Staggered rear shock absorbers with Pickup models.
(2) Included with FX4 Off-Road Package. Unique Rancho shock absorbers with white housing and red bellows.

Appendix B

IST EDR3C-10 Detailed specification and calibration data

CERTIFICATE OF CALIBRATION

Model Number:	EDR-3C-10	**Hardware Version:**	HC11v5A
Serial Number:	689	**Firmware Version:**	3Cv1.61
Memory:	4 MB	**Logic Version:**	9100

Internal Accelerometers:		**CH1** (x)		**CH2** (y)		**CH3** (z)	
Channel Gains (mV/cnt):	$I1V$:	0.03326	$I2V$:	0.03326	$I3V$:	0.03326
Accelerometer Sensitivities (mV/g):	$I1A$:	1.473	$I2A$:	1.427	$I3A$:	1.427
Accelerometer Measurement Range (g):		11.5		11.9		11.9
Accelerometer Measurement Resolution (g):		.023		.023		.023

Temperature Coefficient (per °C): ATC: -0.2 %   Calibration Temperature: 25 °C

Accelerometer Frequency Response: 400 Hz
Accelerometer Resonant Frequency: 1000 Hz

External Accelerometers:

		CH1 (x)		**CH2** (y)		**CH3** (z)	
Channel Gains (mV/cnt):	$E1V$:	.9627	$E2V$:	.9631	$E3V$:	.9659

Temperature Sensor, Humidity and Battery Voltage:

Internal Temperature Sensor (°C per cnt):	ITS:	.6253
Accelerometer Temperature Sensor (°C per cnt):	ATS:	.6253
External Temperature Sensor (°C per cnt):	ETS:	N/A
Humidity Sensor:	HSO: 166.9	HSG: .1569
Battery Voltage Sensor (V/cnt):	BVS: .01484	

Fixed Hardware Operating Characteristics:

Accelerometer Channel Low-Pass Filter (Anti-Aliasing) 3db Cut-Off:

Internal: 90 Hz
External: 90 Hz

Power-Up Voltage: 5.02
Automatic Power-Down Voltage: 4.83
Software Power-Down: 547F

Instrumented Sensor Technology, Inc.'s calibration procedure is traceable to NIST through the following:

Temperature/Humidity Probe:	131081	Date: 04/09/09
DVM:	3146A25274	Date: 01/26/09
Accelerometer(s):	15496	Date: 05/12/09
		Date:
Calibrated by: _TriHuynh_		Date: 07/15/09

IST Instrumented Sensor Technology

4704 Moore Street
Okemos, Michigan 48864
517-349-8487

EDR-3 Series Recorder Specifications

	EDR-3	EDR-3C	EDR-3D
DATA ACQUISITION			
#Selectable High Speed CHs:	3 (3)	3 (3)	6 (6)
#Simultaneous High Speed CHs:	3	3	6
Digitization	10-bit	10-bit	10-bit
#Low Speed CHs:	4	4	8
#Simultaneous Low Speed CHs	4	4	8
Temperature Sensor CHs	1 (1)	1 (1)	2 (2)
Humidity Sensor CHs	(1)	(1)	(2)
Battery Voltage CHs	1	1	2
#Trigger CHs	(1)	(1)	(2)
High Speed Digitization Rate	125-3200 (4800)	125-3200	125-3200
Low Speed	1 sample every 15 sec to 1 sample every 166 hours all models		
Digitization, Agreggate MAX, sps	9600 (14400)	9600	19200
DATA STORAGE			
MegaByte- Non-volatile SRAM	1 (2,4)	1 (2,4)	2 (4,8)
DATA MANAGEMENT			
Fill & Stop Memory Mode	X	X	X
Overwrite Memory Mode	X	X	X
Sliding Window Overwrite Mode™		X	X
Sliding Window Overwrite with Event Type Partitioning			X
Sliding Window Overwrite with Channel Set Partitioning			X
Sliding Window Size	N/A	Selectable 1 min to 30 days	
# Separate Time Windows	N/A	Selectable 1 to 100	

( ) = Optional

Window Overwrite™ (SWO) is a trademark of **Instrumented Sensor Technology, Inc.**

EDR-3 Series Recorder Specifications

	EDR-3	EDR-3C	EDR-3D
DATA COMMUNICATION			
Plug & Play Serial RS-232, modem compatible	9.6kBaud	9.6 to 115kBaud	9.6 to 115kBaud
SENSORS			
Internal Accelerometer: Piezoresistive Triaxial	X	X	X
Accelerometer fs Range Choices		±2, ±5, ±10, ±20, ±50, ±100, ± 200, ±500g all models	
Accelerometer Frequency Responses			
2g, 5g fs		DC-250 Hz, DC-350 Hz	
10g, 50g fs		DC-400 Hz, DC-1000 Hz	
100g, 200g fs		DC-1500 Hz, DC-2000 Hz	
Signal Filtering: 4th Order Anti-Aliasing			
Standard 3dB cutoff choices		60, 80, 90, 110, 140, 170, 200, 340, 420, 510, 620, 750, 930, 1120, 1915 Hz	
Automatic Auto-Zero Offset Correction		1% fs/sec all models	
External Accelerometers:		Voltage mode piezoelectric, 0.5mA, 3.4V bias, 0.5mv/g to 1000 mv/g, all models	
PROGRAMMABILITY			
High Speed Sample Rate	X	X	X
Trigger selection		Internal or external channels and/or external trigger input, all models	
Triggering	X	X	X
Amplitude Threshold	X	X	X
Separate channel thresholds		X	X
Duration (time at level) Threshold	X	X	X
Separate channel thresholds		X	X
Trigger Duration Threshold		1 to 34463 samples all models	
Time Trigger Delay		0 to 35000 seconds all models	
(forced time delay between triggered recordings)			
Time Triggered Recording		1 sample every 15 sec to 1 sample every 166 hours all models	
Maximum Number of Events	5291	5291	10582
Event Length:		Fixed or Data Dependent	
Pre-trigger samples		2 to 9997 all models	
Post-trigger samples		1 to 9999 all models	
Maximum Event Length cutoff:		9999 samples all models	
Memory Modes:	FS, OW	FS, OW, SW	FS, OW, SWO, SWO-ETP,-CSP
OPERATIONAL			
Temperature Recording		Internal & external all models	
Range/Resolution		-40 to +70°C/ ±3°C all models	
Humidity Recording		Internal & external all models	
Range/Resolution		0 to 100% RH / ±3% RH all models	
Usable Temperature Range		1 to 60°C all models	
Digital Clock		Month/Day/Year, Hour:Min:Sec all models	
Date & Time Tagged to each acceleration event			
Resolution/Accuracy		53 msec / ±3 min/Mo all models	
Auto ON and OFF times	X	X	X
Connectors		DB9 for RS-232 serial all models	
		(4-pin microdot for external RS-232, aux. power, all models)	
		(10-32 microdot for external accelerometers)	
Battery Life(Typical) Alkaline C-cell Batteries	30-40 days	20+ days	15+ days
Data Memory Backup		12+ months all models	
PHYSICAL			
Size	4.2"x 4.4" x 2.2"	4.2"x 4.4"x 2.2"	4.2"x 4.4"x 2.5"
Housing		Black Anodized Aluminum, watertight, gasket sealed	
Weight	2.2 lb	2.2 lb	2.6 lb
Operating Temperature Range		-40 to + 70°C all models	
Shock Fragility		500g or 20 x fs, all models	
STANDARD ANALYSES			
(with DM95-BASE Software package)	3-Channel Acceleration waveform graphics, histograms, temp/hum process		
	Resultant Acceleration waveforms		
	Spreadsheet tabulation of max, min, peak, duration, RMS, crest factor,		
	velocity change, temperature, humidity, dew point, battery volt		
	Data editing and sorting by selected event parameters, statistical summaries		
	Digital filtering- low pass, high pass, bandpass		
OPTIONAL ANALYSIS SOFTWARE	DM95-int Velocity and Displacement Waveforms		
	DM95-psd Power Spectral Density (PSD) calculation and analysis		
	DM95-srs Shock Response Spectrum (SRS) calculation and analysis		
	DM95-drop Packaging Drop height - Equivalent impact, Zero-G free fall,		
	package trajectory animation, impact direction & type.		
	DM95-deriv Jerk Waveform calculation and display		
HARDWARE OPTIONS			
Memory expansion	2,4 Mb	2,4 Mb	4,8 Mb
External Channel inputs		3 accel, temp, power, COM, trigger	
Relative humidity sensor		internal and/or external	
Higher digitization rates	X		
Auxiliary battery pack	X	X	X
Hand-Held remote trigger (HRT-1)	X	X	X
Remote Alarm Module (RALM-1)	X	X	X

Printed in the U.S.A. 1/99

Appendix C.

Raw vibration amplitude data

Vibrations experienced during highway travel

Vibration amplitudes associated with ambulance travel over highway road surfaces at low, medium and high speeds for the four ambulances examined in this study are presented in Tables C1, C2, and, C3 and Figures C1, C2, C3and, C4 respectively.

Table C1. *Ambulance vibration amplitudes due to highway travel at speeds ≤ 35mph*

Speed ≤ 35 mph - Highway											
Amb #	Mean r.m.s. accel. (m sec^{-2})			Maximum peak accel. (m sec^{-2})			Mean crest factor			Mean peak accel. (m sec^{-2})		
	Z-axis	Worst axis	Resultant Tri-axial sum	Z-axis	Worst axis	Resultant Tri-axial sum	Z-axis	Worst axis	Resultant Tri-axial sum	Z-axis	Worst axis	Resultant Tri-axial sum
1	0.60	0.60 (z)	0.80	6.92	6.92 (z)	7.48	5.76	5.76 (z)	4.67	3.44	3.44 (z)	3.96
2	0.62	0.62 (z)	0.87	4.81	4.81 (z)	5.58	5.19	5.19 (z)	3.81	3.17	3.17 (z)	3.44
3	0.71	0.71 (z)	0.87	7.90	7.90 (z)	9.13	5.39	6.24 (x)	4.76	3.90	3.90 (z)	4.46
4	0.59	1.80 (x)	1.96	6.38	6.38 (z)	7.69	6.98	6.98 (z)	3.38	4.06	4.06 (z)	5.39

Table C2. *Ambulance vibration amplitudes due to highway travel at speeds 36-64mph*

Speed 36 - 64 mph - Highway											
Amb #	Mean r.m.s. accel. (m sec^{-2})			Maximum peak accel. (m sec^{-2})			Mean crest factor			Mean peak accel. (m sec^{-2})		
	Z-axis	Worst axis	Resultant Tri-axial sum	Z-axis	Worst axis	Resultant Tri-axial sum	Z-axis	Worst axis	Resultant Tri-axial sum	Z-axis	Worst axis	Resultant Tri-axial sum
1	0.84	.84 (z)	0.96	10.32	10.32 (z)	14.63	6.80	6.80 (z)	6.07	5.05	5.05 (z)	6.34
2	0.78	.78 (z)	0.87	4.13	4. 13 (z)	4.21	4.16	4.16 (z)	3.76	3.07	3.07 (z)	3.28
3	1.18	1.18 (z)	1.31	10.80	10.80 (z)	11.05	4.72	4.72 (z)	4.35	5.53	5.53 (y)	6.11
4	0.67	0.67 (z)	0.79	5.94	5.94 (z)	6.38	5.86	5.86 (z)	5.15	3.57	3.57 (z)	4.05

Table C3. *Ambulance vibration amplitudes due to highway travel at speeds ≥ 65mph*

| Speed ≥ 65- Highway											
A m b #	Mean r.m.s. accel. (m sec⁻²)			Maximum peak accel. (m sec⁻²)			Mean crest factor			Mean peak accel. (m sec⁻²)		
	Z-axis	Worst axis	Resultant Tri-axial sum	Z-axis	Worst axis	Resultant Tri-axial sum	Z-axis	Worst axis	Resultant Tri-axial sum	Z-axis	Worst axis	Resultant Tri-axial sum
1	1.12	1.12 (z)	1.36	7.83	7.83 (z)	7.95	4.17	4.17 (z)	3.55	4.45	4.45 (z)	4.89
2	1.02	1.02 (z)	1.26	4.80	4.80 (z)	4.86	4.04	4.04 (z)	3.29	3.50	3.50 (z)	4.15
3	1.63	1.63 (z)	1.81	15.05	15.05 (z)	15.16	4.59	4.59 (z)	4.21	7.25	7.25 (z)	7.62
4	0.96	0.96 (z)	1.12	5.71	5.71 (z)	5.80	4.79	4.79 (z)	4.19	4.40	4.40 (z)	4.69
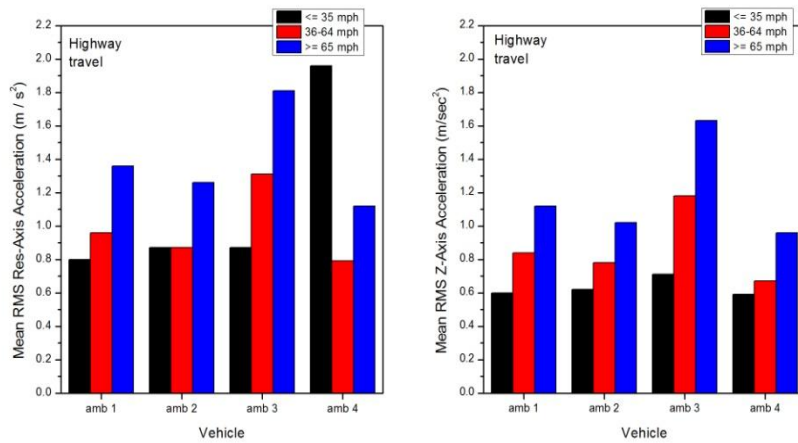
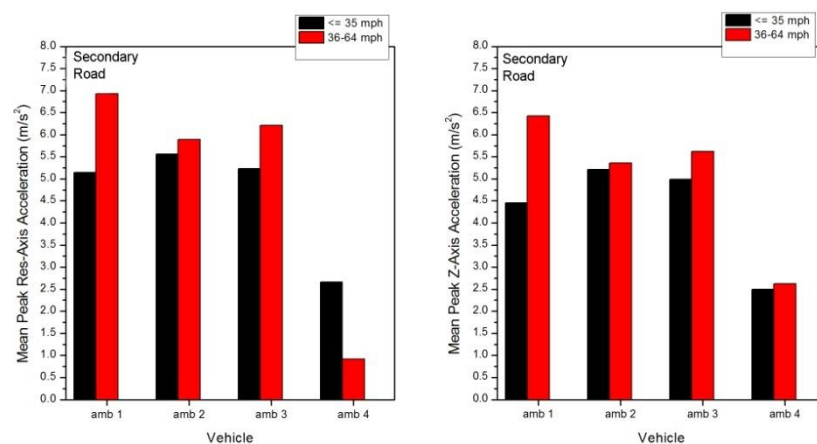Figure C1. *Overall vibration level – highway travel all ambulances all speeds*
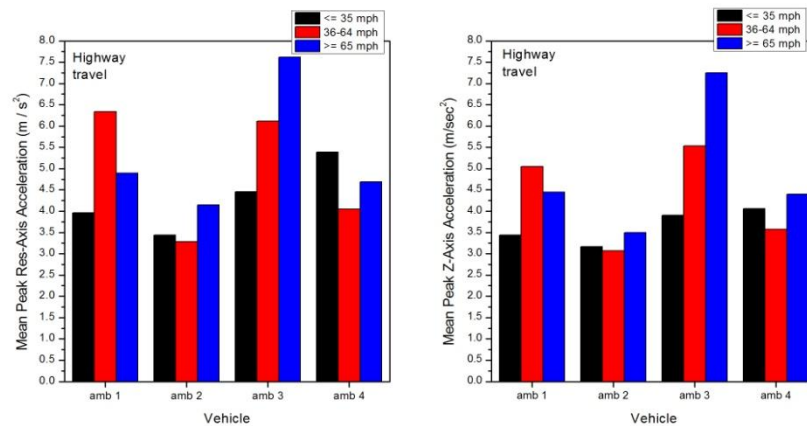
Figure C2. *Mean peak vibration level – highway travel all ambulances all speeds*
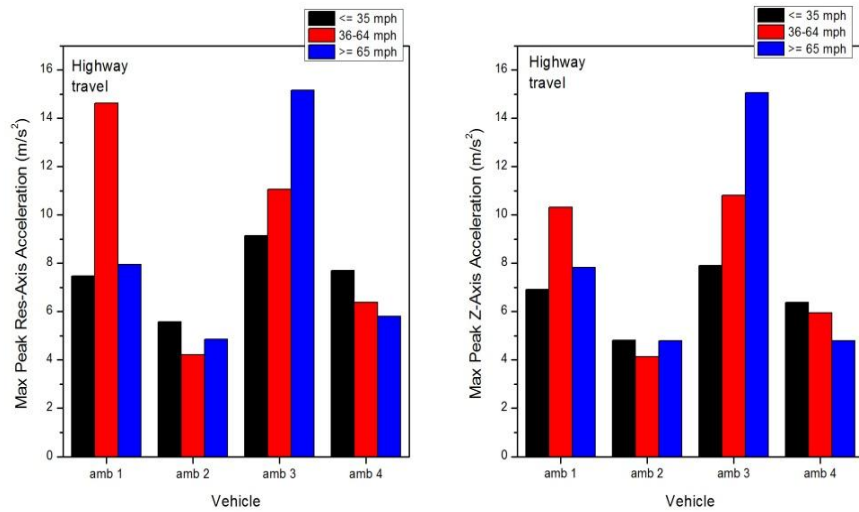
Figure C3. *Max peak vibration level – highway travel all ambulances all speeds*
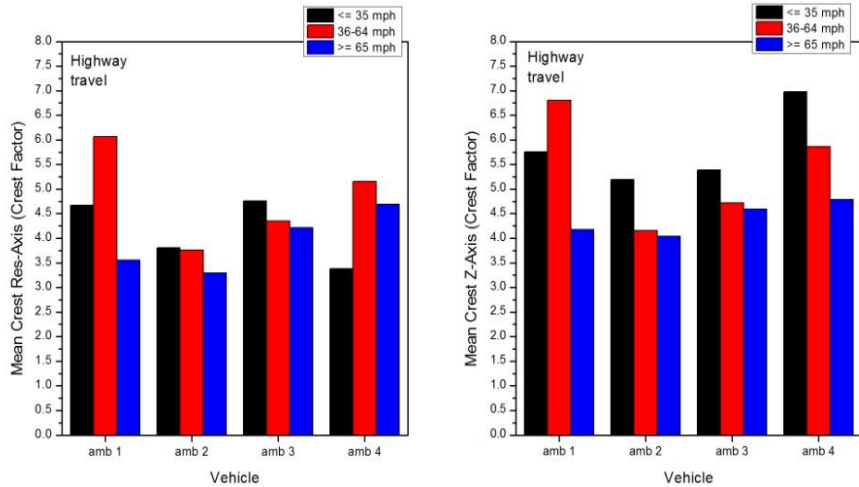
Figure C4. *Mean crest factor – highway travel all ambulances all speeds*

Vibrations experienced during travel over paved secondary roads

Ambulance passenger cabin vibration amplitudes due to travel on secondary road surfaces is shown in Tables C3 and C4 and Figures C5,C6, C7, and, C8, respectively.

Table C3. *Ambulance vibration amplitudes on secondary roads at speeds ≤ 35mph*

Amb #	Mean r.m.s. accel. (m sec^{-2})			Maximum peak accel. (m sec^{-2})			Mean crest factor.			Mean peak accel. (m sec^{-2})		
Speed ≤ 35 mph – Secondary roads												
	Z-axis	Worst axis	Resultant Tri-axial sum	Z-axis	Worst axis	Resultant Tri-axial sum	Z-axis	Worst axis	Resultant Tri-axial sum	Z-axis	Worst axis	Resultant Tri-axial sum
1	0.91	0.91 (z)	1.23	8.28	8.28 (z)	8.35	5.29	5.29 (z)	4.16	4.46	4.46 (z)	5.14
2	0.88	0.88 (z)	1.16	9.04	9.04 (z)	9.04	6.06	6.06 (z)	4.80	5.21	5.21 (z)	5.56
3	0.99	0.99 (z)	1.10	9.72	9.72 (z)	9.72	5.00	5.00 (z)	4.53	4.99	4.99 (z)	5.23
4	0.50	0.50 (z)	0.66	3.47	3.47 (z)	3.94	5.26	5.26 (z)	4.00	2.50	2.50 (z)	2.66

Table C4. *Ambulance vibration amplitudes on secondary roads at speeds 36-64mph*

Amb #	Mean r.m.s. accel. (m sec^{-2})			Maximum peak accel. (m sec^{-2})			Mean crest factor.			Mean peak accel. (m sec^{-2})		
Speed 36 - 64 mph – Secondary roads												
	Z-axis	Worst axis	Resultant Tri-axial sum	Z-axis	Worst axis	Resultant Tri-axial sum	Z-axis	Worst axis	Resultant Tri-axial sum	Z-axis	Worst axis	Resultant Tri-axial sum
1	1.20	1.20 (z)	1.46	7.82	7.82 (z)	7.86	5.60	5.60 (z)	4.85	6.42	6.42 (z)	6.93
2	1.05	1.05 (z)	1.53	7.48	7.48 (z)	8.32	5.31	5.31 (z)	4.01	5.36	5.36 (z)	5.89
3	1.34	1.34 (z)	2.00	8.16	8.16 (z)	8.62	4.20	4.20 (z)	3.13	5.62	5.62 (z)	6.21
4	.60	.60 (z)	.92	3.48	3.48 (z)	4.17	4.72	4.72 (z)	3.56	2.62	2.62 (z)	3.17
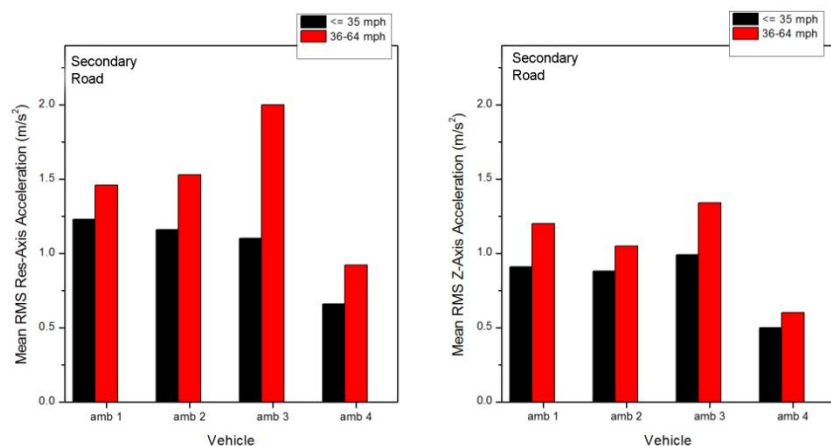
Figure C5. *Overall vibration level – secondary road all ambulances all speeds*

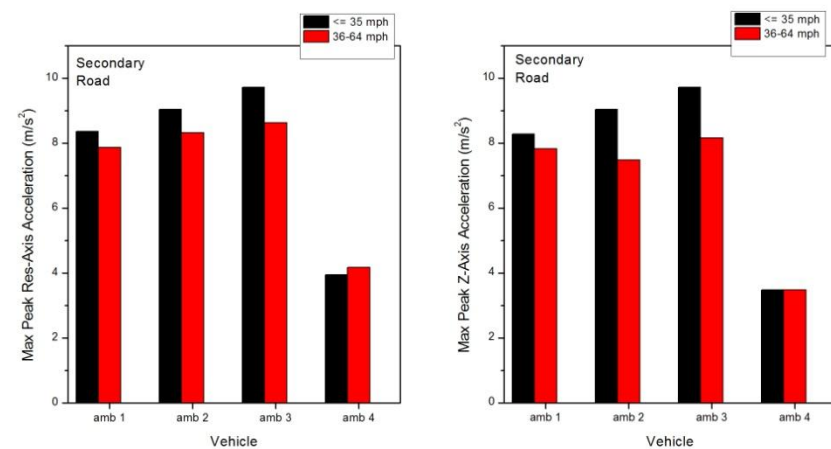Figure C6. *Mean peak vibration level – highway travel all ambulances all speeds*

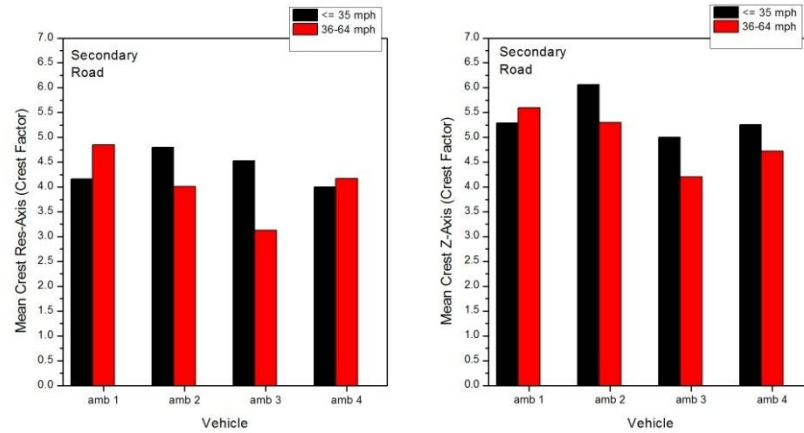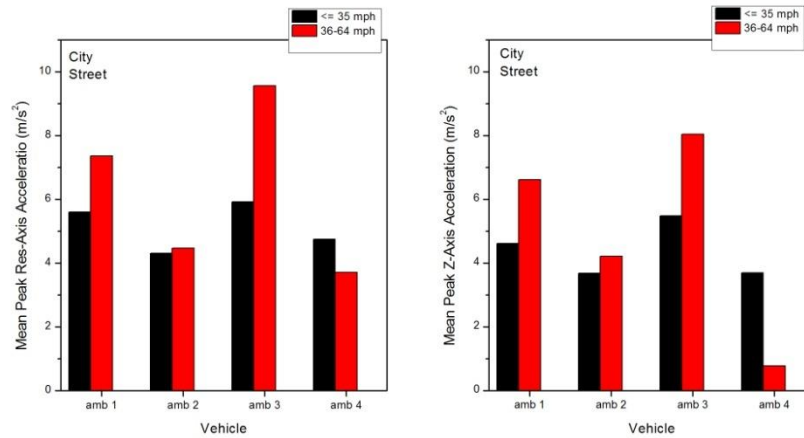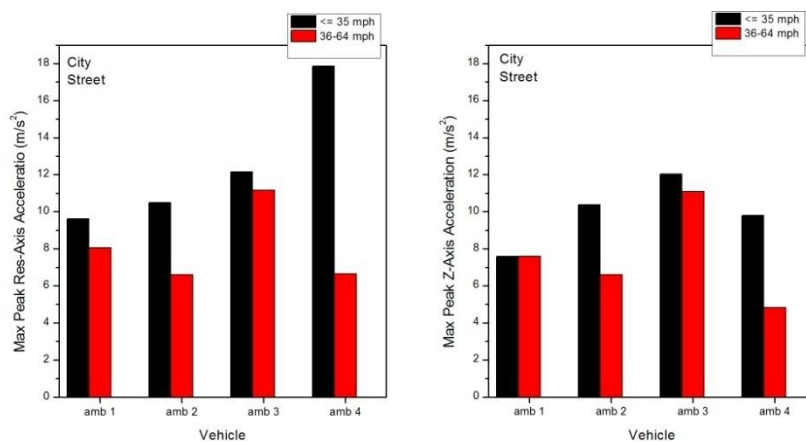Figure C7. *Max peak vibration level – highway travel all ambulances all speeds*
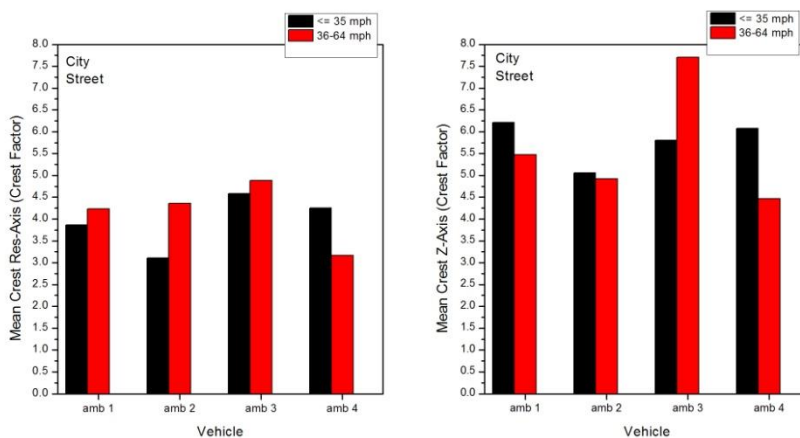
Figure C8. *Mean crest factor – secondary road all ambulances all speeds*

Vibrations experienced during travel over paved city streets

Ambulance passenger cabin vibration amplitudes due to travel on city streets is shown in

Tables C5 and C6, and, Figures C9, C10, C11, and, C12, respectively.

Table C5. *Ambulance vibration amplitudes on city streets at speeds ≤ 35mph*

Speed ≤ 35 mph – City streets											
A m b #	Mean r.m.s. accel. (m sec^{-2})			Maximum peak accel. (m sec^{-2})			Mean crest factor.			Mean peak accel. (m sec^{-2})		
	Z-axis	Worst axis	Resultant Tri-axial sum	Z-axis	Worst axis	Resultant Tri-axial sum	Z-axis	Worst axis	Resultant Tri-axial sum	Z-axis	Worst axis	Resultant Tri-axial sum
1	0.84	0.92 (x)	1.50	7.60	7.60 (z)	9.62	6.21	6.21 (z)	3.86	4.61	4.61 (z)	5.60
2	0.62	0.64 (z)	1.15	10.38	10.38 (z)	10.48	5.06	5.06 (z)	3.11	3.67	3.67 (x)	4.30
3	0.99	0.99 (z)	1.32	12.04	12.04 (z)	12.14	5.80	5.80 (z)	4.58	5.48	5.48 (z)	5.92
4	0.60	0.60 (z)	0.97	9.79	9.79 (z)	17.87	6.08	6.08 (z)	4.25	3.69	3.69 (z)	4.74

Table C6. *Ambulance vibration amplitudes on city streets at speeds 36-64mph*

Speed 36 - 64 mph – City streets											
Amb #	Mean r.m.s. accel. (m sec⁻²)			Maximum peak accel. (m sec⁻²)			Mean crest factor.			Mean peak accel. (m sec⁻²)		
	Z-axis	Worst axis	Resultant Tri-axial sum	Z-axis	Worst axis	Resultant Tri-axial sum	Z-axis	Worst axis	Resultant Tri-axial sum	Z-axis	Worst axis	Resultant Tri-axial sum
1	1.24	1.24 (z)	1.75	7.60	7.60 (z)	8.06	5.47	6.12 (y)	4.23	6.61	6.61 (z)	7.36
2	0.88	0.88 (z)	1.00	6.59	6.59 (z)	6.60	4.92	4.92 (z)	4.35	4.21	4.21 (z)	4.46
3	1.29	1.29 (z)	11.09	11.09	11.09 (z)	11.16	7.70	7.70 (z)	4.88	8.03	8.03 (x)	9.56
4	0.77	0.77 (z)	6.62	4.83	4.83 (z)	6.64	4.47	4.47 (z)	3.17	2.92	2.92 (z)	3.70
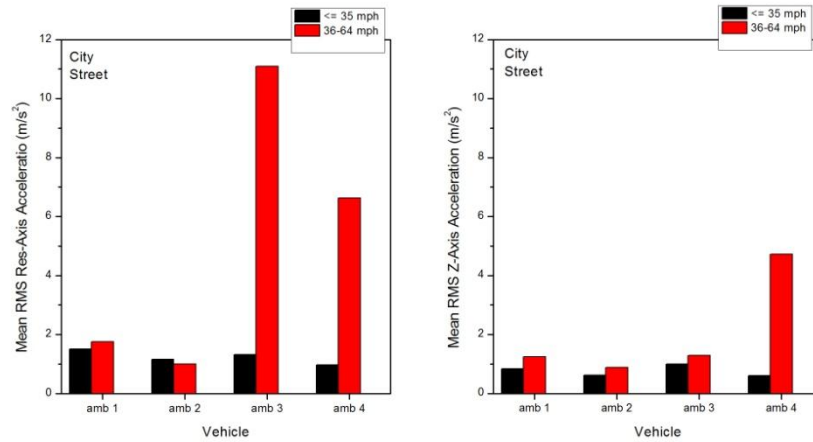
Figure C9. *Overall vibration level – city street all ambulances all speeds*

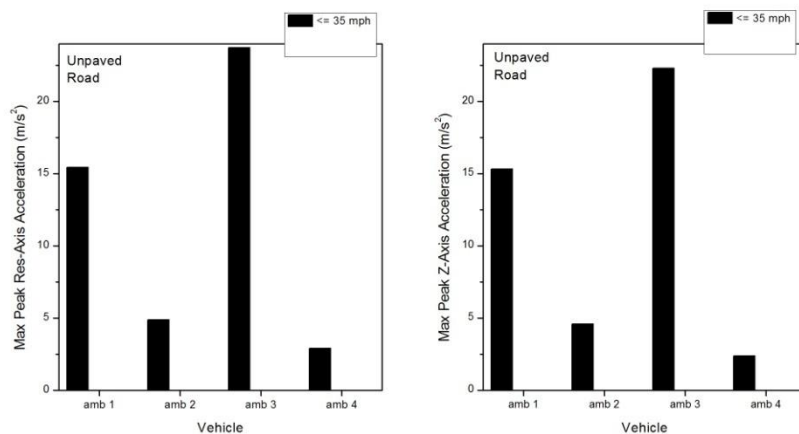Figure C10. *Mean peak vibration level – city street all ambulances all speeds*

Figure C11. *Max peak vibration level – city street all ambulances all speeds*

Figure C12. *Mean crest factor – city street all ambulances all speeds*

Vibrations experienced during travel over unpaved roads

Ambulance passenger cabin vibration amplitudes due to travel on unpaved roads is

shown in Table C7 and Figures C13, C14, C15, and, C16, respectively.

Table C7. *Ambulance vibration amplitudes on unpaved roads at speeds ≤ 35mph*

Speed ≤ 35 mph – Unpaved roads											
A m b #	Mean r.m.s. accel. (m sec^{-2})			Maximum peak accel. (m sec^{-2})			Mean crest factor.			Mean peak accel. (m sec^{-2})		
	Z-axis	Worst axis	Resultant Tri-axial sum	Z-axis	Worst axis	Resultant Tri-axial sum	Z-axis	Worst axis	Resultant Tri-axial sum	Z-axis	Worst axis	Resultant Tri-axial sum
1	2.41	2.41 (z)	2.77	15.31	15.31 (z)	15.43	5.56	5.56 (z)	4.88	13.56	13.56 (z)	13.53
2	0.75	0.75 (z)	0.98	4.58	4.58 (z)	4.86	3.95	3.95 (z)	3.20	2.88	2.88 (x)	3.14
3	2.55	2.55 (z)	2.94	22.29	22.29 (z)	23.72	5.99	5.99 (z)	5.36	15.45	15.45 (z)	16.08
4	0.46	0.63 (x)	0.94	2.36	2.94 (x)	3.65	4.37	4.70 (z)	3.08	1.87	1.88 (x)	2.90
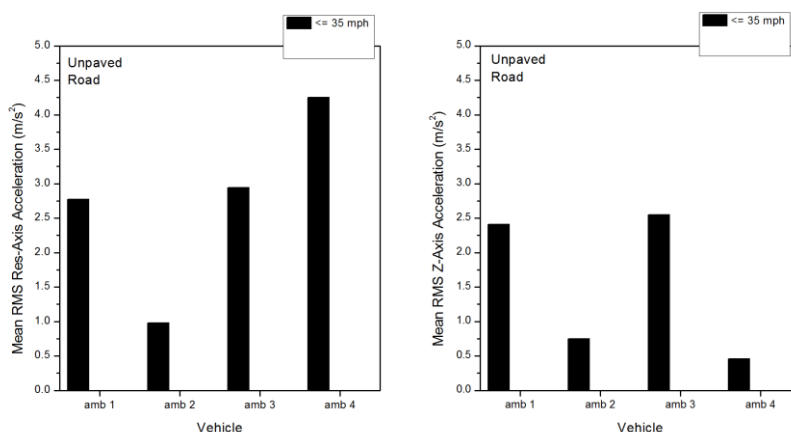
Figure C13. *Overall vibration level – unpaved road all ambulances all speeds*
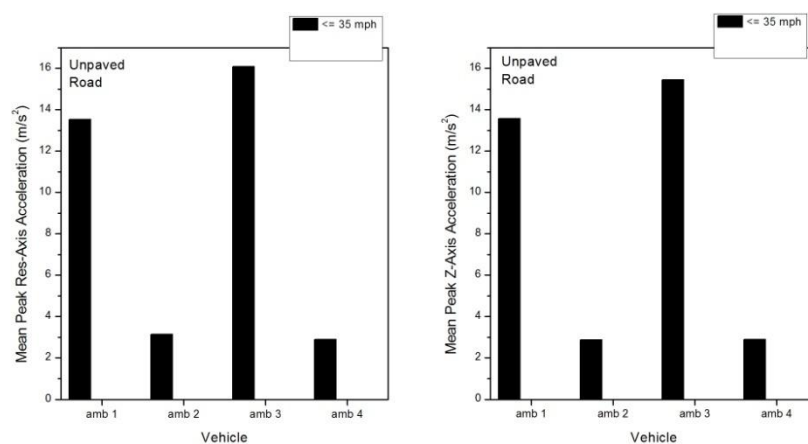
Figure C14. *Mean peak vibration level – unpaved road all ambulances all speeds*

Figure C15. *Max peak vibration level – unpaved road all ambulances all speeds*
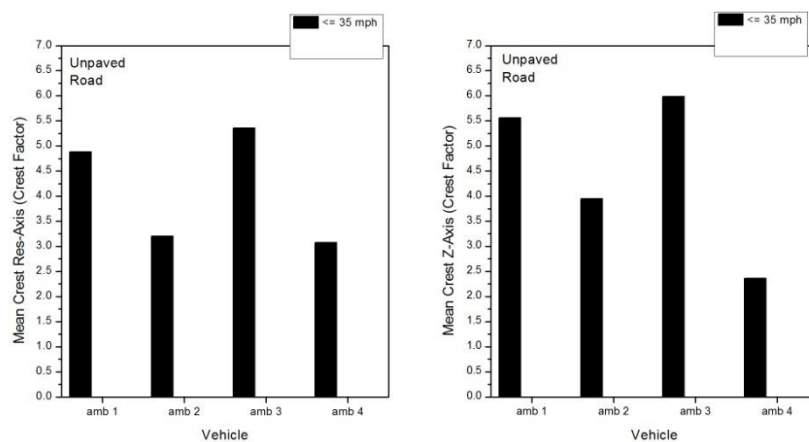
Figure C16. *Mean crest factor – unpaved road all ambulances all speeds*

Appendix D

Sample vibration time history and PSD graphs
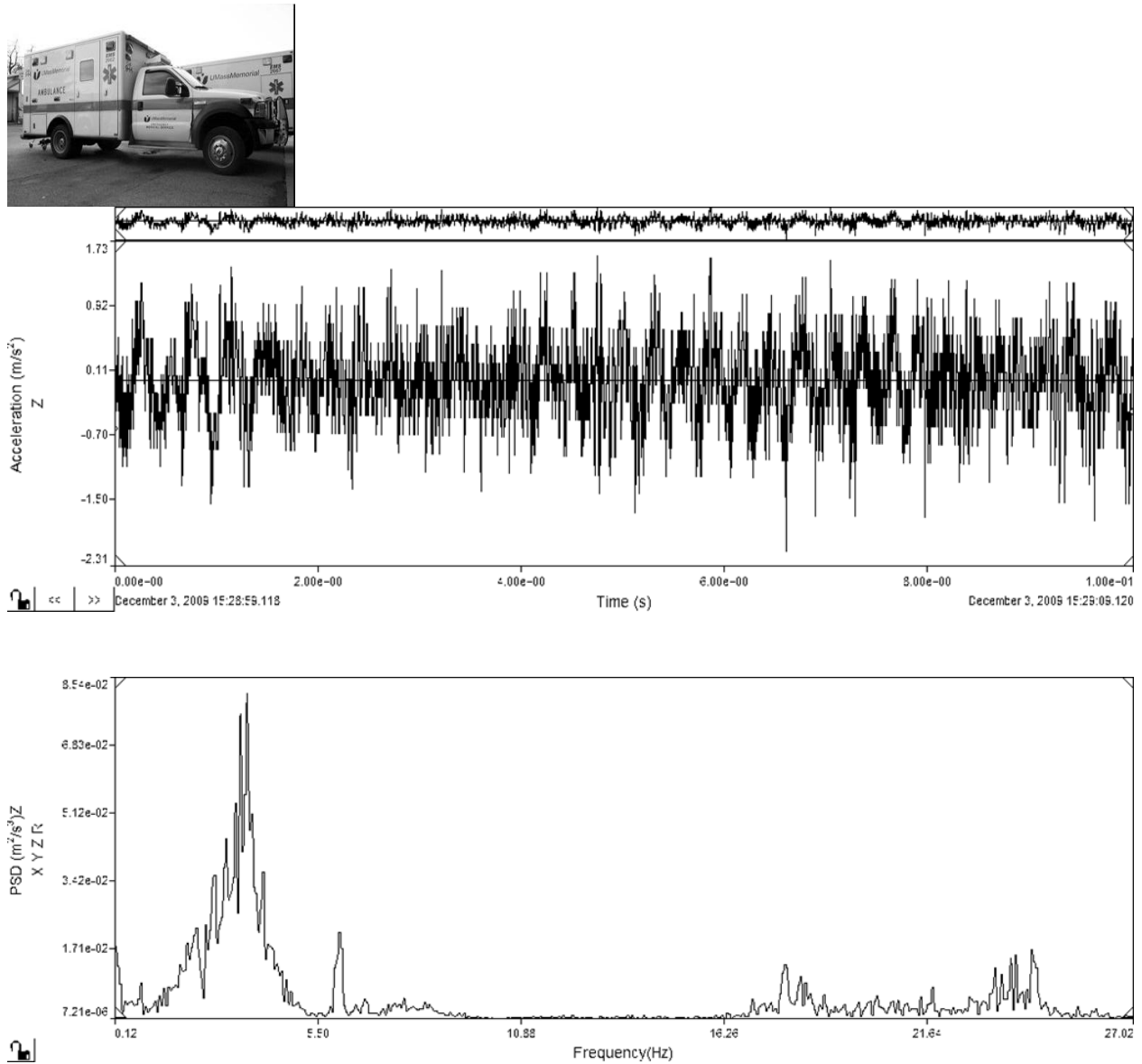
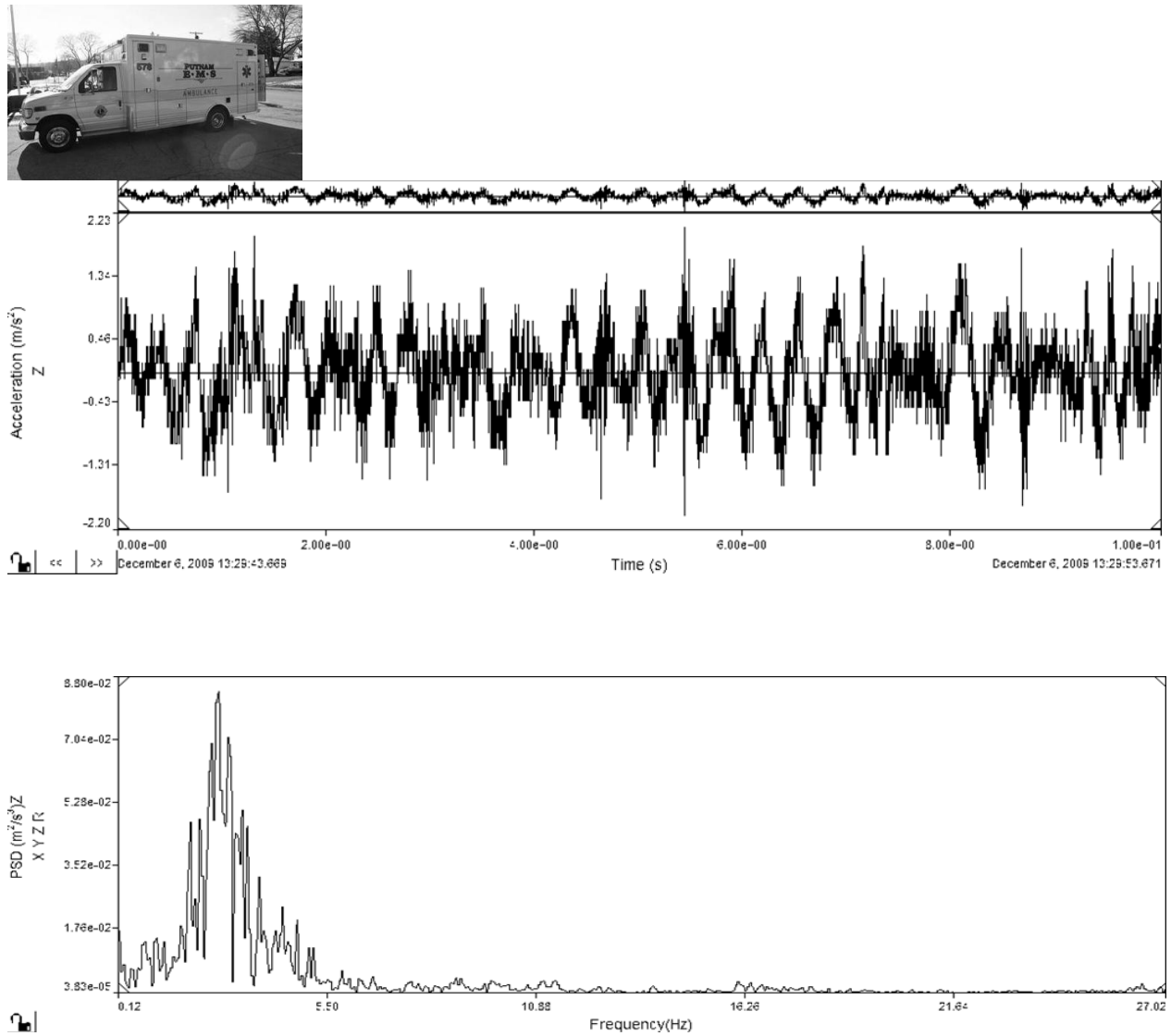Figure D1. *Ambulance #1 – Highway, 35mph, Z-Axis R.M.S., typical 10 sec event interval*

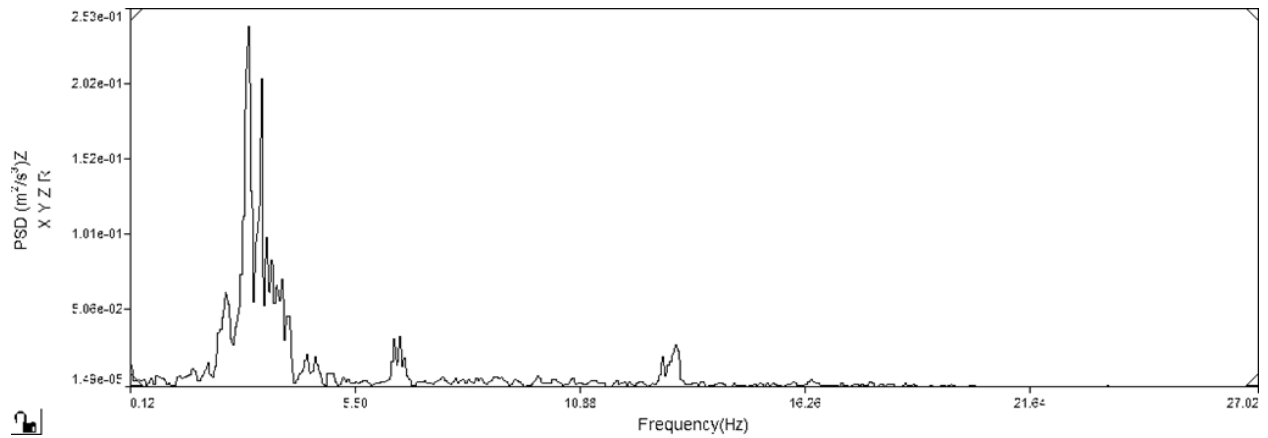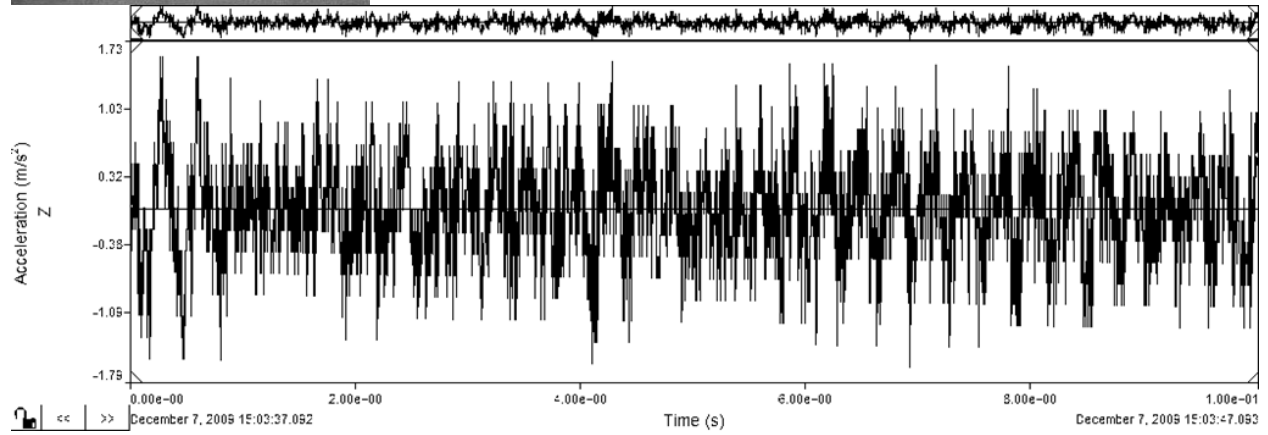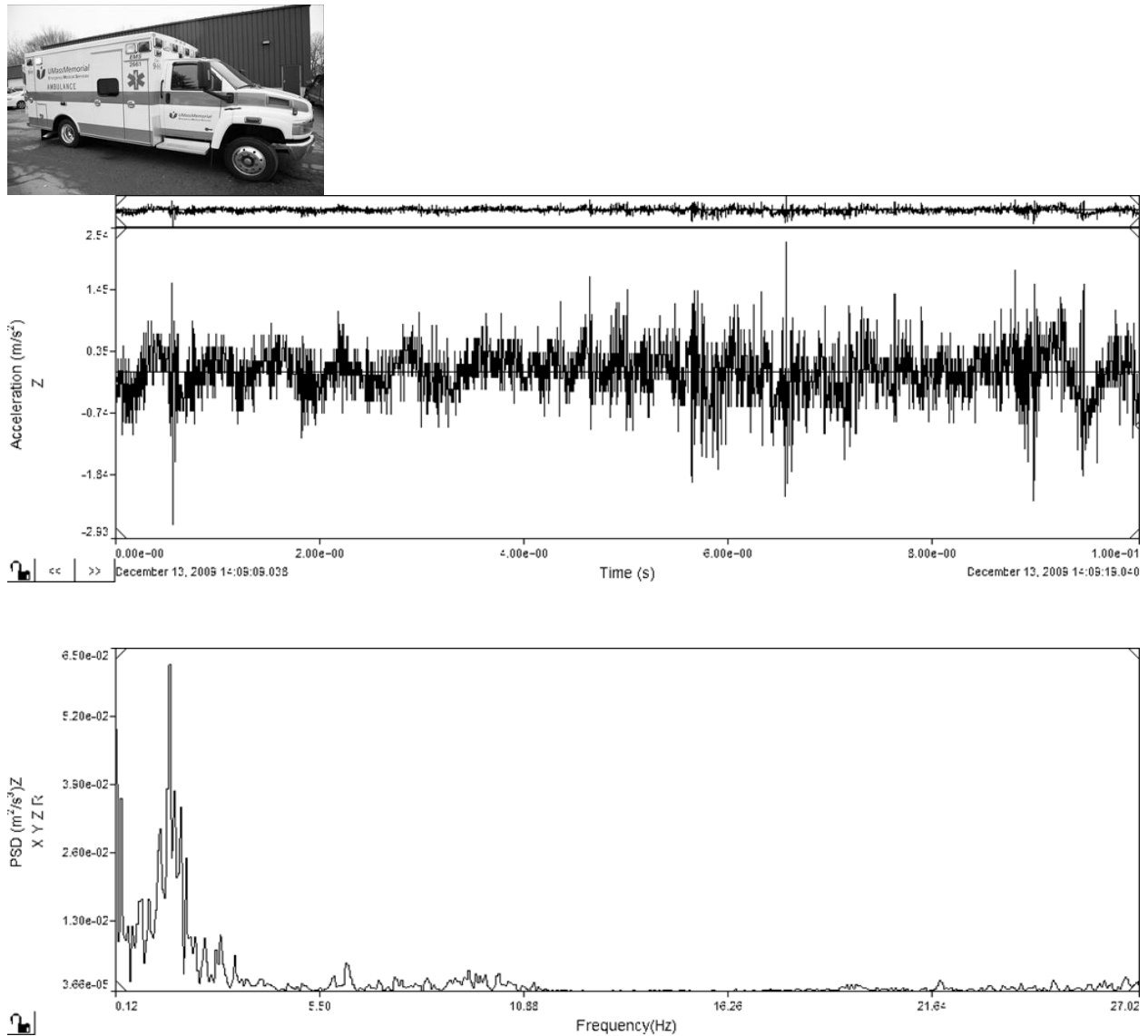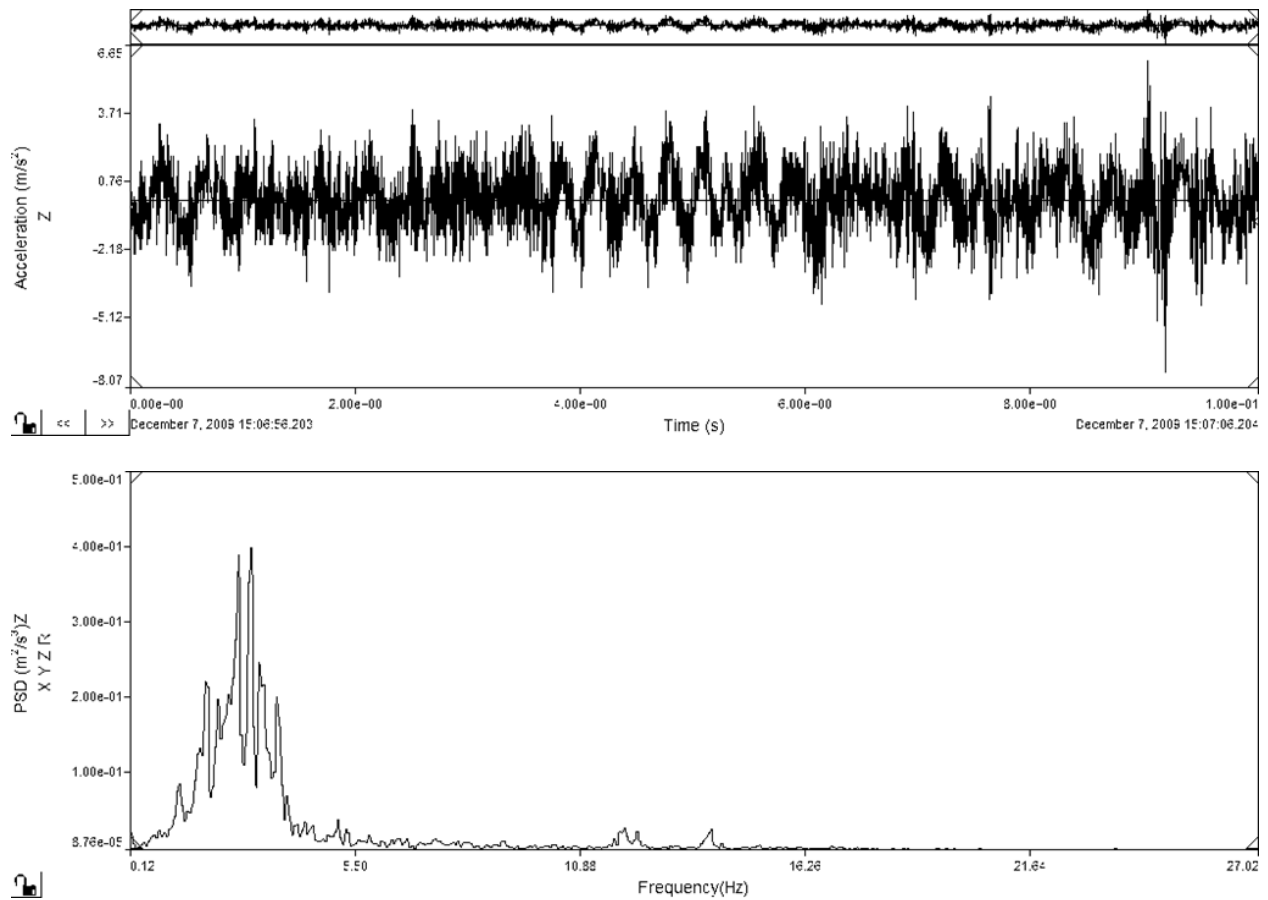Figure D2. *Ambulance #2 – Highway, 35mph, Z-axis R.M.S., typical 10 sec time interval*

Figure D3. *Ambulance #3 – Highway, 35mph, Z-axis R.M.S., typical 10 sec time interval*

Figure D4. *Ambulance #4 – Highway, 35mph, Z-axis R.M.S., typical 10 sec time interval*

Figure D5. *Highway, Ambulance #3, Z-Axis R.M.S.,≥65 mph., typical 10 sec event interval*
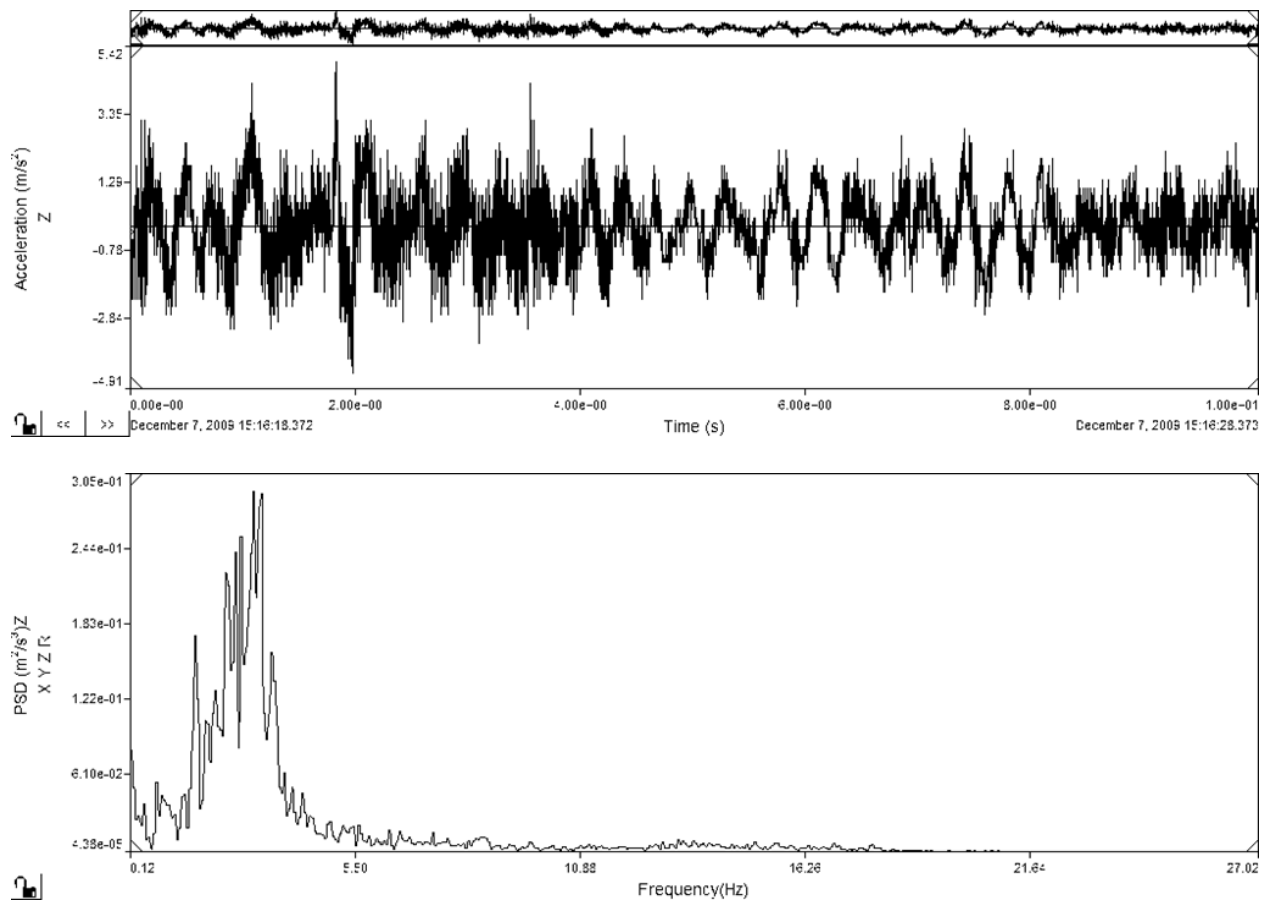
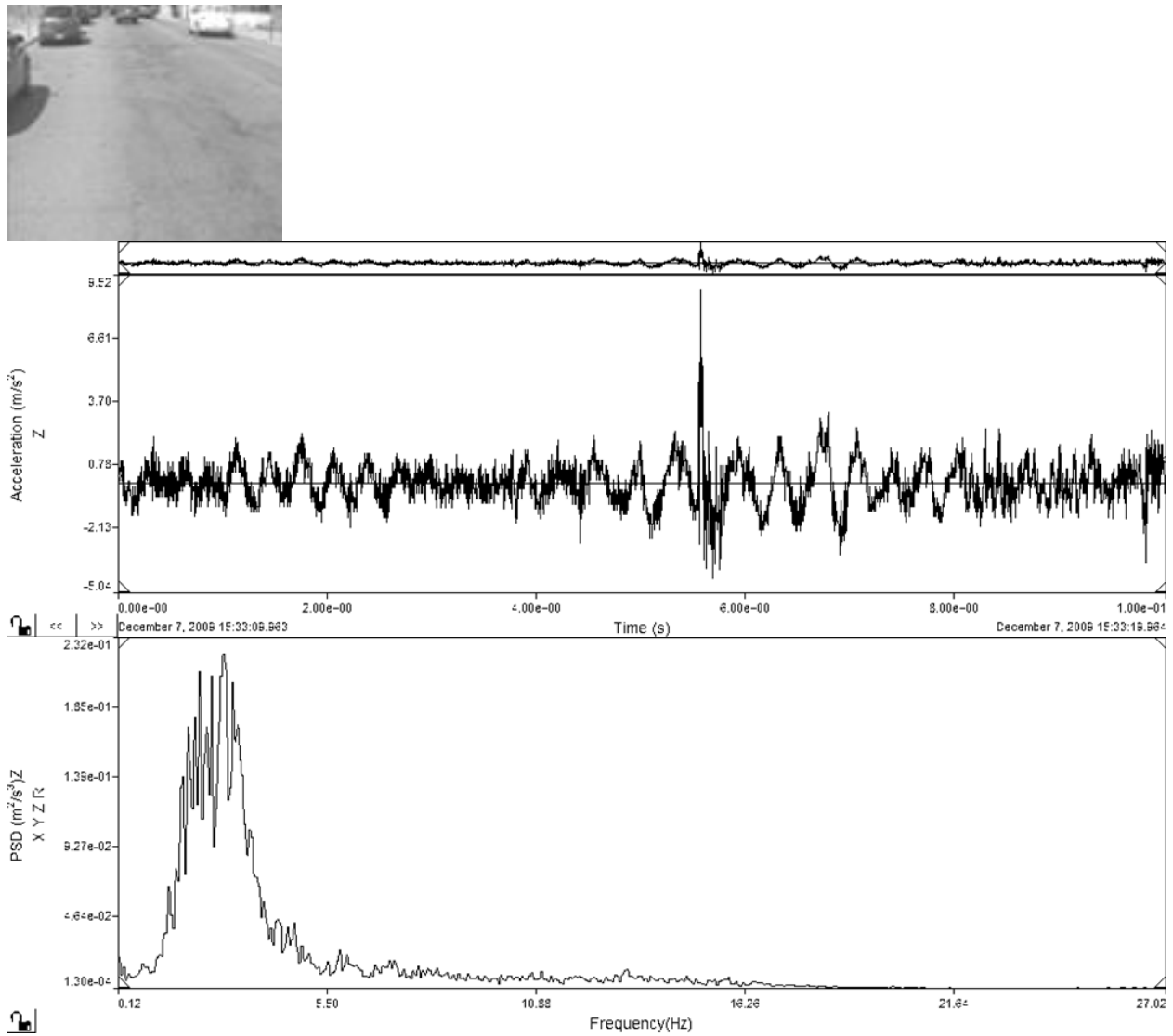Figure D6. *Secondary road , Ambulance #3, Z-Axis R.M.S.,≤35 - 64 mph., typical 10 sec event interval*

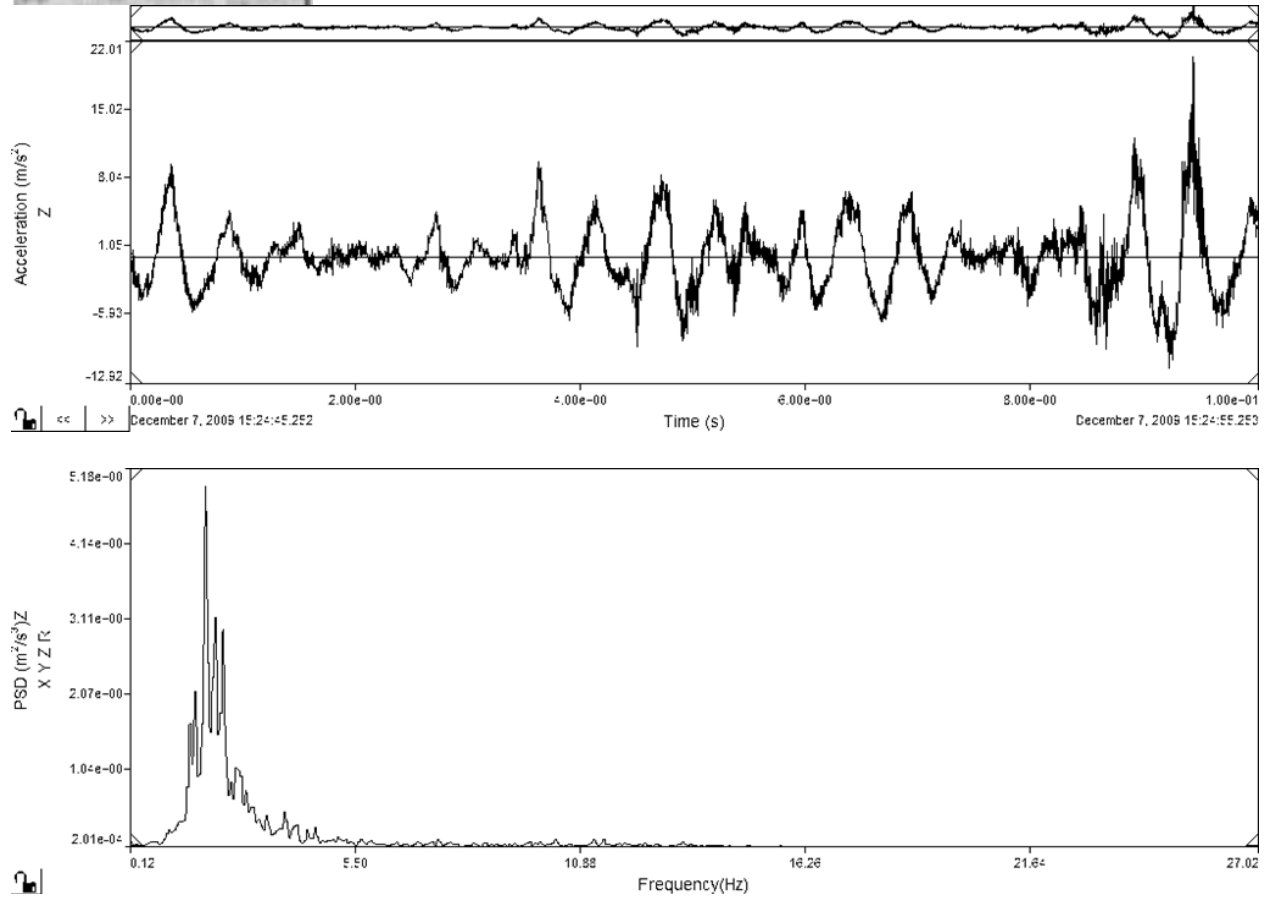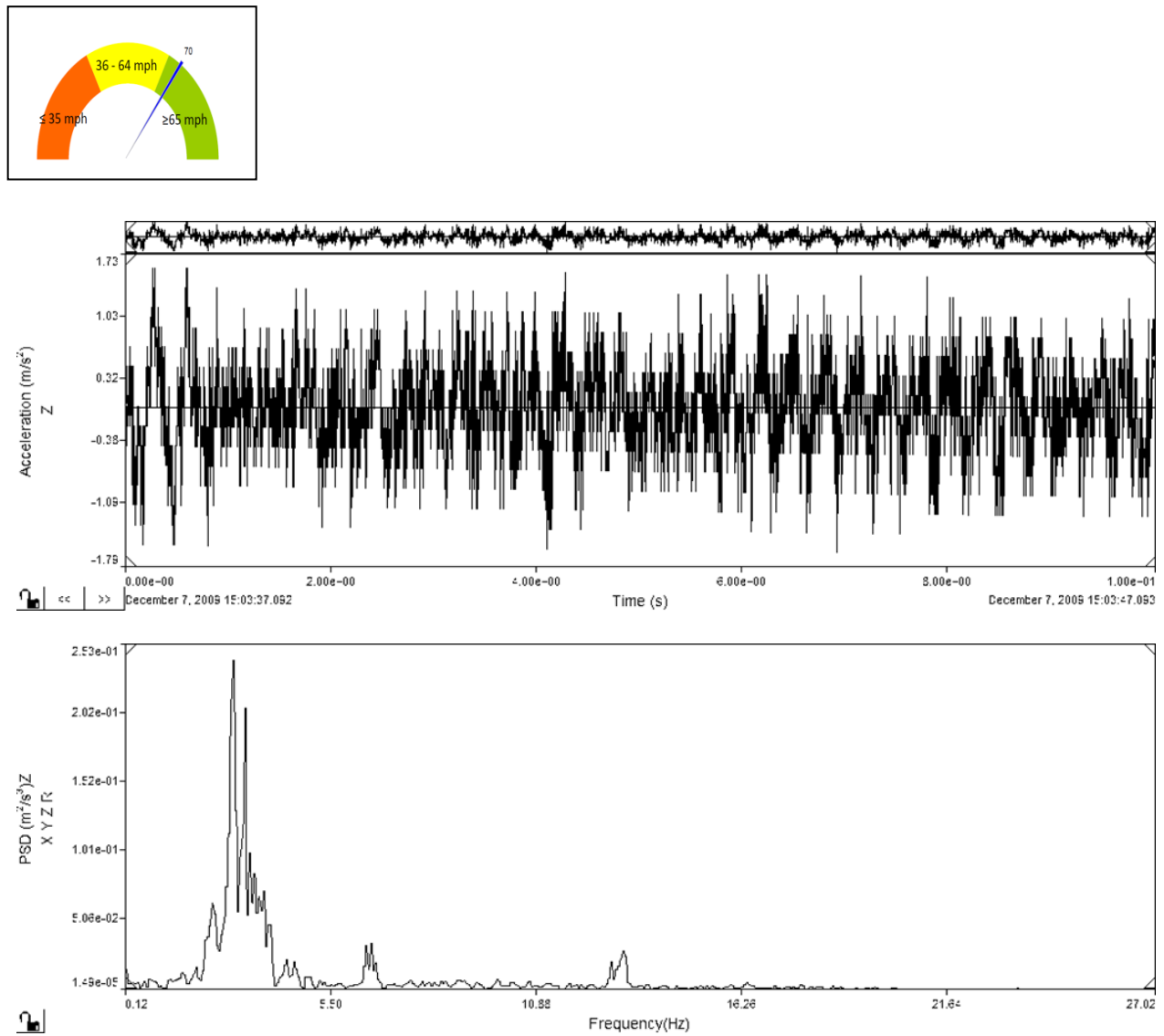Figure D7. *City Street, Ambulance #3, Z-Axis R.M.S.,≤35 - 64 mph., typical 10 sec event interval*

Figure D8. *Unpaved Road, Ambulance #3, Z-Axis R.M.S. ,≤35., typical 10 sec event interval*

Figure D9. ≤35 mph, Highway, Ambulance #3, Z-Axis R.M.S., typical 10 sec event interval
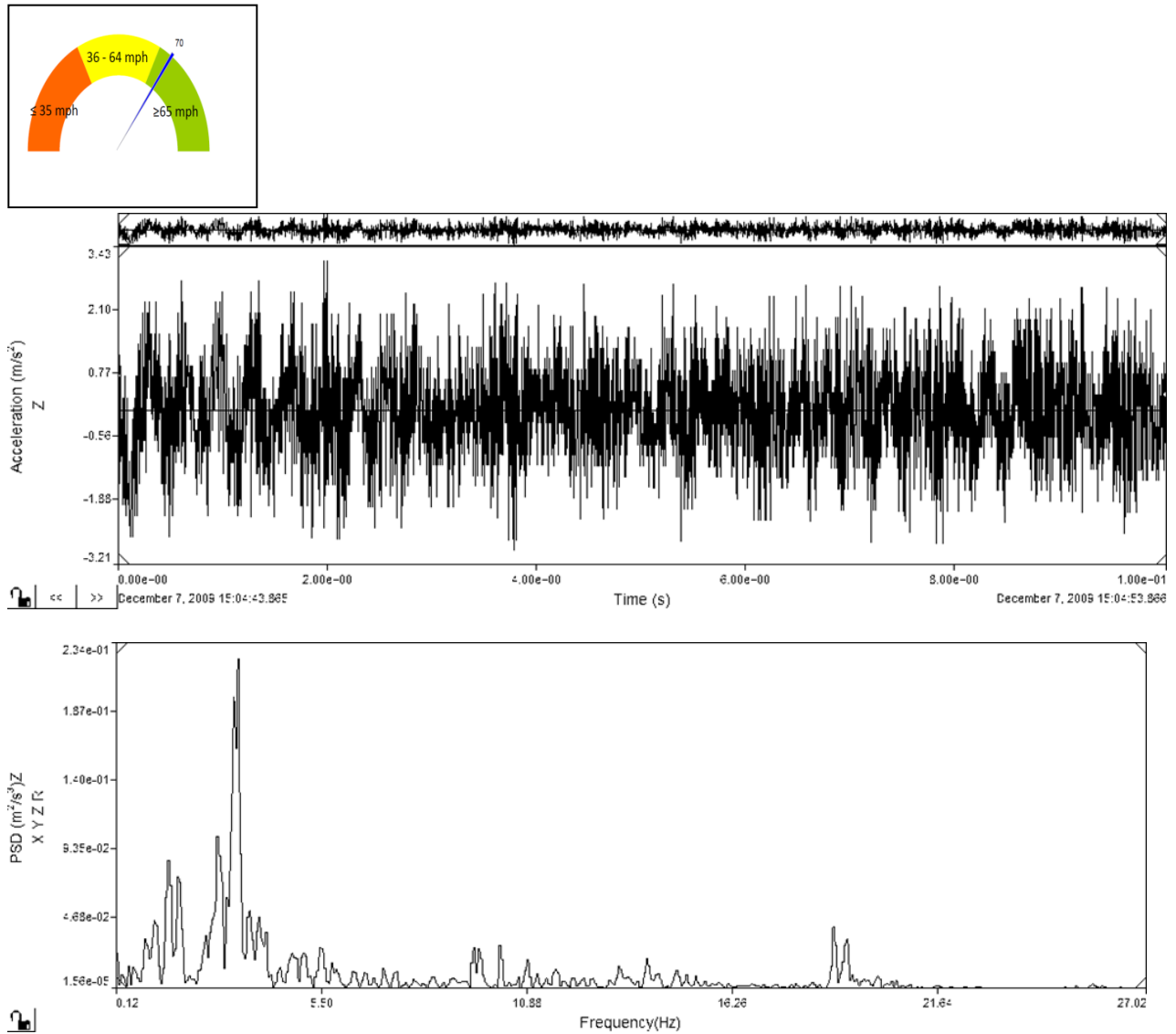
Figure D10. 36-64 *mph, Highway, Ambulance #3, Z-Axis R.M.S., typical 10 sec event interval*
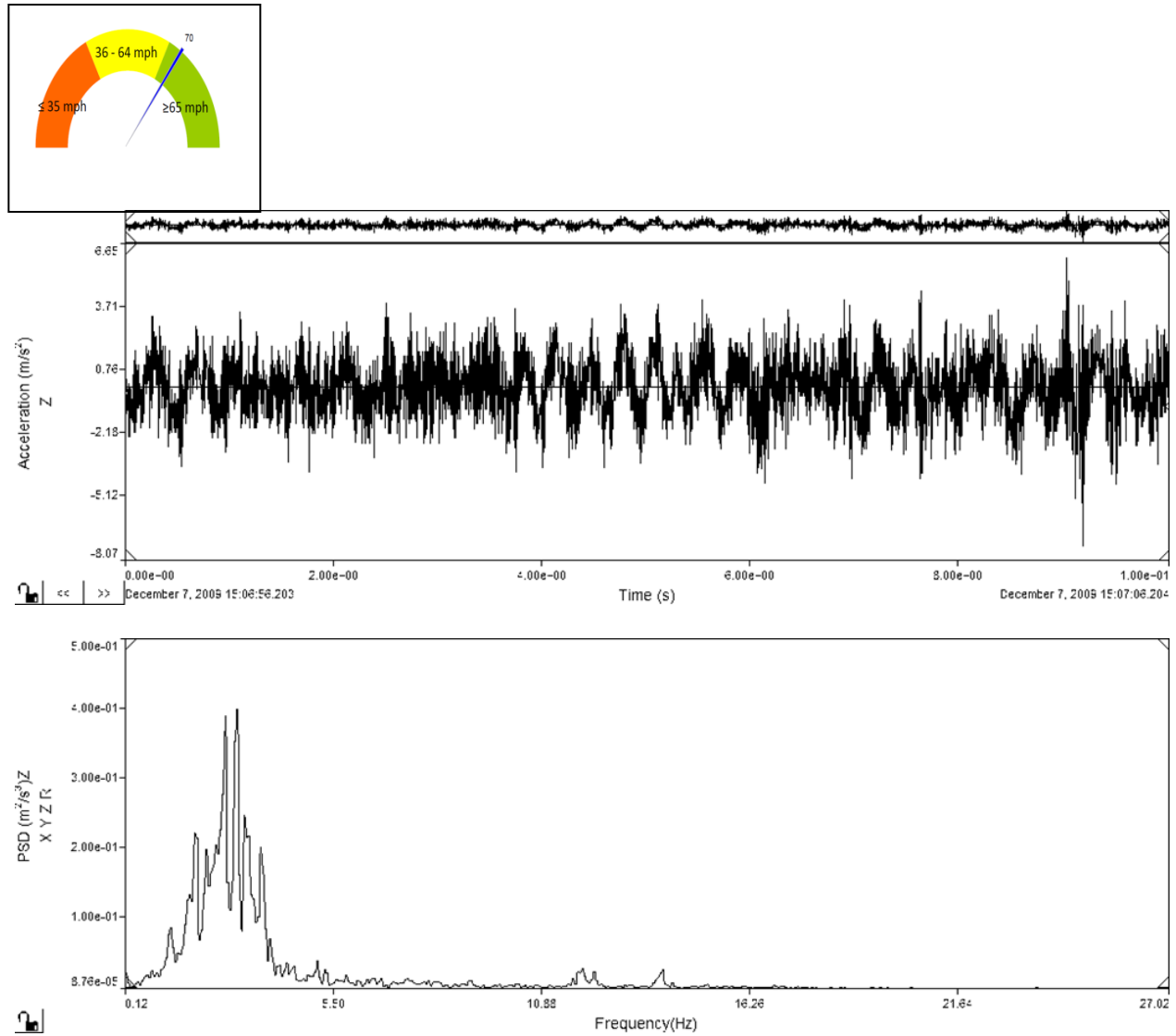
Figure D11. ≥65 mph, Highway, Ambulance #3, Z-Axis R.M.S., typical 10 sec event interval

Appendix E

Sample forcing function graphs

Time Domain Forcing Function — Ambulance #1, Highway - >= 65MPH

Time Domain Forcing Function — Ambulance #1, Highway - <=35MPH

Time Domain Forcing Function

Ambulance #1
Secondary Road - <= 35MPH

Time Domain Forcing Function

Ambulance #1
Unpaved Road - <= 35MPH